

Mechanical Properties Enhancement of Multi-layer thermoplastics using Kevlar- An Experimental Study



Author

Ali Bin Naveed

Regn Number

00000206664

Supervisor

Dr. Shahid Ikramullah Butt

DEPARTMENT

DESIGN AND MANUFACTURING ENGINEERING
SCHOOL OF MECHANICAL & MANUFACTURING ENGINEERING
NATIONAL UNIVERSITY OF SCIENCES AND TECHNOLOGY

ISLAMABAD

September, 2019

Mechanical Properties Enhancement of Multi-layer thermoplastics using Kevlar- An Experimental Study

Author

Ali Bin Naveed

Regn Number

00000206664

A thesis submitted in partial fulfillment of the requirements for the
degree of
MS Design & Manufacturing Engineering

Thesis Supervisor:

Dr. Shahid Ikramullah Butt

Thesis Supervisor's Signature: _____

DEPARTMENT

DESIGN AND MANUFACTURING ENGINEERING
SCHOOL OF MECHANICAL & MANUFACTURING ENGINEERING
NATIONAL UNIVERSITY OF SCIENCES AND TECHNOLOGY
ISLAMABAD

September, 2019

Declaration

I certify that this research work titled “**Mechanical Properties Enhancement of Multi-layer thermoplastics using Kevlar- An Experimental Study**” is my own work. The work has not been presented elsewhere for assessment. The material that has been used from other sources has been properly acknowledged / referred.

Signature of Student

Ali Bin Naveed

2017-NUST-MS-DME-00000206664

Plagiarism Certificate (Turnitin Report)

This thesis has been checked for Plagiarism. Turnitin report endorsed by Supervisor is attached.

Signature of Student

Ali Bin Naveed

00000206664

Signature of Supervisor

It is certified that MS Thesis Titled Mechanical Properties Enhancement of Multi-layer thermoplastics using Kevlar- An Experimental Study by Ali Bin Naveed has been examined by us. We undertake the following:

- (a) Thesis has significant new work/knowledge as compared already published or are under consideration to be published elsewhere. No sentence, equation, diagram, table, paragraph or section has been copied verbatim from previous work unless it is placed under quotation marks and duly referenced.
- (b) The work presented is original and own work of the author (i.e. there is no plagiarism). No ideas, processes, results or words of others have been presented as Author own work.
- (c) There is no fabrication of data or results which have been compiled/analyzed.
- (d) There is no falsification by manipulating research materials, equipment or processes, or changing or omitting data or results such that the research is not accurately represented in the research record.
- (e) The thesis has been checked using TURNITIN (copy of originality report attached) and found within limits as per HEC plagiarism Policy and instructions issued from time to time.

Name & Signiarure of Supervisor

Dr. Shahid Ikramullah

Signature: _____

Thesis Acceptance Certificate

Certified that final Copy of MS thesis written by Mr. Ali Bin Naveed Registration No. 00000206664 of SMME has been vetted by undersigned, found complete in all aspects as per NUST Statues/Regulations/MS Policy, is free of plagiarism, errors and mistakes and is accepted in partial fulfilment for award of MS Degree. It is further certified that necessary amendments as pointed out by GEC members and foreign/local evaluators of the scholar have also been incorporated in the said thesis.

Signature with Stamp: _____

Name of Supervisor: Dr. Shahid Ikramullah Butt

Date: _____

Signature of HoD with Stamp: _____

Date: _____

Countersign By

Signature (Dean/Principal): _____

Date: _____

Form TH-4

Copyright Statement

- Copyright in text of this thesis rests with the student author. Copies (by any process) either in full, or of extracts, may be made only in accordance with instructions given by the author and lodged in the Library of NUST School of Mechanical & Manufacturing Engineering (SMME). Details may be obtained by the Librarian. This page must form part of any such copies made. Further copies (by any process) may not be made without the permission (in writing) of the author.
- The ownership of any intellectual property rights which may be described in this thesis is vested in NUST School of Mechanical & Manufacturing Engineering, subject to any prior agreement to the contrary, and may not be made available for use by third parties without the written permission of the SMME, which will prescribe the terms and conditions of any such agreement.
- Further information on the conditions under which disclosures and exploitation may take place is available from the Library of NUST School of Mechanical & Manufacturing Engineering, Islamabad.

ACKNOWLEDGEMENTS

All praise is for Almighty Allah for bestowing me the courage and honor for successful completion of this project.

Understanding the emerging concept in my project would never be so easy for me without the immense support, able guidance and motivation from my respected advisor Dr Shahid Ikramullah Butt. He not only educated me from his intellect but also helped me in resolving the problems that I faced during the course of this project. I am greatly indebted to his efforts and precious time that he gave even after working hours for the successful completion of my project. I also want to extend my sincere thanks to him, as he was not only a source of motivation for me during my project phase but also helped me learn and explore my own capabilities. I am also thankful to Dr Aamir Mubashir who was always ready to help and guide whenever the project demanded.

I express my utmost gratitude to my parents and family for their kind prayers, support, love and unconditional patience towards my extended working hours. Without their prayers and cooperation, the project could not be a success.

DEDICATION

I dedicate this work to my parents, wife and advisor who have always been a constant source of support and guidance to me.

ABSTRACT

Fused Deposition Modeling (FDM) is a type of Additive Manufacturing (AM) in which structures are formed layer-by-layer directly from CAD model, by using thermoplastics. This technique is capable of net shape parts, however, a serious limitation of the process is lower mechanical properties achieved. These properties are even lower than the same thermoplastic parts produced using conventional techniques such as injection molding. Efforts have been made in recent years to improve mechanical properties by reinforcing the parts produced with high strength parts. This has been achieved by either modifying FDM setups to extrude fibers with thermoplastics and fabricate continuous fiber reinforced thermoplastic composites (CFRTPCs) or employing manual techniques subsequent to part production.

CFRTPCs fabrication procedures have limitations of fiber exposure to environment, no direct control method for volume fraction and poor surface finish. This research work is focused on improving the process of producing CFRTPCs by addressing these limitations using an off-the-shelf dual extruder FDM setup. The process developed was tested for its feasibility using Kevlar fiber as reinforcement for commercially available ABS, PLA, PLA-C and PLA-Cu thermoplastic fibers. Taguchi L16 Orthogonal Array (OA) was used to design experiments while tensile and flexural testing was performed to determine mechanical properties achieved. Tensile strength was improved up to 3 times the baseline value of thermoplastics while flexural strength was improved up to 1.6 times. Subsequently, parts have been produced to show the feasibility of this process in industrial applications.

Contents

Declaration	III
Plagiarism Certificate (Turnitin Report)	IV
Thesis Acceptance Certificate.....	VI
Form TH-4	VII
Copyright Statement	VIII
ACKNOWLEDGEMENTS	IX
DEDICATION.....	X
ABSTRACT	XI
Table of Figures.....	XIV
List of Tables	XV
CHAPTER 1	1
INTRODUCTION	1
Project Overview	1
Project Aim.....	1
Project Milestone.....	1
Project Timeline	2
CHAPTER 2	3
LITERATURE REVIEW	3
Introduction	3
Fused Deposition Modeling (FDM)	3
Design of Experiment	10
Composites & their Properties.....	14
ASTM Standards.....	18
CHAPTER 3	19
METHODOLOGY	19
Introduction	19
Research Gap.....	19
Selecting Equipment & Material.....	20
Operating FDM Setup	21
Operation with Single Nozzle	22
Operation with Dual Extruder	25
Selection of Parameters for Investigation	26
Universal Testing Machine (UTM)	33
Analysis & Confirmatory Experiments.....	34
Minitab	35

CHAPTER 4	36
RESULTS	36
Tensile Properties of Thermoplastics	36
Fracture Mode.....	38
Flexural Properties of Thermoplastics	39
Calculation for Volume Fraction.....	41
Mechanical Properties for the Kevlar Reinforced Thermoplastics	41
Tensile Properties for the L ₁₆ OA	42
Signal-to-Noise Ratio Using Minitab.....	45
Predicted SN Ratios for Full Factorial Design	47
Flexural Properties for the L ₁₆ OA	49
Signal to Noise Ratio Using Minitab	51
Predicted SN ratio for Full Factorial Design	53
Fracture Surface Analysis	55
Theoretical Estimation of Tensile Strength	57
CHAPTER 5	59
DISCUSSION & ANALYSIS.....	59
Research Gap & Process Development	59
DOE & Results	59
Minitab Results.....	62
Fracture Surface Analysis	63
CHAPTER 6	64
CONCLUSION & RECOMMENDATIONS.....	64
Conclusion	64
Recommendations	64
REFERENCES	65
Appendix 'A'	67
G-Code Sheet.....	67

Table of Figures

Figure 1 Categories of Additive Manufacturing (Kruth, 1991)	4
Figure 2 Schematic of FDM Machine (Ning et al., 2017b)	4
Figure 3 Schematic of modified print head (Tian et al., 2016)	10
Figure 4 Schematic of modified print head (Li et al., 2016)	10
Figure 5 Graphical Representation of Taguchi Loss Function	12
Figure 6 General Process Flow for Taguchi DOE	12
Figure 7 Adopted Methodology	19
Figure 8 ANET A-8M Dual Extruder Machine.....	21
Figure 9 Nozzle schematic for fiber in hot-end slot for thermoplastic.....	23
Figure 10 Nozzle schematic with Proposed Modification for fiber.....	23
Figure 11 Thread Pull out at faster print speeds.....	24
Figure 12 Available infill designs.....	25
Figure 13 PLA specimen with Kevlar layer.....	26
Figure 14 Specimens with Dimensions	28
Figure 15 Bending specimen with maximum infill fiber tows.....	28
Figure 16 Feasibility Analysis.....	29
Figure 17 SHIMADZU AGS-X UTM	33
Figure 18 Tensile Test using UTM	34
Figure 19 Flexural Test Using UTM	34
Figure 20 Combined Stress-Strain Curve for Tensile Strength of PLA	36
Figure 21 Combined Stress-Strain Curve for Tensile Strength of ABS.....	37
Figure 22 Combined Stress-Strain Curve for Tensile Strength of PLA-Cu.....	37
Figure 23 Combined Stress-Strain Curve for Tensile Strength of PLA-C.....	37
Figure 24 Fracture Types.....	38
Figure 25 Fracture Surface for thermoplastic specimen	39
Figure 26 Combined Stress-Strain Curve for Flexural Strength of PLA	39
Figure 27 Combined Stress-Strain Curve for Flexural Strength of PLA-C	40
Figure 28 Combined Stress-Strain Curve for Flexural Strength of PLA-Cu	40
Figure 29 Combined Stress-Strain Curve for Flexural Strength of ABS.....	40
Figure 30 Tensile Specimen with Thread Distribution	41
Figure 31 Flexural Specimen with Thread Distribution	41
Figure 32 Schematic of in tandem printing of tensile samples.....	42
Figure 33 Combined Results for Tensile Testing of PLA Composite	43
Figure 34 Combined Results for Tensile Strength of ABS Composites	44
Figure 35 Combined Results for Tensile Testing of PLA-C Composite	44
Figure 36 Combined Results for Tensile Testing of PLA-Cu Composites.....	44
Figure 37 Main Effect plot for Tensile Strength using Minitab.....	46
Figure 38 Combined Results for Flexural Strength of ABS Composites	50
Figure 39 Combined Results for Flexural Strength of PLA-C Composites.....	50
Figure 40 Combined Results for Flexural Strength of PLA Composites	50
Figure 41 Combined Results for Flexural Strength of PLA-Cu Composites.....	51
Figure 42 Main Effects plot for Flexural Strength using Minitab.....	52
Figure 43 Broken Flexural Sample sideview	55
Figure 44 Cross-sectional view of Flexural sample	56
Figure 45 Fiber Pull-out phenomena in Tensile Sample.....	56
Figure 46 Cross-sectional view of Tensile sample and void formation	57

List of Tables

Table 1 Research Timeline	2
Table 2 : Important Process Parameters for FDM	6
Table 3 ANOVA Terminology	13
Table 4 ASTM Standards Utilized	18
Table 5 Product Specifications.....	20
Table 6 Selected Materials.....	21
Table 7 Properties of Technora Fiber.....	22
Table 8 Selected Parameters for Specimen Printing.....	26
Table 9 Specimen Details	28
Table 10 Selected Factors & their levels	29
Table 11 Taguchi OA for Experimentation	30
Table 12 Sample Design.....	32
Table 13 Vmin for all Materials.....	32
Table 14 Volume fractions achievable	33
Table 15 Tensile Properties of thermoplastics	36
Table 16 Flexural Properties for Thermoplastics	39
Table 17 Results for Volume Fraction	42
Table 18 Summary of results for Tensile Testing of Composites.....	43
Table 19 Tensile Modulus for Complete OA.....	45
Table 20 Calculated SN Ratio for Tensile Strength using Minitab	46
Table 21 Response Tables for Tensile Strength using Minitab.....	47
Table 22 Estimated Regression model co-efficient for SN ratio of Tensile Strength	47
Table 23 ANOVA for SN ratios of Tensile Strength	47
Table 24 Predicted SN ratio for full factorial design of Tensile Strength using Minitab	48
Table 25 Results for Flexural Testing of complete OA	49
Table 26 Flexural Modulus for Complete Array	51
Table 28 Response Tables for Flexural Strength Using Minitab.....	53
Table 29 Estimated Regression Model Coefficients for SN ratio of Flexural Strength	53
Table 30 ANOVA for SN ratio of Flexural Strength.....	53
Table 31 Predicted SN ratio for full factorial design of Flexural Strength using Minitab	54
Table 32 Tensile Strength Estimation using ROM.....	58

CHAPTER 1

INTRODUCTION

Project Overview

1. Fused Deposition Modeling (FDM) is the most common technique of Additive Manufacturing being used in industry. In this technique, fused thermoplastic is deposited layer by layer through a heated nozzle assembly to form a part according to the input CAD model.
2. Strength of the parts is a function of bonding between the layers, as the part is fabricated one layer at a time. This bonding is limited due to the complex thermal cycle of the process. Therefore, the strength of a part fabricated using FDM is much lower than the strength of a part fabricated conventional techniques such as injection molding etc. Thus, limiting the use of this technique to prototyping instead of serial manufacturing in the industry.
3. In the recent years, much research has been focused on improving mechanical properties of the parts produced by FDM. One such attempt has been to produce continuous fiber reinforced thermoplastic composites (CFRTPCs) by modifying nozzle assembly. This technique has improved strength of the parts manifold, however, bonding related defects become even more pronounced. While intricate shapes cannot be produced due to use of larger diameter nozzle to accommodate fiber.
4. In this project an attempt at improving the mechanical properties of the FDM produced parts has been made by using a dual extrusion system. Premise is to only reinforce the interior of a part while the exterior is produced by thermoplastic. Proposed technique will enhance the acceptability of FDM as it is a far cheaper and less time-consuming technique. The established technique can produce any shape while the flexibility of producing small intricate features remains intact.

Project Aim

5. The aim of this research was to devise a novel CFRTPCs fabrication technique to enhance mechanical properties of parts involving Kevlar fiber produced using FDM.

Project Milestone

6. Aim of this research along with study of the project related issues lead to the establishment of milestones which ensured smooth execution of the required task. Milestones of the project devised after feasibility analysis of the project objectives are following:
 - (a) **Understanding the project.** Includes understanding of aim of the project and establishing the feasibility of fabrication of CFRTPCs using dual extrusion FDM system.
 - (b) **Detailed investigation on Concepts of Additive Manufacturing.** Detailed study on concepts of various AM techniques, their requirements, limitations and development over the years.

- (c) **Procuring and Developing expertise on Dual Extrusion FDM system.** Feasibility study of commercially available FDM systems and selection of suitable setup within budget constraints. Hands-on experience on the system and its relevant software along with identification of critical process parameters.
- (d) **Study of Theoretical Techniques to determine Volume fraction and Mechanical properties.** Identification of established techniques for determining volume fractions and estimated mechanical properties.
- (e) **Experimental Design.** Investigation into different Design of Experiment (DoE) techniques and identifying desired parameters for DoE.
- (f) **Preparation of Specimens.** Includes preparation of CFRTPCs samples for mechanical testing.
- (g) **Testing & Analysis.** Mechanical testing of prepared specimens using Universal Testing Machine (UTM) followed by optimization of parameters.
- (h) **Project Documentation and Presentation.** Documenting the developed technique and outcomes achieved in the form of a good project report and making the final presentation.

Project Timeline

7. Based on preliminary research, following is the proposed timeline for this project:

Table 1 Research Timeline

TASK	2018						2019						
	Jul	Aug	Sept	Oct	Nov	Dec	Jan	Feb	Mar	Apr	May	Jun	Jul
Literature Review													
Procuring Eqpt													
Eqpt Setup & Procedure Development													
Experimentation & Mechanical Testing													
Study, Investigation and Comparison of Results													
Report Writing and Defense													

CHAPTER 2

LITERATURE REVIEW

Introduction

1. Manufacturing technologies can be broadly categorized as Formative, Subtractive or Additive (Onuh and Yusuf, 1999). Formative and Subtractive technologies cover processes such as forging and machining etc. While concepts of Rapid Prototyping come under the umbrella of Additive Manufacturing (AM). Rapid Prototyping (RP) is a modern-day manufacturing technique which outshines conventional manufacturing technologies, subtractive and forming alike, in that this technique is less time consuming, highly flexible, fully automated and produces nearly zero waste.

2. A manufacturing organization that achieves excellence along aforementioned dimensions is called a World class manufacturing organization (Liou, 2007). World Class Manufacturers generate more revenues as compared to conventional manufacturers. Modern Industry is driven by rapidly changing customer needs, which in turn requires technology with the ability of quickly adapting to these needs and bringing desirable products to light. AM encompasses this ability to cope up with rapid design changes and quick product turn over. AM can utilize metals, ceramics, polymers (liquid or filament), composites (polymers with natural/synthetic fibers) and alloys. However, a single system cannot be utilized for all these materials as a specific set of parameters and conditions are required for each material category. Several classifications have been proposed over the years based upon materials utilized, energy source utilized and the material processing technique. The most relevant classification technique here is based upon the material utilized shown in Figure 1 (Kruth, 1991).

3. The commercial inception of AM in 1982 by Charles Hull started out as a technology only capable of producing prototypes, however, with the recent advances this technology is now capable of producing near net shape and net shape objects. Several techniques have been developed with the aim to manufacture parts layer-by-layer in a totally automated and flexible environment. This research aims at Fused Deposition Modeling (FDM), a type of solid based AM system, its operating principle and advancements in the technique in recent years.

4. Based upon the budget, resources and time availability experimental design was devised that would yield maximum information for least number of experimental runs, Taguchi DOE was selected for this purpose. Specimen were fabricated according to established ASTM standards while Rule of mixtures (ROM) was used to perform theoretical analysis of strength and determination of volume fraction of the specimens produced.

Fused Deposition Modeling (FDM)

5. FDM was invented and patented by Steven Scott Crump, co-founder and chairman of Stratasys Ltd., in 1989. However, similar technology has also been utilized by other companies such as Fused Filament Fabrication (FFF) used by Brooklyn-based MakerBot®. This technology is amongst the most widely used AM technologies due to its low material and machine cost, low operating temperature, reasonably reduced part production time and process accuracy (Noorani, 2006, Sood et al., 2010).

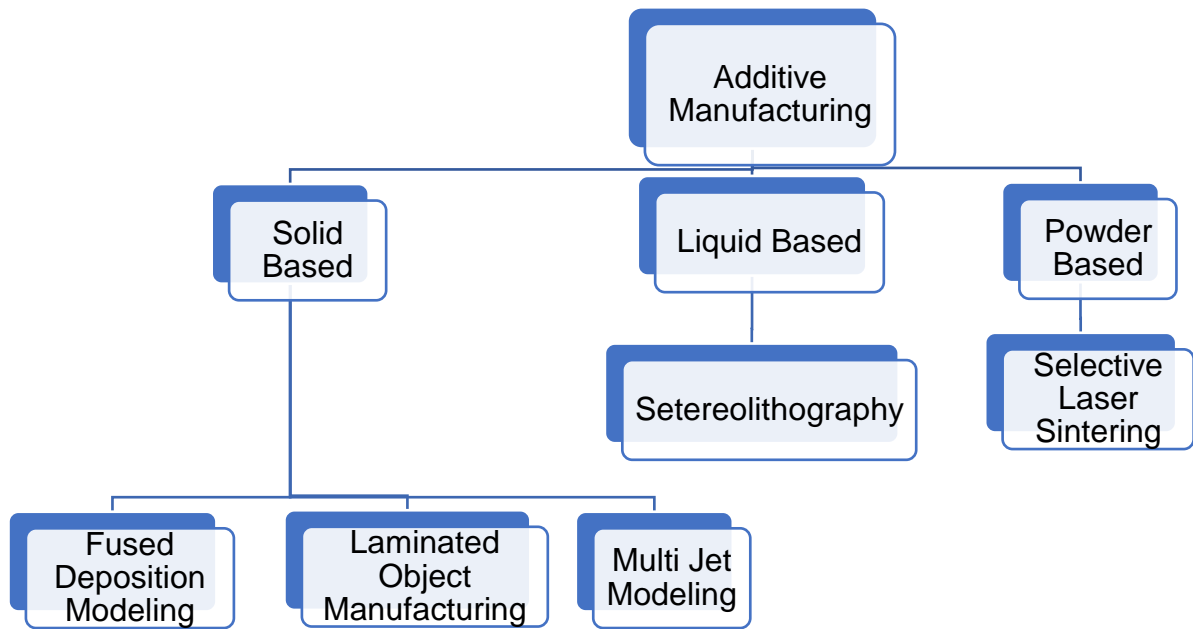


Figure 1 Categories of Additive Manufacturing (Kruth, 1991)

6. FDM technology involves melting and depositing feedstock thermoplastic filament layer-by-layer according to the 2D cross-section of the object. These cross-sections of the object are obtained from CAD model once it is converted into FDM machine readable format, STL file. Melting in FDM machine is achieved with the help of heated nozzle assembly while deposition is controlled by an extruder assembly which forces filament in the heated nozzle at a controlled rate (Ning et al., 2017b). Usually two kinds of material are used, a modeling material that forms the finished part, and an easily removable support material that supports overhanging structures in the part as it is being printed. Schematic in Figure 2 shows a generic construction of FDM machine. However, instead of support material, another build material can also be used to achieve a multicolor part, a part fabricated from two different types of materials etc.

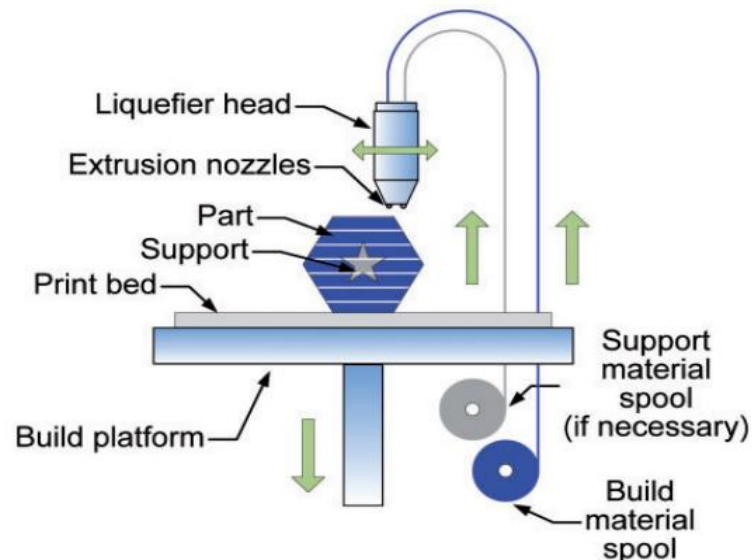


Figure 2 Schematic of FDM Machine (Ning et al., 2017b)

7. Common thermoplastics in use for part production using FDM include Acrylonitrile Butadiene Styrene (ABS), Polylactic Acid (PLA), Polycarbonate (PC), Polyetherimide (PEI), Polyether Ether Ketone (PEEK), Polyurethane (PU), Polyamide (PA or Nylon) and Polyphenylene Sulfone (PPSF). PLA and ABS are more commonly used due to their abundant availability and lower melting points.

8. Parts produced by FDM process are primarily dependent upon the bonding between layers of the molten filament extruded through the nozzle. Bellehumeur et al. (2004) modeled the dynamics of bond formation in FDM and the impact of different manufacturing parameters on bond formation. Investigation was focused on ABS bond formation with assessment that voids are created due to cooling of previously deposited layers before bonding can take place. Moreover, nozzle temperature has a more significant effect on bond formation than the envelope temperature.

9. Here following few terms commonly used in FDM printing must also be explained briefly:

(a) **Top layer.** It is the last layer of the part that is printed.

(b) **Bottom layer.** It is the first layer of the part that is printed.

(c) **Walls.** Side boundaries of a part are commonly called walls.

(d) **Shell.** Top, bottom layers and walls collectively are called shell. This constitutes the outer boundaries of a part that is visible to any observer.

(e) **Infill.** The inner part structure whether printed in the same pattern or as a different pattern is called infill. Modern software provide the flexibility to modify infill independent of the outer structure/ shell.

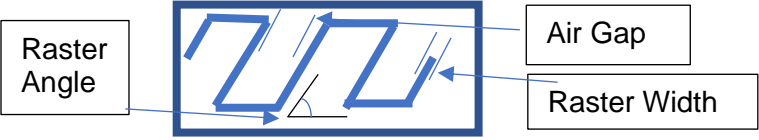
10. Over the years RP technologies have been thoroughly investigated for industrial application, especially application of FDM for making master patterns in investment casting. Lee et al. (2004) performed in-depth analysis on FDM produced patterns for investment casting. Authors have postulated that for small to medium batch production FDM patterns present the advantages of significant time and cost saving with a very small overall error. However, for mass production conventional methods for pattern production become suitable as the cost of initial tooling is offset by number of parts produced. Similarly, Hafsa et al. (2014) evaluated ABS & PLA master patterns produced through FDM for Investment Casting. ABS material provided higher part quality & surface finish compared to PLA for patterns before use. While PLA pattern gave better dimensional accuracy & surface roughness to metal parts produced by using them as master pattern.

11. Analysis has shown that using FDM for parts production is an optimization problem. Table 2 shows the common parameters affecting the quality of the parts produced. In the same context, Sood et al. (2010) have presented a comprehensive study on effect of certain parameters on mechanical properties of FDM processed parts. Authors have considered raster angle, raster width, raster gap, layer thickness and part orientation for DOE. Central Composite Design (CCD) has been used to optimize these parameters. Tensile, flexural and impact testing has been carried out to determine mechanical properties. Subsequently, full quadratic response surface model has been used for analytical analysis. Based on this analysis, authors have

presented optimized parameters to achieve highest possible tensile, impact and flexural strength using FDM. Similarly, Onwubolu and Rayegani (2014) studied the effects of layer thickness, part orientation, raster angle, raster orientation and air gap on tensile strength using full factorial DOE. Minimum layer thickness, zero-degree part orientation, maximum raster orientation, minimum raster width and negative air gap yield the best tensile strength. Based on these 5 parameters a MATLAB based group method of data handling (GMDH) mathematical model has been designed. Using this model in Differential evolution (DE) method of optimization, optimal parameters have been identified analytically and found to agree with experimental findings.

12. Beniak et al. (2015) studied the effects of part orientation within X-Y plane, Taguchi DOE has been employed for experimentation. ABS, PLA and PC materials have been used, while orientation of 0, 45, 90 deg has been investigated. This study proves that the strength of parts produced by FDM is lower than conventionally produced parts because of lower part density achieved in FDM even with negative airgap. Also, that orientation within the plane also affects part strength. Similarly, Afrose et al. (2016) Investigated PLA produced FDM samples for fatigue strength. Build orientation of 0, 45 and 90 deg has been investigated. Authors have established that the 45 deg samples had the highest fatigue strength. While further investigation is required to fully optimize the many process parameters involved.

Table 2 : Important Process Parameters for FDM

S No	Parameter	Description
1	Raster Angle	 <p>The diagram illustrates a 3D perspective of a printed layer. It shows a zig-zag raster pattern. A box labeled 'Raster Angle' points to the angle between adjacent raster lines. Another box labeled 'Air Gap' points to the space between the raster lines. A third box labeled 'Raster Width' points to the width of a single raster line.</p>
2	Raster Width	
3	Air Gap	
4	Layer Thickness	Height of each layer
5	Printing Speed	Speed with which the print head moves
6	Nozzle Diameter	Diameter of the heated nozzle, controls material extruded
7	Nozzle Temperature	Temperature of the print head
8	Part Build Orientation	Axis in which the part is built w.r.t to FDM machine

13. Effects of raster angle has a significant effect on the strength of parts produced by FDM process. Ziemian et al. (2012) carried out research for developing understanding of dependence of mechanical properties on raster angle and assess part capability of sustaining in-service loading. Tensile, compressive, flexural, impact and fatigue strength properties have been analyzed in comparison to injection molded ABS parts. ANOVA was utilized for results. It was found that raster orientation significantly impacts mechanical properties with 0° showing highest tensile, bending, fatigue and impact strength. However, these mechanical properties are lower than the injection molded parts. Similar study has also been carried out by Magalhães et al. (2014) to evaluate influence of deposition strategy (raster angle) on mechanical properties and stiffness behavior in FDM. Classical Lamination theory (CLT) was used for behavior prediction analytically. CLT results were found inaccurate, however, deposition strategy significantly impacts the tensile strength and bending strength of the part compared to default

deposition technique of the machine. While further study is required to evaluate relationship between size of void, its shape and deposition strategy.

14. Wu et al. (2015) have established the feasibility of using PEEK for 3D printing of parts. A 3D system capable of printing PEEK was custom built due to higher temperature requirement. Prime factors considered in this research are layer thickness and raster angle. Tensile, compressive & bending strength of PEEK samples were compared to ABS & found greater than ABS samples. Injection molded parts have higher strengths than FDM printed parts for both ABS & PEEK. However, further optimization of parameters for printing PEEK is required both for defect reduction and improving fabricated part quality.

15. As with ABS, attempts to optimize parameters for PLA printing have also been carried out. Chacón et al. (2017) have investigated the effects of build orientation, layer thickness and feed rate on mechanical properties of PLA structures. Layer thickness of 0.06, 0.12, 0.18, 0.24 mm were investigated. Feed rates of 20, 50, 80 mm/sec were investigated while build orientation of Flat, on-edge and upright were investigated. Optimal results were achieved for on-edge orientation, flat specimen yielded higher tensile strength while flexural strength was lower. Upright samples failed under lower loads in both instances.

16. Time required for fabricating parts is one of the most important and determining factor in process selection. Tanoto and Anggono (2017) have investigated processing time and material consumption required for fabricating ABS and PLA parts with FDM machine. ABS was found more efficient than PLA in time required while PLA consumed lesser material quantity. However, selection of material should also include parameters such as mechanical properties required and dimensional accuracy desirable.

17. Some research has also been performed on dual material printing in FDM setup. Kim et al. (2017) have reported the results of tensile tests conducted on single material specimen to analyze impact of several manufacturing factors. Subsequently, experiments have been performed with dual materials to investigate effectiveness of dual materials. ABS & PLA were used for investigation. Several structural arrangements have been considered. Common defects of voids and interfacial immiscibility have been detected. These can be minimized by controlling the sequence of deposition of multiple materials.

18. It is pertinent to mention here that albeit the easy availability of ABS and PLA and flexibility and automation offered by FDM, mechanical properties (tensile strength, flexural strength etc.) of the parts produced are low. This does not allow for their use in functional parts, therefore, in recent years researchers have focused research on use of additives, such as short carbon, glass and Kevlar fibers, in thermoplastics which exhibit better mechanical properties of the parts produced. Similarly, researchers in the past decade have shifted their focus on FDM machine and modifying its stock material or the machine itself to produce high strength functional parts at a much lower cost.

19. These researches can be broadly classified into two main categories:

- (a) Short Fiber reinforced Stock thermoplastic materials
- (b) Continuous Fiber reinforced thermoplastic composites (CFRTPCs)

(a) Short Fiber reinforced Stock thermoplastic materials

Much research has been carried out on short fiber reinforced thermoplastics using conventional techniques and then converting it to stock filament form for utilization in FDM machines. Working on the same lines, Zhong et al. (2001) investigated the feasibility of using reinforced ABS instead of pure ABS for FDM process, as pure ABS has lower strength. Short fiber reinforced GF-ABS for use as FDM stock material was investigated. It was found to improve strength of ABS, however, addition of GF reduced flexibility & handleability of ABS thus the composite could not be formed into filament rolls as it was brittle. This was then improved by adding compatibilizer & plasticizers. Twin screw extruder technique was used to mix the stock material and form pellets. Single screw extruder was subsequently used to form filaments of GF-ABS with better results compared to pure ABS. Perez et al. (2014) have developed ABS filament blends for FDM with TiO₂, Jute and Thermoplastic Elastomer (TPE) using twin screw extruder machine. Tensile strength and SEM analysis has been performed on samples fabricated in flat and top-up orientations. Comparison of the samples has been performed with samples of pure ABS. Results show that the ABS-TiO₂ blend improves the tensile strength of the samples while other additives reduced the tensile strength. TPE addition improved the surface roughness of the samples produced.

Ning et al. (2017a) have investigated the effects of FDM machine parameters on the print quality of Short Carbon fiber (SCF)-ABS filament with 5% wt. of SCF. Tensile testing has been carried out for 70 samples to perform detailed analysis on four parameters under consideration. The parameters investigated are raster orientation, infill speed, print speed and layer thickness. Authors have proven experimentally that the parameters have significant impact on the quality of printed parts. Best results have been yielded for 0.15 mm layer thickness, 25 mm/s infill speed, 220 nozzle temp and [0,90] raster orientation. Similarly, Ning et al. (2017b) have further worked with Graphite-ABS and SCF-ABS as stock materials for FDM printing of samples with the same 5% wt. composition. They have identified that SCF-ABS samples exhibit better tensile properties. However, inherent porosity in SCF-ABS is much larger than Graphite-ABS. Graphite can be used in SCF-ABS to reduce porosity of the parts produced.

(b) Continuous Fiber reinforced thermoplastic composites (CFRTPCs)

Fabricating high strength composites requires continuous fiber reinforcement instead of short fiber with a metal or polymer resin. These composites are termed as Continuous fiber reinforced thermoplastic composites (CFRTPCs). Conventional fabrication facilities for CFRTPCs have a very steep operating and setup cost involved with them. In the recent past, efforts have also been made by researchers to fabricate CFRTPC parts directly using FDM machines.

Matsuzaki et al. (2016) have modified a single extruder nozzles of commercially available FDM printers to produce CFRTPCs of CFR-PLA and Jute-PLA. For CFR-PLA nichrome wire has been used to preheat carbon fiber while Jute has been supplied as-is. Tensile testing has been performed of the samples produced and CFR-PLA composite has been found to have superior properties as compared to pure PLA and Jute-PLA composite. CFR-PLA produced has also been compared with similar

composite available in literature that have been produced by other 3D printing techniques and found superior than them. No treatment of CFR and Jute was performed to improve permeation with PLA. Authors have coined the term of Composite 2.0 for CFRTPCs printed using AM technology while CFRTPCs developed using conventional techniques have been termed as Composite 1.0.

Li et al. (2016) have evaluated the feasibility of achieving Carbon fiber reinforced (CFR)-PLA composite through FDM. FDM machine was developed by using off the shelf parts with print head modification to support introduction of carbon fiber. CFR was modified to improve the interfacial properties of the composite. Subsequently, comparison of PLA with PLA-CFR composite and PLA-modified CFR composite was carried out. Drastic improvement in mechanical properties was achieved along with success in printing composite directly from FDM process.

Similar research work has also been conducted by Tian et al. (2016) where CFR-PLA composite was manufactured by modifying print head with a 2 mm nozzle. Parameters selected for DOE were Temperature, Layer thickness, Filament feed rate, hatch spacing and printing speed. Authors have identified that temp of 200-230 °C, layer thickness of 0.4-0.6 mm, feed rate of 80-100 mm/sec, hatch spacing of 0.6 mm and printing speed of 100 mm/min yielded the best results. Carbon fiber content in the composite can be easily controlled using layer thickness, feed rate and printing speed.

Further building upon the aforementioned work, Yang et al. (2017) have used the same setup to print CFR-ABS composite via 0.8 mm nozzle and mechanical properties (tensile strength, flexural strength & interlaminar shear strength) have been found comparable (but less) to injection molded CFR-ABS but far greater than pure ABS. SEM analysis has also been performed which showed loss of strength due to voids at the interface between fiber and polymer.

To add to their previous research work in the field of fabricating CFRTPCs through FDM, Liu et al. (2018) proposed free hanging 3D printing of CFRTPC (CFR-PLA) with formation and testing of samples for mechanical properties. This required the authors to redesign the print head of FDM machine. High strength & low weight environmentally friendly structures have been achieved. The proposed methodology also eliminates the need of forming complex moulds for fabrication of CFRTPCs with complex curved shapes.

Albeit the many advantages of the aforementioned improvement in FDM process, part building process becomes slower as compared to fabricating a plastic part. This additional time further reduces bonding between consecutive layers of the part resulting in weaker part integrity. Addition of fiber also reduces the available surface for bonding between the fused plastic. Also, as the thread is exposed to environment, deterioration may also set in over time which would degrade the mechanical properties of the structure.

20. Another suggested technique for improving mechanical properties of thermo-polymers is to add reinforcement to the main load bearing path (Brooks and Molony, 2016). This reinforcement can enhance stiffness, tensile & bending strength. The method used involves

reinforcing the load paths of a structure with Carbon, Kevlar, basalt or SS 316 wire. Polymers used for FDM are ABS & PLA while PA12 has been used for SLA. However, limitation of this technique is that the success of this process depends on load applied, as structure reinforcement will only improve strength in a specific direction while in any other direction structure strength will be like polymer's load bearing capacity. Moreover, this method involves manual labor to overlay the reinforcement on the polymer part produced from AM techniques.

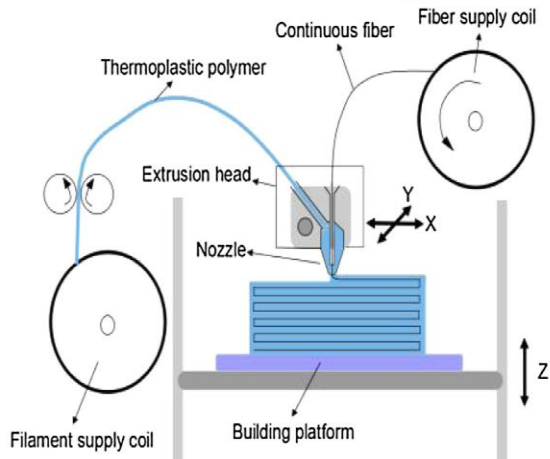


Figure 3 Schematic of modified print head (Tian et al., 2016)

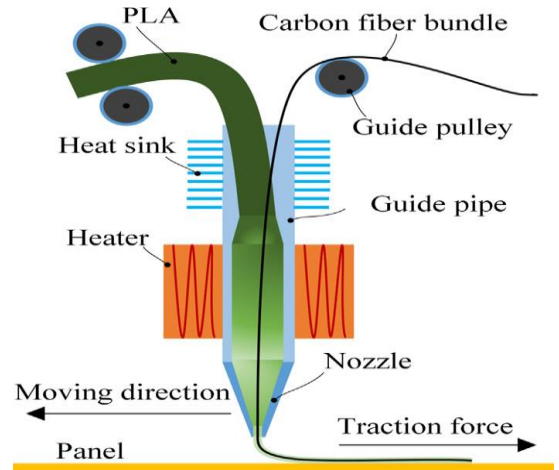


Figure 4 Schematic of modified print head (Li et al., 2016)

21. Another method that has been devised by commercial FDM filament producers is to provide continuous fibers infused with thermoplastic. These are available in filament form and can be used to produce parts using FDM setups. Dickson et al. (2017) have reported results of tensile & bending tests conducted for Nylon with Carbon, Glass & Kevlar fiber composites. The Carbon, Kevlar and glass fiber is readily available with commercial FDM filament supplier. Strength of these composites were found to improve beyond Aluminum. Here a dual extruder has been used to form the composite which extrudes nylon filament from one nozzle and carbon, glass or Kevlar fiber from the other according to the designed part. Carbon fiber with Nylon was found to be the strongest composite. A similar research on same nylon impregnated continuous Glass and Carbon fiber has also been carried out to assess the mechanical properties of these stock filaments. Goh et al. (2018) have established that good mechanical properties can be achieved by using these filaments, however, the company claimed strength could not be achieved. Also, authors have established that this process cannot replace existing composite manufacturing processes. This is primarily because of the high mechanical properties achieved by using conventional techniques. The filaments are currently only available as composites of Nylon with Carbon, Glass and Kevlar fiber. Therefore, the process does not afford the flexibility to fabricate any combination of fiber matrix other than the aforementioned materials.

Design of Experiment

22. Ross (1996) has defined DOE as the strategic variation of multiple factors at predefined levels to assess their effect on the outcome of a process or characteristic. The prime focus of experimentation is to learn about a system, identify variable effecting it and to develop understanding of the different system responses. If required, experimentation can also be used to improve system performance based upon the system knowledge. This improvement is termed as system optimization which reduces variation in the process and hence losses

resulting can be minimized. DOE can take on different forms depending upon factors like the budget, time, complexity of the information required and resources available.

23. DOE first came into focus when Dr R A Fisher applied full factorial experiments to resolve agricultural issues in England in 1920s. The equation below is a representation of full factorial experimentation. Here 'L' represents the levels of the factors under consideration while 'k' represents the number of factors.

$$\text{Number of Trials} = L^k$$

24. Dr Taguchi in 1940s realized that the experimental setup for a full factorial requires a lot of time and effort. This may become impractical where cost and time are important constraints. Therefore, a new DOE was established which uses a set of Orthogonal Arrays, that are standardized Fractional Factorial experimental design. This was done in order to ensure that engineers performing same experiments in different part of the world may yield comparable results. This would save time and effort while the data generated would remain statistically significant.

25. Any designed system has a target value, an Upper Specification Limit (USL) and a Lower Specification Limit (LSL). USL and LSL combined are also termed as allowable tolerance. Though any system operating in these limits is termed as satisfactory, it cannot be termed as optimum. Dr Taguchi suggests that any variation from the target value results in quantifiable loss. This may be in terms of lower quality of the product or loss due to warranty claims by the customer. This loss was quantified by Dr Taguchi in the form of following mathematical relationship

$$L(Y) = k(Y - Y_o)^2$$

Where, $L(Y)$ = Loss

k = constant, dependant upon the manufacturing process

Y = Value achieved

Y_o = Target value

A general graphical representation of this mathematical relationship is shown in Figure 5. The graph shows that the loss is minimum at the target value while it increases with the deviation form target value. Even if the product is within the allowable tolerances, loss will incur.

26. Taguchi DOE yields two primary benefits, it is a systematic technique of exploring possible system configurations especially helpful when complex problems are being investigated. It provides a means to investigate possible alternatives cost-effectively. Basic steps involved in implementing Taguchi Method are shown in Figure 6.

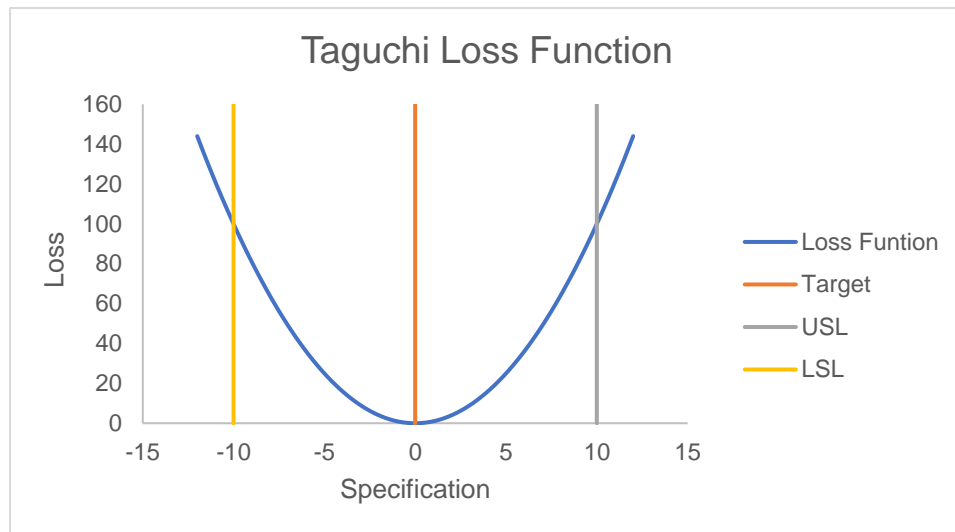


Figure 5 Graphical Representation of Taguchi Loss Function

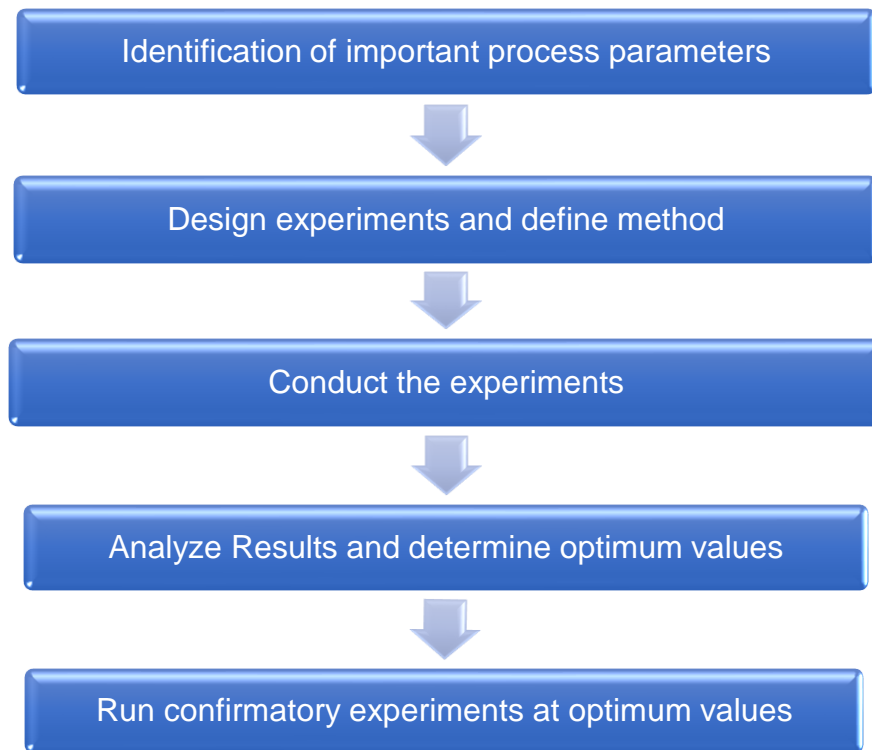


Figure 6 General Process Flow for Taguchi DOE

27. Orthogonal Arrays are the sequence of experiments that have yielded results with high confidence levels over the period of years of statistical research. They are constructed in a manner that a balanced relationship is achieved within and between columns of any selected array. It should be kept in mind that a single Orthogonal Array is suitable for several experimental designs. Following steps may be taken to determine the required orthogonal array:

- (a) Brainstorming to determine the factors to be analyzed and levels of each factor

(b) Determine Degree of Freedom (DOF) of the system based upon factors and their levels. General mathematical relationship is given as under, while the array selected should have trial runs at least equal to DOF of the system.

$$DOF = 1 + (No. of Factors) * (Factor levels - 1)$$

(c) Select the Orthogonal Array (OA) which contains experimental runs more than or equal to the DOF of the system.

(d) Assign factors to the column arbitrarily, if no interaction is included in the experiments.

(e) Define combination of experimental runs, number of repetitions and order of the runs. It is preferred to run experiments in random order, common practice is to select a setting and complete all the repetitions that setting.

28. Data acquired from experimentation can be analyzed using the following approaches:

(a) Calculating Signal to Noise (S/N) ratio for response value if repetitions have been performed, this converts the results into a logarithmic scale. This determines the most robust condition amongst the experiments conducted by identifying parameters that exhibit the least variance. Larger S/N ratio represents a smaller scatter, Taguchi recommends this technique if the outcome is in numeric figures.

(b) Determining the main effects and influence of factors in qualitative terms. In this case, variation in results is used to determine the relative influence of each factor.

(c) Performing Analysis of Variance (ANOVA) to determine statistical significance of each factor. ANOVA also identifies the relative influence of each factor on the experimental outcome in quantitative terms. Table 3 give a brief summary of the factors calculated, their meaning and mathematical relations for their calculation.

Table 3 ANOVA Terminology

S No	Quantity	Definition	Description
1	S	Sum of Squares	$S = (\text{Square of response at } 1^{\text{st}} \text{ level} / \text{Number of trial}) + (\text{Square of response at } 2^{\text{nd}} \text{ level} / \text{Number of trial}) - CF$
2	S'	Pure Sum of Squares	$S' = \text{factor sum of squares} - (\text{DF of factor}) \times (\text{Error Variance})$
3	V	Mean Square (Variance)	$V = \text{Sum of square of factor} / \text{DF of factor}$
4	f / DF	Degree of Freedom	$f / \text{DF} = \text{Number of levels of a factor} - 1$
5	e	Error	Amount of variation in the response left unexplained by the model
6	F	Variance Ratio	$F = \text{Variance of a factor} / \text{Variance of Error}$
7	P	Percent Contribution	$P = (\text{factor sum} / \text{Total sum}) \times 100 \%$
8	p	-	-
9	T	Total of results	$T = \text{Sum of all results}$
10	N	Number of Experiments	-
11	CF	Correction factor	$C.F = T^2 / N$
12	n	Total Degrees of Freedom	$n = \text{Sum of degrees of freedom}$

29. The desirable outcome of the experiments may be one of the following:

(a) **Smaller is better.** This means that the outcome variable needs to be minimized such as noise in an engine etc. In case of S/N ratio, following mathematical relationship represents smaller is better:

$$S/N \text{ ratio} = -10 \log \left(\frac{1}{n} \sum_{i=1}^n y_i^2 \right)$$

(b) **Nominal is best.** This means that the process needs to be maintained at a certain value to achieve optimum outcome. S/N ratio for this condition becomes:

$$S/N \text{ ratio} = -10 \log \frac{1}{n} \left(\sum_{i=1}^n (y_i - y)^2 \right)$$

(c) **Larger is better.** This means that the outcome variable needs to be maximized such as yield of a production process. S/N ratio for this condition becomes:

$$S/N \text{ ratio} = -10 \log \left(\frac{1}{n} \sum_{i=1}^n \frac{1}{y_i^2} \right)$$

30. Once optimum levels of all the factors under consideration have been selected, it is recommended to perform confirmation experiments. As OA represent only a fraction of complete factorial experiment, it rarely happens that experimental run has already been performed at optimized values of the factors.

31. Taguchi method offers a technique to estimate the value of outcome variable at optimized condition. Roy (1990) presents a generalized mathematical relation for calculation of this optimum value.

$$Y_{Opt} = \frac{T}{N} + \left(\text{Average of 1st factor's optimum level} - \frac{T}{N} \right) + \left(\text{Average of 2nd factor's optimum level} - \frac{T}{N} \right) + \dots$$

Here, Y_{Opt} = Estimated optimum response

T = Grand total of all the results

N = Total number of results

Composites & their Properties

32. Composite materials are formed by the combination of two dissimilar materials to produce a new material with better properties (mechanical and chemical) than the constituent materials. Most common examples of such materials are high strength fiber held in a matrix with the help of a binder. Fiber reinforcement is usually preferred because most materials have

far greater mechanical properties in fiber form than in bulk condition. However, fibers cannot be used alone as their mechanical properties perpendicular to the fiber direction are very poor. This is because of the orientation of molecules along the fiber direction. A matrix or a binder (gluing agent) is therefore required to provide acceptable properties in transverse direction.

33. Though the matrix/ binder holds the fiber together, their mechanical properties are far inferior to the fibers. Therefore, mechanical properties of the composite are also inferior to that of the fibers. This effect is more pronounced in the direction perpendicular to the fiber layup. Extreme loss of mechanical properties in transverse direction to fibers also necessitates that the fiber be lay up in multiple direction to achieve acceptable properties in multiple directions for complex loading systems.

34. Barbero (2017) classifies composite materials in the following categories:

(a) Based on Reinforcement. A material can be reinforced with the help of continuous, discontinuous fibers or with the help of particles or whiskers (elongated crystals) to form a composite with superior mechanical properties.

(b) Based on Laminate configuration. Laminate is formed by overlaying a high strength reinforcement such as a fiber with a plastic or some low strength material. These laminates can be bonded together to form composites. The direction of these laminates determines mechanical properties of a composite. Configuration of the laminate can be unidirectional, laying up laminates in different directions or the composite can be formed directly in bulk form.

(c) Hybrid Structures. Composites can also be produced with addition of more than one type of reinforcement in different laminates and then bonding them together. These materials are often called sandwich structure, where a lightweight core is used to provide structure to high strength fibers.

35. In available literature, properties of fiber and matrix are often reported separately. These properties can be combined for the purpose of composite composition by using mathematical relationships provided in micromechanics literature. Micromechanics is the study of composite materials considering the interaction of constituent materials in detail. These formulas allow designers to predict the properties analytically for a given combination of fiber and matrix.

36. Fiber and matrix are dissimilar materials exhibiting contrasting properties. Micromechanics allows designers to represent this heterogeneity with an equivalent homogeneous material that is anisotropic in nature. However, it must be noted that these mathematical formulas can predict stiffness very accurately while the prediction of mechanical properties, such as strength, is not accurate. Therefore, composite properties are banked upon experimental data. Handbooks are available for mechanical properties of composite materials for different matrix and reinforcement combinations.

37. Availability of experimental data eliminates the need for use of micromechanics, however, producing infinite combinations for experimentation is an arduous task that requires large investment and allocation of resources. Research is still on going for determining better theoretical methods. Researchers usually use a hybrid approach for determining properties of a composite of interest. Fiber and matrix properties are taken from available literature and a

few experiments are performed to determine baseline values. These values are then used in micromechanics to further predict properties of the composite. This also provides a method to calculate and adjust the difference between theoretical and experimental values.

38. Continuous fibers are often used to produce high strength and stiffness composites although the manufacturing process for continuous fiber composite manufacturing are slow and costly. In contrast, discontinuous fiber composites cost low but have lower strength. Maximum strength achieved by a discontinuous fiber reinforced composite is characterized by the critical length L_c of the fiber. Most common fibers used in both continuous and discontinuous fiber composites are Carbon and Glass fibers.

39. For manufacturing Polymer Matrix Composite (PMC), fabrication technique used is determined by the composite structure desired, cost, production volume and required production rate. Hand layup or wet layup is the most common technique in use in the modern industry. Composites also offer us the opportunity to design their mechanical properties as desired by changing the amount of constituent materials. While in case of metals, selection is primarily based upon the availability.

40. PMCs are produced as a combination of amount of fiber and matrix, represented by fiber and matrix volume fraction. These fractions can be varied as desired to achieve desired physical properties. Mathematically they can be defined as,

$$V_m = \frac{\text{Matrix Volume}}{\text{Total Volume}} \quad ; \quad 0 \leq V_m \leq 1$$

$$V_f = \frac{\text{Fiber Volume}}{\text{Total Volume}} \quad ; \quad 0 \leq V_f \leq 1$$

$$V_f + V_m = 1$$

41. Similarly, weights of the fiber and matrix can also be determined. The fiber volume/weight fraction can also be calculated analytically if the materials properties are known as follows,

$$V_f = \frac{\eta \text{TEX}}{1000 \rho_f t_c}$$

Where, η = number of tows per unit width perpendicular to fiber direction (tows/mm)

TEX = weight of the tow (gm/km)

ρ_f = density of fiber in gm/cm³

t_c = thickness of laminate in mm

42. It must be noted that volume fraction can take any value depending upon the process being used by the manufacturer. The selection of a particular value of volume fraction is determined by the properties required. As already established that composite properties are

primarily based upon experimental data, however, this is not practical due to resource, cost and time limitations. Trade-off here is to perform tests at one value of V_f and then using the actual measured values to calculate properties at other value of V_f using micromechanics.

43. Micromechanics formulas use the concept of Representative Volume Element (RVE), which is the smallest portion of a laminate that contains all the peculiarities of complete structure. This is a heterogeneous area containing fiber, matrix and defects. Based on RVE and individual properties of fiber and matrix, equations have been derived for properties estimation.

44. For Elastic modulus of the composite laminate containing unidirectional fibers, rule of mixtures (ROM) equation can be used for prediction. For deriving this equation following assumptions are made:

- (a) RVE is replaced with an equivalent homogeneous element, which means that the bonding between matrix and fibers is perfect.
- (b) Strain in the direction of the fibers is equal in both matrix and fibers which also implies that the bond between fiber and matrix is perfect.
- (c) All fibers exhibit same tensile strength whereas in reality fiber strength exhibits a Weibull distribution (Barbero, 2017).
- (d) Fibers and matrix exhibit a linear behavior up till the point of failure.
- (e) Fibers are stiffer and brittle than the matrix.

45. Under the aforementioned limitations, ROM equation is written as follows:

$$F_{1t} = F_{ft} \left[V_f + \frac{E_m}{E_f} (1 - V_f) \right]$$

Where, F_{1t} = Tensile strength of the composite measured experimentally

F_{ft} = Apparent tensile strength of the fibers, the strength of fibers suggested in literature is often too high and not achievable under real condition. It is advisable to perform experiments and determine this factor experimentally for a certain V_f and use it for subsequent estimation of F_{1t}

E_m = Elastic Modulus of the matrix

E_f = Elastic Modulus of fibers

46. Underlying purpose of fabricating a composite material is to produce a structure which exhibits superior properties than the matrix. If addition of fiber does not yield any improvement in strength, then its addition is not advised. This minimum quantity of fiber is called minimum volume fraction. Mathematically it is represented as,

$$V_{min} = \frac{F_{mt} - \sigma_m^*}{F_{ft} - \sigma_m^*}$$

$$\sigma_m^* = F_{ft} \frac{E_m}{E_f}$$

Where, σ_m^* = Stress in the matrix at failure

F_{mt} = Tensile Strength of Pure Matrix

47. While for predicting flexural strength, no such analytical formulas exist. Hence reliance is made on experimental data for determination of flexural properties.

ASTM Standards

48. These standards outline widely accepted test procedures for determining strength of materials. As part of the research, flexural and tensile testing of the PMCs and plastics was carried out to determine feasibility of the procedure developed. The summary of ASTM Standards used is presented in Table 4:

Table 4 ASTM Standards Utilized

S No	ASTM Standard	Details
1	D3039 Standard (2003)	Standard Test Method for Tensile Properties of Polymer Matrix Composite Materials
2	D638 Standard (2009)	Standard Test Method for Tensile Properties of Plastics
3	D790 ASTM (2007)	Standard Test Methods for Flexural Properties of Unreinforced and Reinforced Plastics and Electrical Insulating Materials
4	D7264 International (2015)	Standard Test Method for Flexural Properties of Polymer Matrix Composite Materials

49. Flexural test standards delineate the procedures for conducting three point bending and four point bending test. In this study, only three point bending test has been performed.

50. Sample design details will be discussed in the forthcoming chapter. It has been attempted to use standard dimensions mentioned in these standards, while the applied load has been kept same across all tensile and bending samples.

CHAPTER 3

METHODOLOGY

Introduction

1. This part of the report covers the method adopted to complete the research work. Figure 7 represents process flow adopted for this experimental study. Subsequently each step of the process is explained in detail.

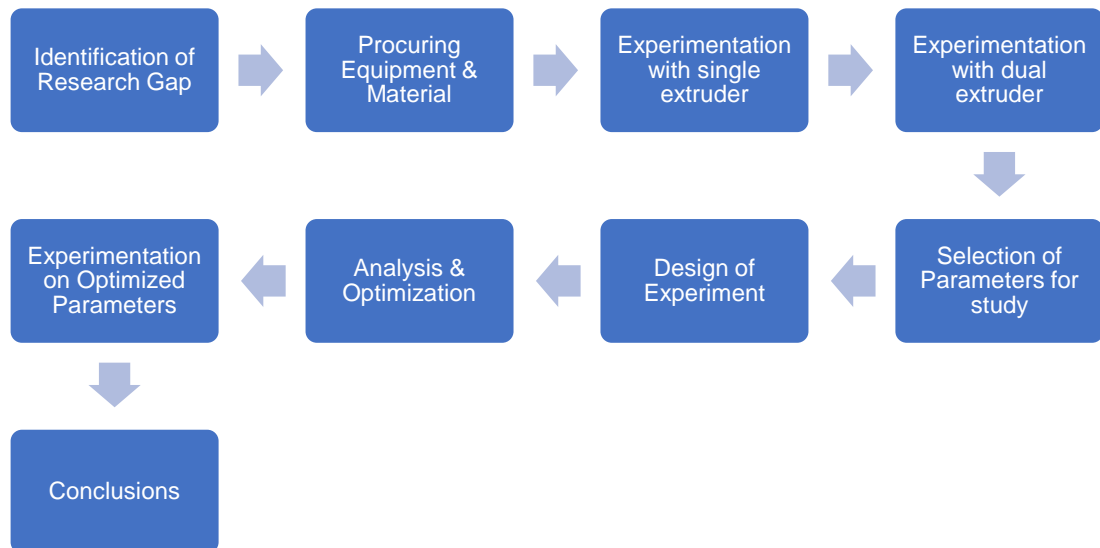


Figure 7 Adopted Methodology

Research Gap

2. Extensive literature review was carried out to understand FDM and other 3D printing techniques. Subsequently, research was further enhanced to cover modern day improvements and trends. Based upon the literature review, following were the identified areas of interest:

(a) Several researches have been made to optimize FDM parameters and enhance the strength of the parts produced using Short fibers as well. These researches have already been covered in detail in the previous chapter.

(b) Researchers have been successful in modifying FDM setups to fabricate high strength unidirectional composite parts (Li et al., 2016, Matsuzaki et al., 2016, Tian et al., 2016, Liu et al., 2018). However, the parts produced have low quality surface finish and the fiber is exposed to atmospheric effects which will affect the part performance over time. Large sized nozzles were used to accommodate fiber which also reduces the part quality, this is a common fact known for FDM fabrication. Also, there is no direct method of controlling the volume fraction of parts produced. Authors have tried managing it by modifying the flow rate of thermoplastic.

(c) Brooks and Molony (2016) have successfully increased 3D printed part strength manifold. The devised process involves simulation of the part to identify the load carrying path in a structure and then reinforcing that path manually with the help of metallic and non-metallic fibers. Plastic parts were produced using FDM and SLA in this research. As stated, this process involves manual labor thus degrading the automation advantages of 3D printing.

3. After gaining firsthand knowledge on the subject, brainstorming was done to identify the results of the literature review. Conclusions that can be drawn from above mentioned areas of interest are as follows:

(a) Optimized parameters for part fabrication using FDM are readily available in literature and may be used to achieve higher strength parts.

(a) It is possible to improve strength of FDM produced parts by fabricating CFRTPCs instead of thermoplastic parts. However, the strength may degrade over time as the fiber is exposed to atmospheric effects (Barbero, 2017). Moreover, low quality surface finish of parts may reduce the industrial acceptability of this technique.

(b) Improving mechanical properties of parts produced using 3D printing is of prime importance to enhance use of these automated and flexible techniques. However, this may be achieved without effecting the primary purpose of these processes i.e. flexibility and automation.

4. Aforementioned conclusions led to the research gap that has been explored in this research work. The aim selected for this research was to explore the possibility of fabricating CFRTPCs using dual extrusion system in which one small sized nozzle prints thermoplastic shell to provide good surface finish and protection to nonmetallic fiber. While the other large sized nozzle may be modified to make it capable of extruding fiber along with fused thermoplastic.

Selecting Equipment & Material

5. First step in the successful implementation of this idea was to select suitable FDM setup within the budget constraints and availability along with materials. Pakistan has no manufacturers of FDM machines and raw materials. Therefore, vendors were identified who could import equipment and materials from China. Figure 8 shows the selected FDM setup (ANET A-8M) while its salient features are listed in Table 5:

Table 5 Product Specifications

S No	Specification	Values
1	Printing Speed	Upto 120 mm/sec
2	Material	ABS, PLA
3	Dual Nozzle Extrusion	√
4	Build Plate Temperature	Upto 100 °C
5	Nozzle Temperature	Upto 260 °C
6	Build Plate Size (LxWxH)	220x220x240 mm
7	Compatible Software	Repetier-Host, Cura

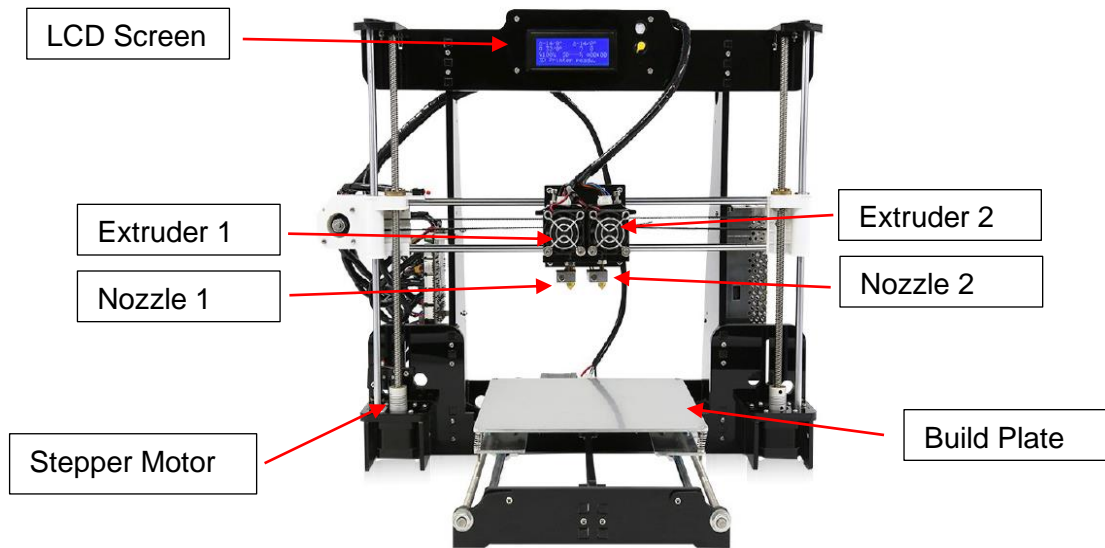


Figure 8 ANET A-8M Dual Extruder Machine

6. Following materials were procured for the purpose of this research:

Table 6 Selected Materials

S No	Material	Composition
1	PLA	-
2	ABS	-
3	PLA-C	PLA with 15% (by wt.) short Carbon Fiber
4	PLA-Cu	PLA with 20% (by wt.) Copper
5	Kevlar Fiber	66 tex fiber from Hyosung Corporation

Operating FDM Setup

7. The Setup was received in dismantled condition with all operating and assembling instruction in a flash drive. Documents were reviewed in detail and items were inspected for any defects before assembly. It was found that the setup uses four stepper motors to ensure movement in three axes while material is pushed into the heated nozzle with the help of two separate stepper motors, one for each nozzle. 01 Stepper motor for Z-Axis movement and motors for pushing plastic filament (Extruder 1 & 2) have been shown in figure 8 for ease of reference.

8. There was no past experience with the operation of FDM setup therefore for gaining experience fabrication was started with a single nozzle operation. Adjustment of machine and different machine settings were explored in detail. Over 100 trial runs were carried out to sort out all the parameters and their effects. This also involved understanding and exploring 02 software applications Ultimaker Cura and Repetier-Host, compatible with the FDM setup. It was found that all 3D printing setups, just as CNC machines, operate on G-code. This code is same as the tool path generated for motion of CNC tool.

9. All the possible parameters can be easily adjusted using Cura, however, the G-code once generated by Cura cannot be edited. Here, Repetier-Host proved useful as it allows the flexibility of editing G-code generated by the software itself and also, if imported into the software. Important parameters, on which extensive research has already been carried out, have been listed in Table 1. It must be noted that the FDM setup use a whole spectrum of different software, in case of the FDM setup procured software mentioned in Table 5 were compatible.

10. A list of standard G-codes and their meaning has been attached as Appendix 'A' for ready reference and ease of understanding. Simulation capability of the software in use plays a pivotal role in correct understanding and editing of G-code. The file generated by both software is essentially a tool path file, similar to the file generated for CNC machining. Here additional lines are however added to control movement of the extruders and controlling temperature of the nozzle and build plate. G-code file generated using Cura for a single sample constituted over 10000 lines of code.

Operation with Single Nozzle

11. Kevlar (para-aramid) fiber produced by Hyosung Corporation Korea was procured from their Branch in China. This fiber has properties close to K29 Kevlar fiber produced by Dupont®, detailed specifications of this fiber are available at their website. A few important fiber properties which have been directly used during calculations of the composite properties are listed in Table 7.

Table 7 Properties of Technora Fiber

S No	Characteristic	Value
1	Density (ρ_f)	1.4 gm/cm ³
2	TEX	66 gm/km
3	Modulus (E_f)	100 GPa

12. Here two approaches were selected for investigation, initially the thread was inserted in same slot designed for inserting thermoplastic filament in hot-end as shown in figure 9. If this approach failed or the thread got damaged due to friction force exerted by the moving thermoplastic filament as shown in figure 10. As the initial approach proved fruitful without affecting fiber, it was used for the rest of experimentation. Although the modification to nozzle assembly was also successful, it was not used.

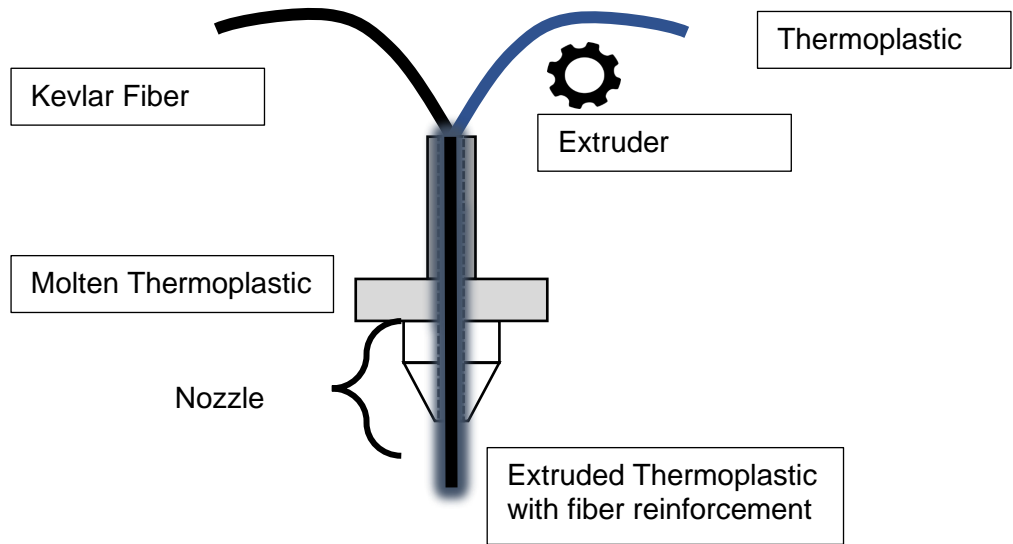


Figure 9 Nozzle schematic for fiber in hot-end slot for thermoplastic

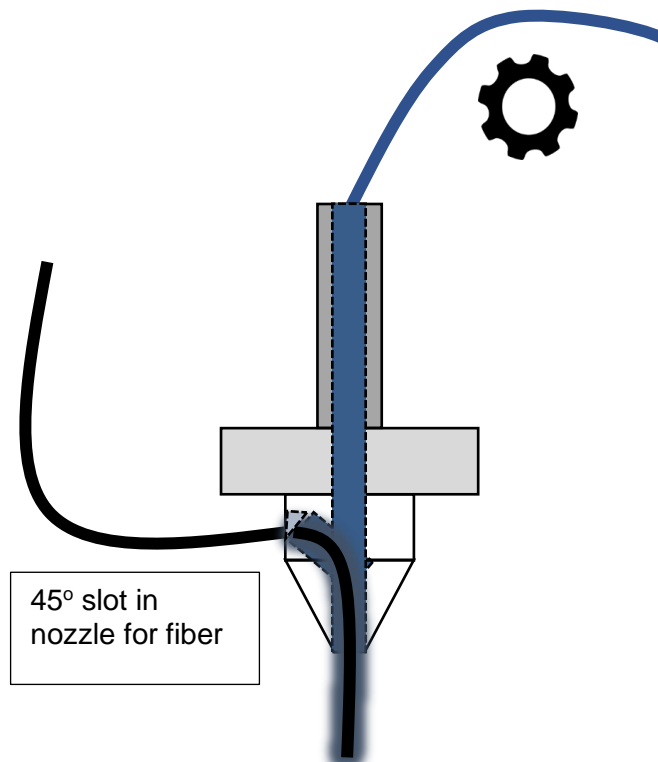


Figure 10 Nozzle schematic with Proposed Modification for fiber

13. Based on the available literature, machine parameters were kept constant and fiber was inserted with filament into the nozzle. From the trial runs performed, following conclusions were drawn:

- (a) Initial attempts for printing fiber with 0.4, 0.5 & 0.6 mm nozzles failed as flow of the thermoplastic became restricted due to presence of fiber. This resulted in loss of adhesion of thermoplastic layers with each other and with build plate.
- (b) Range of temperature from 180-230 °C for PLA and 230-260 °C for ABS was explored to ease tension on the thread and increase flow of thermoplastic. However, with this increase in flowability the time to cooling also increased and resulted in thread pull out whenever nozzle direction would change during print.
- (c) Thread chaffing with the nozzle could also be observed. Subsequently, nozzle size was increased from the default size of 0.4 mm to 1 mm. It flowed easily from the hot nozzle with the plastic filament and deposition was achieved.
- (d) G-code generated by Cura was analyzed in Repetier-Host and commands were edited while the printing nozzle approached corners to slow the movement while turning. However, this did not yield any fruitful results as slowing nozzle also kept plastic in molten form which made it easier for the thread to pull out.
- (e) It was also revealed that optimum printing speed for CFRTPCs is 3-5 mm/sec. For printing speeds greater than 5 mm/sec, the thread started to tear out of molten thermoplastic at turns. While, the time for printing became very large for speeds slower than 3 mm/sec. Figure 11 shows the thread pull out phenomena at faster speeds.
- (f) Fiber pull out phenomena became pronounced when print direction of fiber was changed by 180°. This phenomenon was considerably reduced when the angle at corners was reduced from 180° to 90°. Therefore, printing was carried out in concentric pattern instead of lines pattern. Moreover, maximum strength is also achieved when the fiber is placed in concentric pattern (Beniak et al., 2015, Onwubolu and Rayegani, 2014).

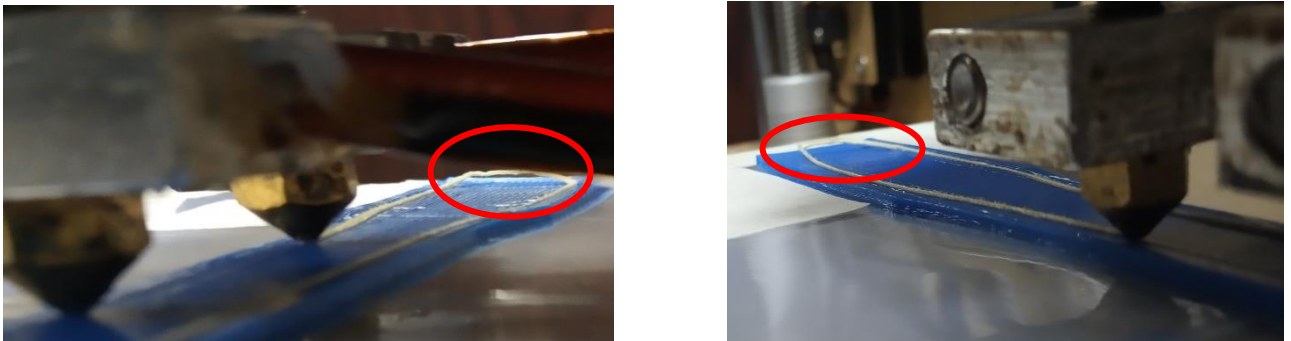


Figure 11 Thread Pull out at faster print speeds

- (g) Flexibility of printing other orientations is also possible in the developed technique. However, separate experimentation is required for each orientation to determine the appropriate fiber printing speed. A few of the printable orientations are shown in figure below.

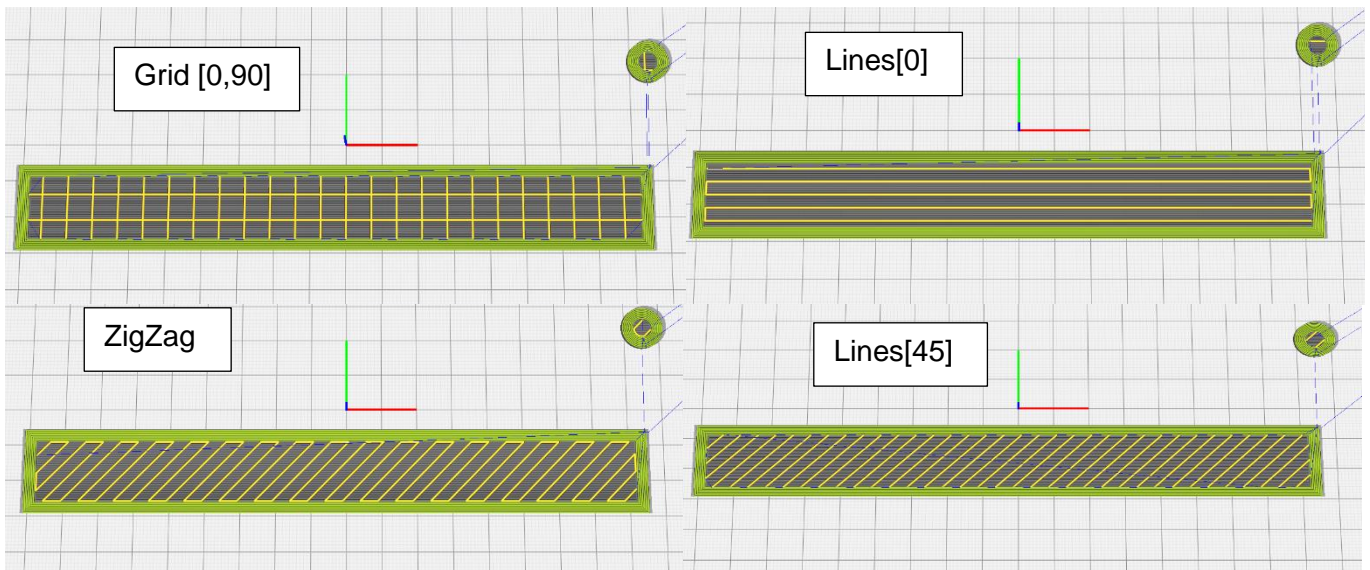


Figure 12 Available infill designs

Operation with Dual Extruder

14. After improving grasp on single nozzle operation, dual nozzle operation was started. Upon initiating the process calibration parts were printed to ensure the alignment of the dual nozzle system, it was found well aligned. During calibration initially 0.4 mm nozzles were installed with both extruders and then it was carried out with 1 mm nozzle at Extruder 1 and 0.4 mm at Extruder 2.

15. After calibrating the system, Kevlar fiber was added in Extruder 1 and printing was performed. During this initial period of 'Proof of Concept' only ABS and PLA filaments were used. Figure 13 shows a specimen with a layer of Kevlar fiber being deposited on PLA. Following conclusions were drawn from the 50 trial runs that were carried out to sort out possible disruptions during actual specimen printing:

- (a) Thread at the end of printing a single layer needed to be cut. Therefore, a nozzle priming part was also modeled along with specimen. It is a small part outside of the specimen, this would allow ample time to cut the fiber.
- (b) Leveling of the nozzles play a pivotal role, any difference in the level of nozzle tips will distort the print quality.
- (c) Print speed of the shell can easily be maintained at a decent pace while the print speed of infill (fiber) must be kept between 3-5 mm/sec to achieve positive bonding between layers of thermoplastic.
- (d) Layer height of each layer needed to be at least equal to the height of fiber to ensure that enough thermoplastic can be extruded with the fiber. This will ensure bonding between layers of thermoplastic.

(e) It is not possible to print fiber at multiple heights by using Cura only. This is because the software limits use of infill at only 1 location. G-code editing will be required to print thread alternatively with thermoplastic.

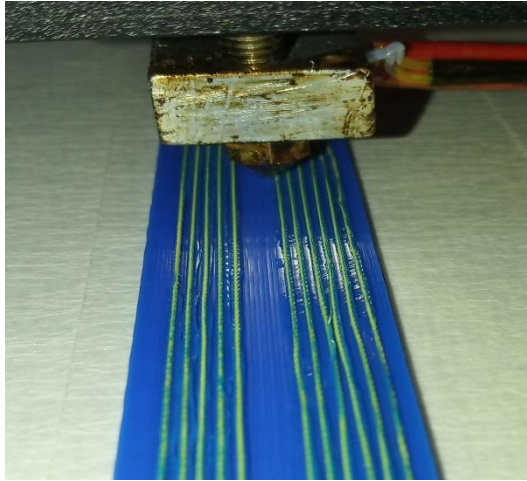


Figure 13 PLA specimen with Kevlar layer

Selection of Parameters for Investigation

16. Table 2 shows the parameters primary to FDM printing. Much research has been carried out on optimizing these parameters to ensure best possible part quality and strength. Due to plethora of research already available, all these parameters were set at their delineated optimal. Table 8 shows the values selected for all the materials.

Table 8 Selected Parameters for Specimen Printing

S No	Parameter	Selected Value
1	Build Plate Temperature	60 °C for PLA & 85 °C for ABS
2	Nozzle Temperature	210 °C for PLA & 230 °C for ABS
3	Shell Print Speed	60 mm/sec
4	Infill Print Speed	4 mm/sec
5	Infill Pattern	Concentric
6	Shell Pattern	Lines [90]
7	Layer Height	0.2 mm
8	Shell Nozzle Diameter	0.4 mm
9	Infill Nozzle Diameter	1 mm
10	Shell Extruder	Extruder 2 (Ref Figure 8)
11	Infill Extruder	Extruder 1 (Ref Figure 8)

17. For designing the specimen, following considerations were taken into account:

(a) **Diameter of Kevlar fiber.** It is to be noted that a larger layer height reduces part quality but decreases part build time and vice versa. As per the OEM provided information, diameter of the Kevlar fiber was 0.2 mm. To ensure a positive flow of the

fiber from the nozzle the layer height was kept at 0.2 mm. This was a fair compromise between allowance for fiber and part build quality.

(b) Build Plate Dimensions. One of the limiting factors for printing specimens was the available print area (220x220 mm). The specimen dimensions must be well within the limits of the build plate.

(c) Considered Variables for DOE. Literature review suggested that a comparison, if any, was only available for ABS & PLA while a single study that comprehensively covered the effects of different materials on part strength is not available. Therefore, four materials were procured to perform a comprehensive study on their properties and interaction with Kevlar fiber. Also, it was found in the literature review that there was pronounced void formation in parts produced using FDM printing of CFRTPCs due to lack of bonding between successive layers (Li et al., 2016). Thus, a hypothesis was formed to test the improvement of part strength by printing the fiber reinforced layers with thermoplastic layers between them. In conjunction with the printing of thermoplastic layers between fiber reinforced layers, number of fiber layers were also considered for this study to ascertain the optimum level of fiber.

(d) Outcome Variables. The outcome variables selected for the study were tensile and flexural strength. Tensile and 3-point bending tests were performed using SHIMADZU UTM machine with a load cell of 20 kN.

(e) ASTM Standards. ASTM standards pertaining to flexural testing and tensile testing were studied in detail. These standards provide parametric sample designs and general guidelines for testing and recording results. Standards considered are presented in Table 4. Based upon the finalized parameters and the system limitations, dimensions of the samples were determined. The dimensions have been covered in Table 9 while Figure 14 presents these specimens. It should be noted that the smaller part with the specimen represents a nozzle priming area, it was designed to simplify cutting fiber on completion of each layer. This assembly also serves the purpose of priming area for nozzle whenever nozzle are interchanged with each other. Simple G-code modification was done to achieve it.

Table 9 Specimen Details

Characteristics	Tensile Specimen		Flexural Specimen	
	Plastic	Composite	Plastic	Composite
Specimen Type	Dog Bone	Constant Rectangular Cross-section		
Grip/ Overhang	30 mm	30 mm	10 mm	10 mm
Gauge/ Support Span	50 mm	90 mm	100 mm	100 mm
Width at Grip	18 mm	20 mm	13 mm	13 mm
Width at Gauge	13 mm	20 mm	13 mm	13 mm
Thickness	3.2 mm	3.2 mm	3.2 mm	3.2 mm
Total Length	136 mm	150 mm	120 mm	120 mm
Total layer	16			
Rate of crosshead motion for testing	5 mm/min	2 mm/min	5 mm/min	1 mm/min

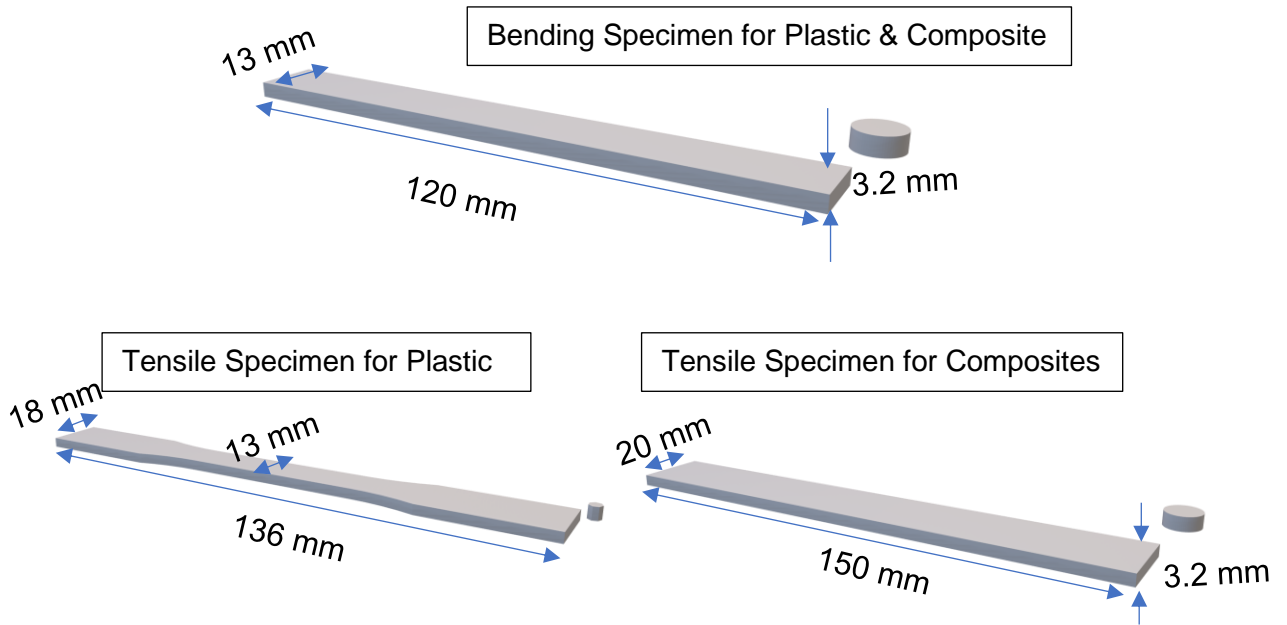


Figure 14 Specimens with Dimensions

(f) Fiber tows deposited per layer. One of the primary objectives of this research work was to deposit fiber in a manner that it is not exposed to atmospheric conditions. Therefore, layer design for fiber deposition was carried out with wall thickness just enough to avoid thread exposure. Bending specimen has the smaller cross-section, therefore, it was used to determine maximum possible tows. This resulted in a maximum of 12 tows per layer of fiber with a wall thickness just enough to shelter the fiber as shown in Figure 15. Therefore, one layer of fiber is equivalent to 12 fiber tows, here on referred as thread count. The same number of fiber tows was also utilized to design tensile specimen. It must be noted here that the fibers have been counted across the volume of each specimen. Therefore 4 layers of fiber is equivalent to 48 thread count.

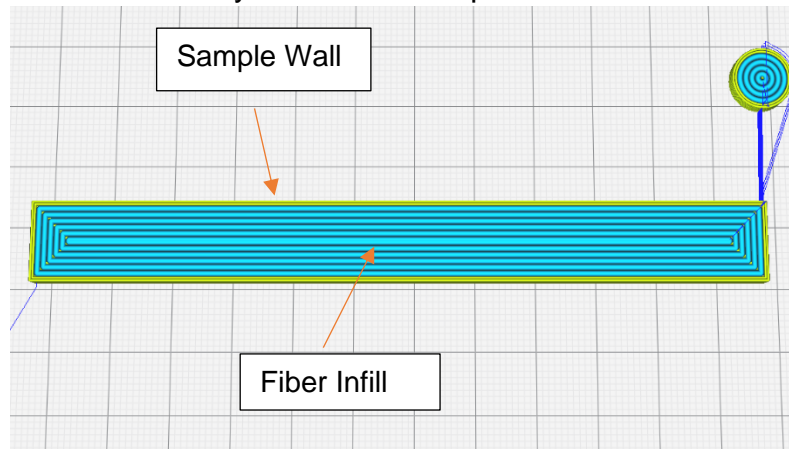


Figure 15 Bending specimen with maximum infill fiber tows

(g) Selection of Orthogonal Array. After finalizing dimensions, the important step was to determine the analysis matrix. This means that the factor levels needed to be finalized. As already mentioned, there are 04 material types that will be analyzed during

the course of this research work. Now, the important step was to find the possible combinations that could be explored and determine any further design limitations. As shown in table 9, total layers in which each sample was divided was 16. Similar layer height was kept across the board to simplify the sample design and subsequent analysis. Area under the curve in Figure 16 is a graphical representation of the combinations that can be achieved by combining all the design parameters and limitations. While the axes have been represented in numerical terms as well as physical dimensions for ease of understanding. Each layer of specimen can be represented as 0.2 mm in terms of height of the specimen. Similarly, as already described, each fiber layer is equivalent to 12 threads printed in a single layer.

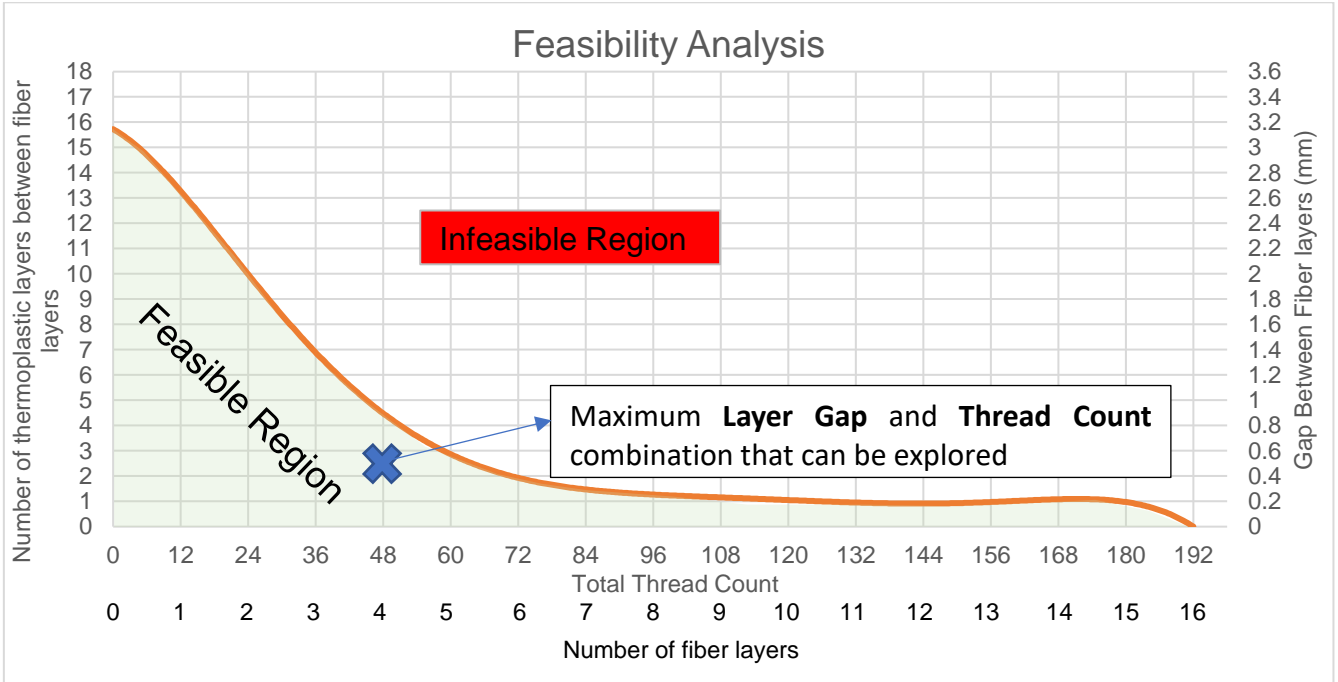


Figure 16 Feasibility Analysis

Graph above shows the feasible region based upon the design parameters, variables under consideration and system limitations. It can be deduced from this representation that with thread count beyond 48, layer gap begins to reduce. Therefore, the finalized parameters for this experimental study are shown in Table 10.

Table 10 Selected Factors & their levels

S No	Factors	Levels
1	Material	PLA ABS PLA-C PLA-Cu
2	Thread Count	12 24 36 48
3	Layer Gap	0 1 2 3

Now, if a full factorial design is made for this experimental design then a total number of trial runs become as follows,

$$\text{Trial runs} = L^k$$

$$\text{Trial runs} = 4^3$$

$$\text{Trial runs} = 64$$

Repetitions are a must for such experiments to make the data statistically viable. For only 02 repetitions the trial runs are doubled. So, a total of 128 experiments will be required to only cover tensile testing and this number will increase to 256 for two repetitions each for all possible combinations for both tensile and flexural samples. Taguchi DOE on the other hand will reduce the number of experiments drastically. In this case DOF of the system is given by,

$$DOF = 1 + (\text{No. of Factors}) * (\text{Factor levels} - 1)$$

$$DOF = 1 + (3) * (4 - 1)$$

$$DOF = 10$$

Therefore, the array selected is L₁₆ OA, DOE of the system in this case takes the shape shown in table 11. This table was generated using Minitab software.

The selection of L₁₆ OA reduced the number of experiments from total of 256, including repetitions to a total of 64 with generation of almost the same information. It was also decided to perform more trial runs for the array that generates results with a difference of more than 10% for tensile as well as flexural testing.

Table 11 Taguchi OA for Experimentation

S No	Material	Thread Count	Layer Gap
1	PLA	12	0
2	PLA	24	1
3	PLA	36	2
4	PLA	48	3
5	ABS	12	1
6	ABS	24	0
7	ABS	36	3
8	ABS	48	2
9	PLA_C	12	2
10	PLA_C	24	3
11	PLA_C	36	0
12	PLA_C	48	1
13	PLA_Cu	12	3
14	PLA_Cu	24	2
15	PLA_Cu	36	1
16	PLA_Cu	48	0

Following must be mentioned here for the handling of special conditions:

- i. Number of threads was used instead of using number of layers to accommodate settings such as 12 threads with 03 layer gap. In such instances, the number of threads was divided into 02 layers with 06 threads each and printed at the layer gap against the setting.
- ii. As already mentioned, G-code for each setting was generated using Cura. However, Cura does not afford the flexibility of printing thread (infill) at more than one places. Therefore, OA trial runs where thermoplastic had to be printed between layer of threads could not be printed by just using Cura. In such cases, initial G-code was generated using Cura and then imported in Repetier-Host software where it could be edited line by line as desired. Each code generated by Cura was over 10000 lines and a thorough understanding of each line was required to edit the code. Also, for each setting and material a different set of code was required.
- iii. Similarly, as the dimensions for each flexural and tensile sample was different, a different code was required. G-codes designed for each setting were made separately and 02 samples (both bending or both tensile) for each setting were printed in tandem. It must be noted that analysis and editing of G-code for each setting took at least an hour.
- iv. As all the settings were not tested there is a chance that the optimized setting lie outside of these experimental runs. Therefore, it may be necessary to perform confirmatory experiments on the optimized settings subsequent to analysis.
- v. Theoretical specimen design of 16 layers was carried out prior to fabricating actual specimens to confirm that the bracket under consideration could be fabricated. Table 12 shows the sample design for all layers in respect of fiber and thermoplastic, where 'K' represents Kevlar and 'P' represents thermoplastic. The table confirms that all the combinations can be easily fabricated. It may also be noted here that combination of thread count exceeding 48 (4 layers) with layer gap of 3 or above cannot be printed in the current sample design.

Volume Fraction Analysis. The final step performed before beginning actual experimentation was to ascertain that the parameters selected have a positive impact on the outcome variables (tensile and flexural strength). Barbero (2017) suggests that if addition of a fiber in a structure has no positive impact on the tensile strength of the specimen then it is below the minimum volume fraction V_{min} . Such addition will only add to cost and no improvement will be achieved. Therefore, initially pure plastic samples were printed to determine the baseline thermoplastic characteristics. Subsequently, composite samples were printed for each material category with minimum thread count (12 threads) and calculation were made for apparent fiber properties. These were then used to calculate the V_{min} values for each material and volume fractions V_f , though very low, were above the V_{min} values. Thus, this condition was met satisfactorily. Summary of

the results achieved by experiments and using formulas listed in Chapter 2 are listed in Table 13.

Similarly, maximum volume fraction achievable for tensile and flexural samples can also be computed. V_f computed in the table 13 is volume fraction achieved for a single layer, therefore, max volume fraction for the current design of specimen becomes volume fraction achieved for 14 layers of thread with 1 layer for top and bottom and wall thickness kept the same. Table 14 represents the change in volume fraction with the number of layers. Here also it is evident that the difference between the V_f for tensile samples is less but comparable to the V_f achieved for a corresponding flexural sample within the region explored. Therefore, the sample design was kept the same. However, it may be noted that the at maximum V_f achievable using the above defined process parameters has a considerable difference for corresponding tensile and flexural samples.

Table 12 Sample Design

Sample	Layer Height															
	0.2	0.4	0.6	0.8	1	1.2	1.4	1.6	1.8	2	2.2	2.4	2.6	2.8	3	3.2
12-0	P	P	P	P	P	P	P	K	P	P	P	P	P	P	P	P
24-1'	P	P	P	P	P	P	K	P	K	P	P	P	P	P	P	P
36-2'	P	P	P	P	K	P	P	K	P	P	K	P	P	P	P	P
48-3'	P	K	P	P	P	K	P	P	P	K	P	P	P	K	P	P
12-1'	P	P	P	P	P	P	K	P	K	P	P	P	P	P	P	P
24-0	P	P	P	P	P	P	P	K	K	P	P	P	P	P	P	P
36-3"	P	P	P	K	P	P	P	K	P	P	P	K	P	P	P	P
48-2'	P	P	P	K	P	P	K	P	P	K	P	P	K	P	P	P
12-2'	P	P	P	P	P	P	K	P	P	K	P	P	P	P	P	P
24-3'	P	P	P	P	P	K	P	P	P	K	P	P	P	P	P	P
36-0	P	P	P	P	P	P	K	K	K	P	P	P	P	P	P	P
48-1'	P	P	P	P	K	P	K	P	K	P	K	P	P	P	P	P
12-3'	P	P	P	P	P	K	P	P	P	K	P	P	P	P	P	P
24-2"	P	P	P	P	P	P	K	P	P	K	P	P	P	P	P	P
36-1'	P	P	P	P	P	K	P	K	P	K	P	P	P	P	P	P
48-0	P	P	P	P	P	P	K	K	K	K	P	P	P	P	P	P

Table 13 Vmin for all Materials

S No	Material	Tensile Properties							
		F_{mt}	E_m	F_{1t}	η	V_f	F_{1t}	σ_m^*	V_{min}
1	PLA	37.50	682.1601	-					
2	E PLA	-		65.99	0.882353	0.012999	3344.335	22.81372	0.004422
3	ABS	24.27	476.9205	-					
4	E ABS	-		42.15	0.882353	0.012999	2136.137	10.18768	0.006623
5	PLA-C	36.29	713.8315	-					
6	E PLA-C	-		60.31	0.882353	0.012999	3056.476	21.81809	0.004768
7	PLA-Cu	29.49	806.1426	-					
8	E PLA-Cu	-		52.3	0.882353	0.012999	2650.534	21.36708	0.003091

Table 14 Volume fractions achievable

Layers	Tows	Tensile Samples		Flexural Samples	
		η	V_f	η	V_f
1	12	0.882353	0.012999	1.052632	0.015508
2	24	1.764706	0.025998	2.105263	0.031015
3	36	2.647059	0.038997	3.157895	0.046523
4	48	3.529412	0.051996	4.210526	0.06203
5	60	4.411765	0.064995	5.263158	0.077538
6	72	5.294118	0.077994	6.315789	0.093045
7	84	6.176471	0.090993	7.368421	0.108553
8	96	7.058824	0.103992	8.421053	0.12406
9	108	7.941176	0.116991	9.473684	0.139568
10	120	8.823529	0.129989	10.52632	0.155075
11	132	9.705882	0.142988	11.57895	0.170583
12	144	10.58824	0.155987	12.63158	0.18609
13	156	11.47059	0.168986	13.68421	0.201598
14	168	12.35294	0.181985	14.73684	0.217105

Universal Testing Machine (UTM)

18. To evaluate the mechanical properties of the CFRTPCs fabricated, UTM was used for tensile testing and 3-point bending test. SHIMADZU AGS-X Series UTM was used with a 20kN load cell, figure below shows the setup. Figure 18 & 19 show reinforced thermoplastic being tested under tensile and flexural loads. The software associated with this machine is 'Trapezium' which has the capability to provide a number of different graphs, excel data sheet and a complete report for each type of test conducted.



Figure 17 SHIMADZU AGS-X UTM



Figure 18 Tensile Test using UTM

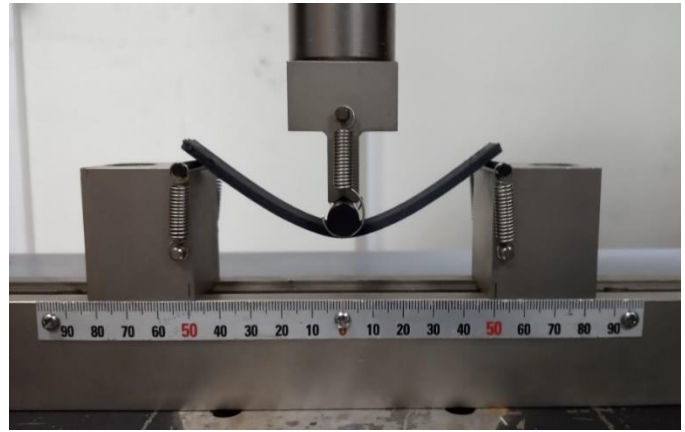


Figure 19 Flexural Test Using UTM

19. This software is quite simple in design and requires little to no experience for understanding and operating it. As output, excel data sheet, complete report and stress-strain graphs were obtained using Trapezium. It must be noted that the machine generates a single excel sheet with 30000 data points. For flexural testing, data points exceeded 100000 data points due to the low strain rate selected for this research work. Therefore, 4-5 excel sheets were generated for a single flexural test. These sheets were combined to produce a single sheet for ease of analysis and reporting. For tensile test a single excel workbook was generated by the software.

Analysis & Confirmatory Experiments

20. After completion of result compilation, following analysis were performed to draw inferences:

(a) **Signal to Noise Ratio.** S/N ratios for the experimental data was performed to identify the most suitable factor levels. Here aim was to maximize the tensile and flexural strength, therefore, larger the better S/N ratio were calculated.

(b) **Regression Analysis.** To determine the statistical significance of each factor, regression analysis of the factors has been performed. Minitab was used for this purpose, it determines the p-value of each factor by determining coefficients for factor levels one less than the total factor levels. Note that p-value is the probability that measures a value against the null hypothesis. Thus, a lower p-value represents higher significance of a factor. General practice is to select a Confidence Interval of 95% ($\alpha=0.05$), which will be used for this study. A value larger than Confidence interval here means that the value achieved for a certain factor is significant enough to explain 95% of the data. Therefore, any factor level having p value ($1 - \alpha$) less than 0.05 has significant effect on the outcome variable.

(c) **ANOVA.** Analysis of Variance (ANOVA) was performed to identify the percentage contribution of each factor and to determine the significance of each factor. For more than two factors operating at more than two level it is recommended that Two way ANOVA be performed (Roy, 1990). Here F-ratio and p-value are calculated based upon

the data variance, F-ratio is the ratio of individual variance to error variance of a system named after Sir Ronald Fisher while p-value here is the same C.I as discussed above (Ross, 1996).

(d) **Analytical Estimation using ROM.** Using ROM, tensile strength were estimated and compared with experimental results. Subsequently, comparison with experimental results has been carried out.

21. As discussed in the previous chapter, confirmatory experiments on optimized settings is a must as only a fraction of all the possible trial runs are performed in Taguchi's DOE. There is always the off chance that optimized setting is one of the trials runs already completed.

Minitab

22. Although Excel manages and manipulates data quite efficiently, it is better to use specially designed software for data analysis. Minitab is a powerful statistical software that helps in data analysis and management. Statistical software have the advantage of providing large data handling capability while conduct of analysis and graphical representation can be carried out in an efficient and cost-effective way. The main advantage of Minitab is that using this software does not require any programming skills or statistical expertise. All options are listed in drop down menus and required expertise can be gained by using Tutorials and 'Help' features integrated in the software.

23. Moreover, Design of Experiment techniques such as Taguchi, Response Surface Methodology (RSM), mixed and full factorial design can also be carried out using Minitab. This software basically provides an effective method for data input, manipulation, trends and patterns identification and then extrapolation as required. Originally designed for teaching statistical techniques, this software provides a wide range of statistical analysis tools for efficient data management, visualization, fast analysis and streamlining workflow.

24. In this experimental study, Orthogonal Array for Taguchi DOE was formed using this software. Also, Signal-to-Noise ratio and ANOVA analysis were also performed using this software. Details of the standard procedure for DOE and subsequent analysis can be easily found through internet, software 'Help' and Tutorials.

25. It must be noted that the software has certain limitations and standard procedures, these must be followed to avoid any error in results. For example, response variables are only assigned one column each. If two different response variables are added in consecutive columns and S/N ratios are calculated then Minitab assumes these two response columns to be replications of each other.

CHAPTER 4

RESULTS

Tensile Properties of Thermoplastics

1. Initially, tensile samples according to ASTM standard were fabricated to develop the baseline and provide a comparison to the achieved properties for composites. These specimens were not part of the DOE, therefore, the total experiments increased from 64 to 88. Figure 14 shows the dimensions and design of the sample generated using Pro-E®. Results of experiments are presented in Table 15. Here the value of Young's Modulus has been calculated using stress strain curves for each of the materials. Also, F_{mt} is the average tensile strength of the thermoplastic. Figure 20-23 represent stress-strain curves achieved for all the materials. Here it must be noted that the values achieved were in close relation to the values available in literature reaffirming the quality of the material used. It can be seen that the strongest out of the four materials under investigation is PLA.

Table 15 Tensile Properties of thermoplastics

S No	Material	Tensile Test					
		T1	T2	T3	T4	F_{mt}	Y
1	PLA	39	37.22	37.2	36.58	37.50	682.16
2	ABS	24.04	24.499			24.27	476.921
3	PLA-C	36.14	36.434			36.29	713.832
4	PLA-Cu	29.08	29.905			29.49	806.143

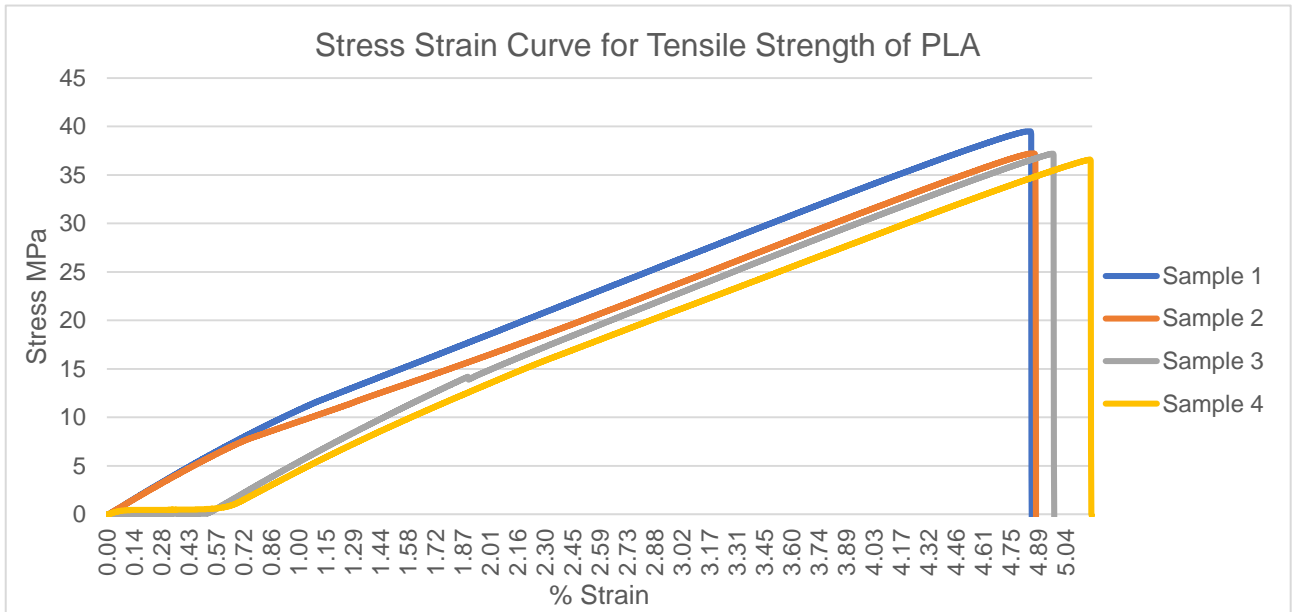


Figure 20 Combined Stress-Strain Curve for Tensile Strength of PLA

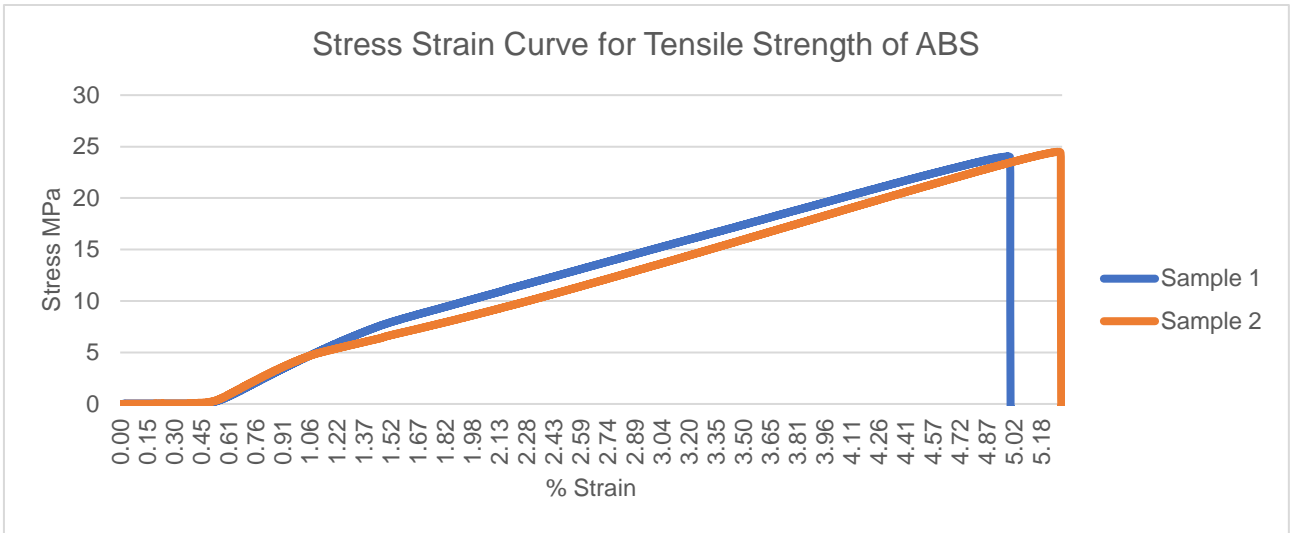


Figure 21 Combined Stress-Strain Curve for Tensile Strength of ABS

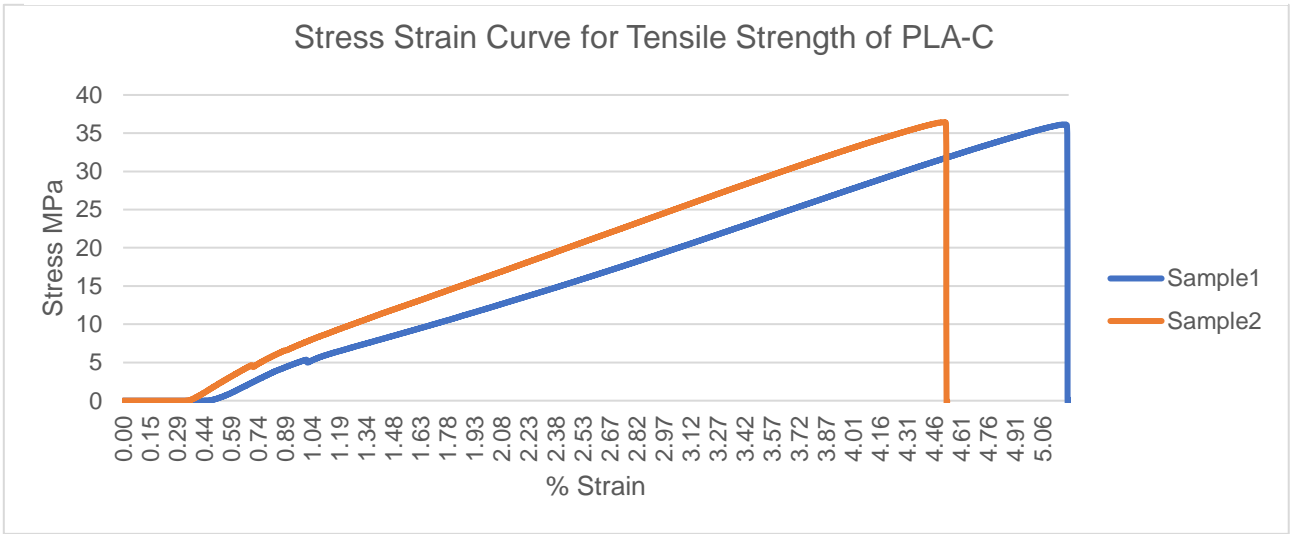


Figure 23 Combined Stress-Strain Curve for Tensile Strength of PLA-C

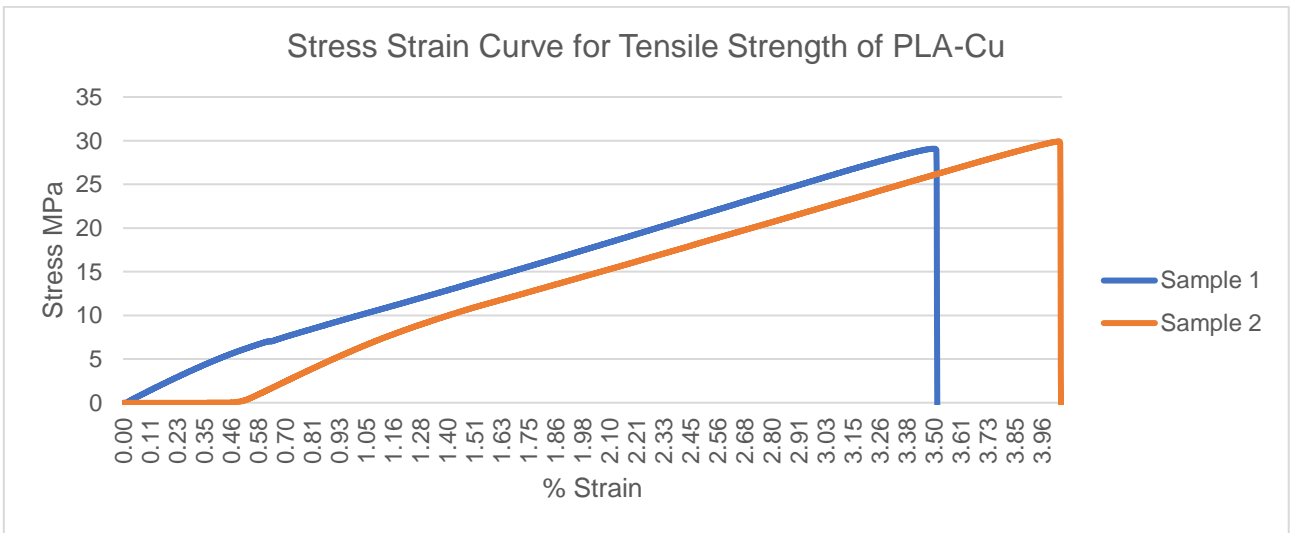


Figure 22 Combined Stress-Strain Curve for Tensile Strength of PLA-Cu

Fracture Mode

2. Brittle fracture is the type of fracture in which material shows little to no deformation before fracture. Crack propagation in this type of fracture is rapid and surface of the specimen is usually rough with a granular look. In this type of failure, the crack propagates across the specimen under tensile load, that is the axis of fracture is nearly perpendicular to the axis of tensile load. A part that has undergone a brittle failure can be placed together to get the original part with actual dimensions, this means that there is no deformation in the part at a macroscale. While in ductile failure, the part becomes elongated losing its original cross-section and length at the failure point. Brittle fracture is often termed as trans-granular failure as the fracture occurs by breaking bonds between atoms.

3. In inorganic materials, the crack initially propagates resulting in a smooth surface which is followed by instantaneous failure. This abrupt failure gives rise to a rocky/ grainy failure surface. Moreover, stress-strain curves for a brittle material have no discernable yield point. Figure 24 shows a schematic of difference between a ductile and brittle fracture.

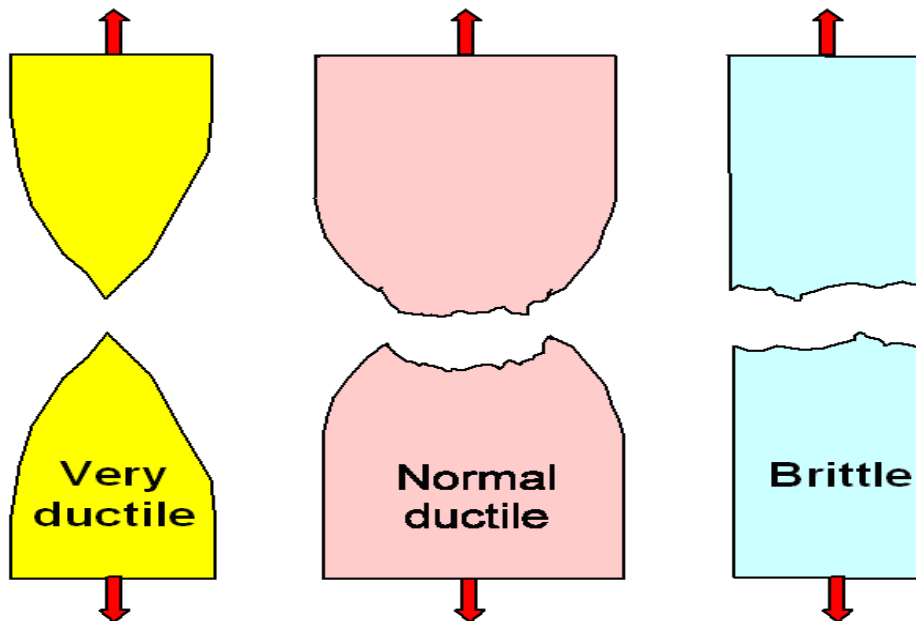


Figure 24 Fracture Types

4. Broken samples were analyzed visually for the fracture type, all the samples broke in nearly a straight line without necking. That is a manifestation of brittle fracture. This is also evident from the stress-strain graphs where no appreciable curvature is observed prior to failure. Moreover, figure 25 shows the fracture surface of a few samples. The surface has roughness with smooth patches at the edges suggesting crack propagation for a small region and instantaneous fracture for the remaining surface common in brittle materials. Therefore, it is clear that all thermoplastics used in this research work exhibit brittle behavior. The same is also supported by available literature (Beniak et al., 2015, Perez et al., 2014).

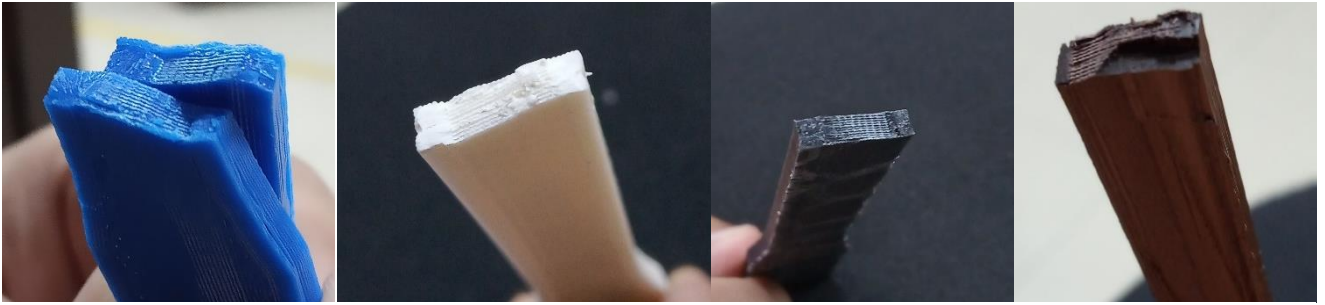


Figure 25 Fracture Surface for thermoplastic specimen

Flexural Properties of Thermoplastics

5. Subsequently, flexural specimen were fabricated for all thermoplastics and tested using 3 point bending test on UTM. The results yielded were used to calculate Ultimate Flexural Strength and Flexural Modulus for each material. Table 16 and Figure 26-29 shows graphical data obtained from bending tests. Here also the flexural modulus was calculated using the stress strain curves for each sample and then taking average for each material. Results show that the addition of Copper to PLA yields the highest flexural properties. As flexural modulus is inversely related to deflection of a material, therefore, higher flexural modulus means a higher capacity to bear load. It is evident by the experimental results that addition of copper to PLA improves material stiffness.

Table 16 Flexural Properties for Thermoplastics

S No	Material	3 Point Bend Test			
		B1	B2	Avg	E
1	PLA	78.2669	78.49	78.3762	3214.36
2	ABS	64.2684	61.63	62.9502	2630.64
3	PLA-C	82.5689	81.92	82.2429	3907.44
4	PLA-Cu	90.1771	89.57	89.8726	4763.67

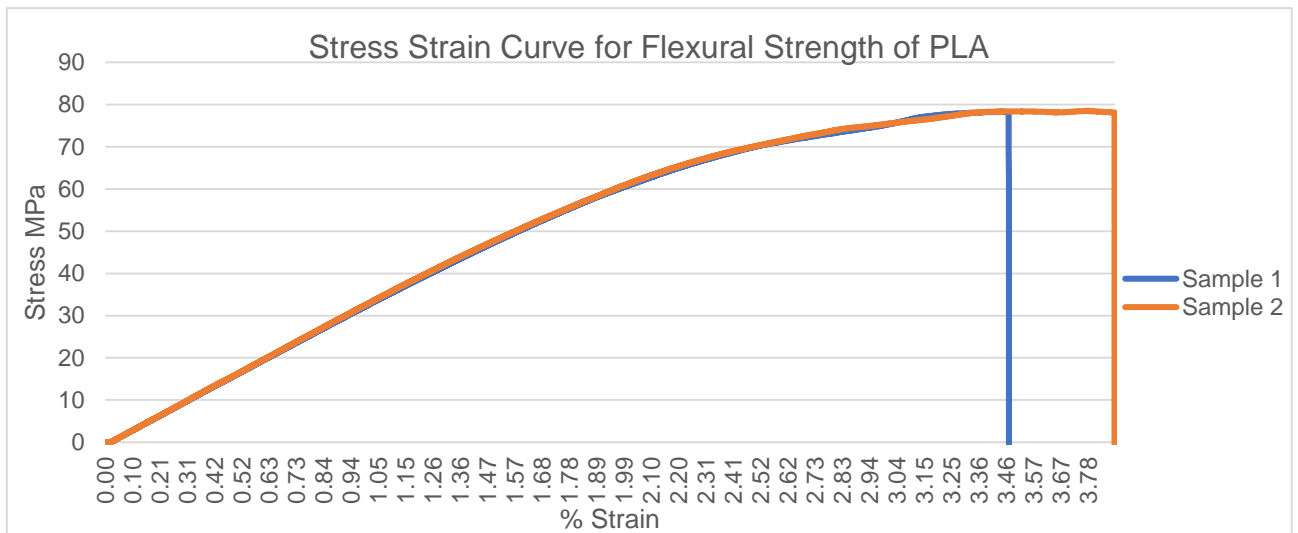


Figure 26 Combined Stress-Strain Curve for Flexural Strength of PLA

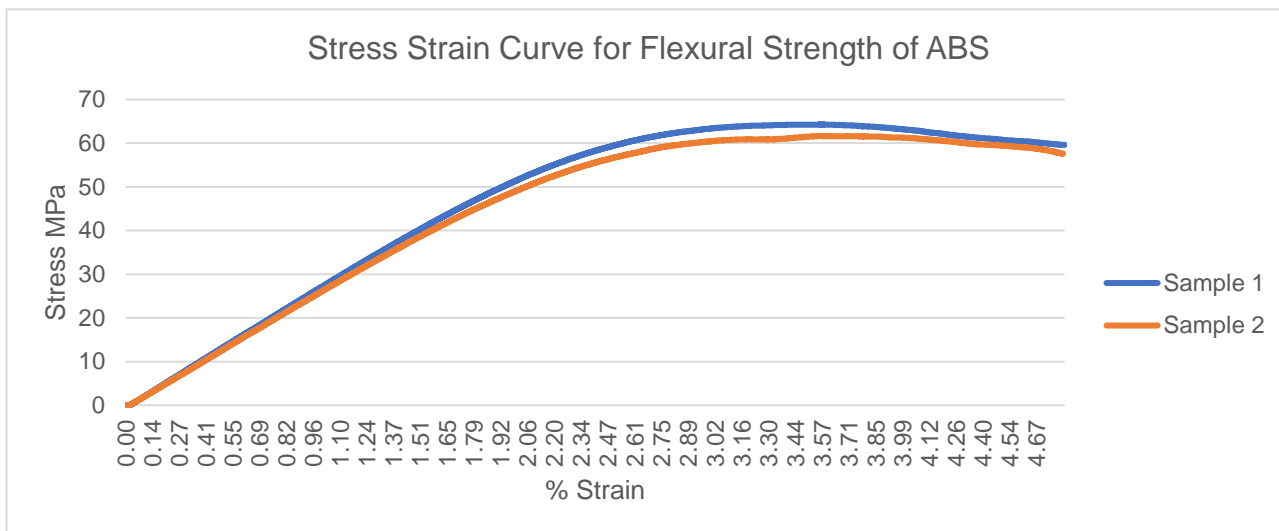


Figure 29 Combined Stress-Strain Curve for Flexural Strength of ABS

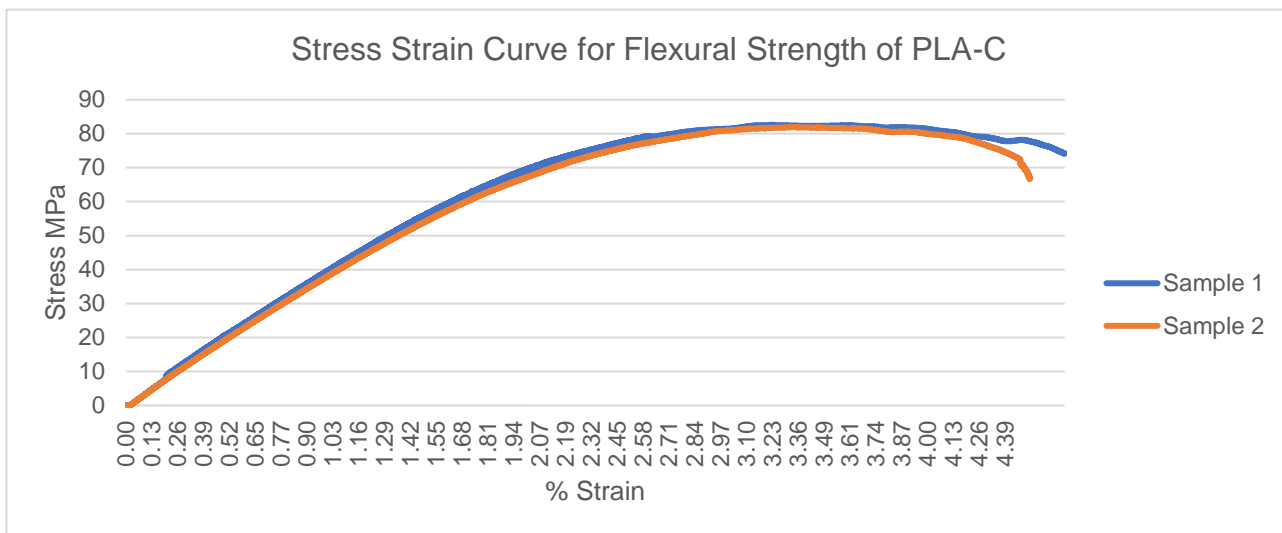


Figure 27 Combined Stress-Strain Curve for Flexural Strength of PLA-C

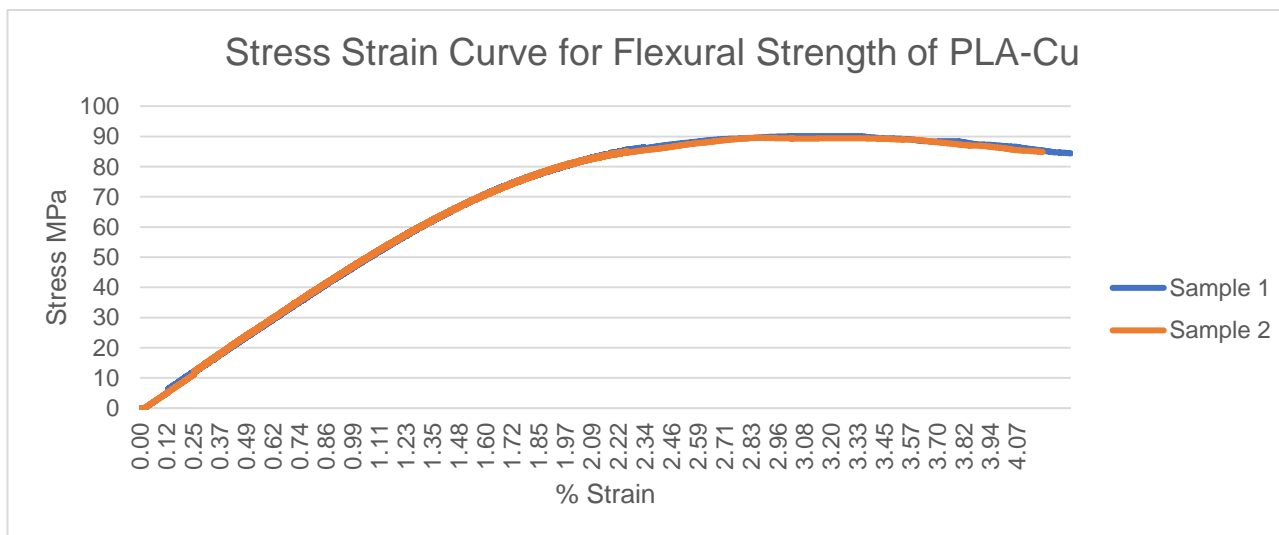


Figure 28 Combined Stress-Strain Curve for Flexural Strength of PLA-Cu

Calculation for Volume Fraction

6. The process developed for fabricating CFRTPCs in this research offers the flexibility to control volume fraction as desired. Figure 16 shows the region that could be explored under the given process parameters. Therefore, thread count up to 04 layers that correspond to 48 threads was explored. Figure 30 & 31 shows thread distribution for a single layer for both tensile specimen and a flexural specimen with dimensions, respectively.

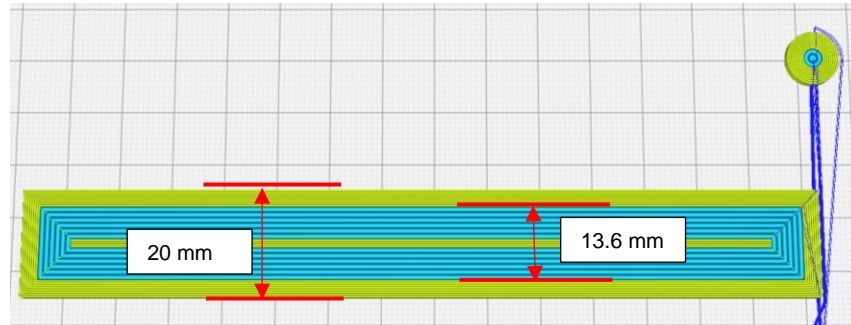


Figure 30 Tensile Specimen with Thread Distribution

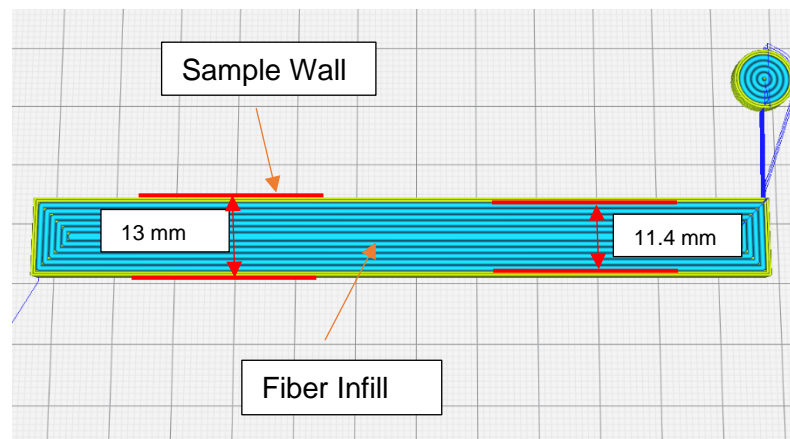


Figure 31 Flexural Specimen with Thread Distribution

7. Using the above shown dimensions and equations already described in Chapter 2, volume fractions for each case of tensile and flexural specimen were estimated. Table 17 summarizes these calculations for the complete Orthogonal Array selected for this research. It is evident even from the figures that thread concentration for flexural specimen is higher than for tensile specimen, however, the difference is negligibly small. Therefore, no changes were made in specimen design to cater for the difference.

Mechanical Properties for the Kevlar Reinforced Thermoplastics

8. Subsequent to completion of thermoplastic results, G-codes for all the settings according to the selected OA were generated. Then samples were printed at random as suggested by literature. Time required for printing the samples directly depended upon size of the sample and number of threads to be printed. A sample with 12 threads took around one hour and thirty minutes to print while a sample with 48 threads took over three hours of printing. Therefore, it took over six weeks to just print these samples.

Table 17 Results for Volume Fraction

S No	Material	Count	Gap	Tensile Specimen			Flexural Specimen		
				η	V_f	% V_f	η	V_f	% V_f
1	PLA	12	0	0.88	0.0129989	1.30	1.05	0.0155075	1.55
2	PLA	24	1	1.76	0.0259979	2.60	2.11	0.031015	3.10
3	PLA	36	2	2.65	0.0389968	3.90	3.16	0.0465226	4.65
4	PLA	48	3	3.53	0.0519958	5.20	4.21	0.0620301	6.20
5	ABS	12	1	0.88	0.0129989	1.30	1.05	0.0155075	1.55
6	ABS	24	0	1.76	0.0259979	2.60	2.11	0.031015	3.10
7	ABS	36	3	2.65	0.0389968	3.90	3.16	0.0465226	4.65
8	ABS	48	2	3.53	0.0519958	5.20	4.21	0.0620301	6.20
9	PLA-C	12	2	0.88	0.0129989	1.30	1.05	0.0155075	1.55
10	PLA-C	24	3	1.76	0.0259979	2.60	2.11	0.031015	3.10
11	PLA-C	36	0	2.65	0.0389968	3.90	3.16	0.0465226	4.65
12	PLA-C	48	1	3.53	0.0519958	5.20	4.21	0.0620301	6.20
13	PLA-Cu	12	3	0.88	0.0129989	1.30	1.05	0.0155075	1.55
14	PLA-Cu	24	2	1.76	0.0259979	2.60	2.11	0.031015	3.10
15	PLA-Cu	36	1	2.65	0.0389968	3.90	3.16	0.0465226	4.65
16	PLA-Cu	48	0	3.53	0.0519958	5.20	4.21	0.0620301	6.20

9. Due to limited availability of UTM, testing of samples was carried out once a week, hence, the samples had to be stored. To avoid any environmental effects on the fabricated samples, they were kept in Ziplock bags with silica gel bags. Sample fabrication was managed in a way that all the samples fabricated were tested in the same week.

10. It was ensured that the sample fabrication is kept random. Printing of Flexural and Tensile samples of the same setting was also randomized. However, due to sparsity of time two samples were fabricated in a single go i.e. tensile & flexural samples of the same trial run were printed together. This reduced the material change and setup time for each setting. Figure 32 shows a schematic of two tensile samples on the print bed.

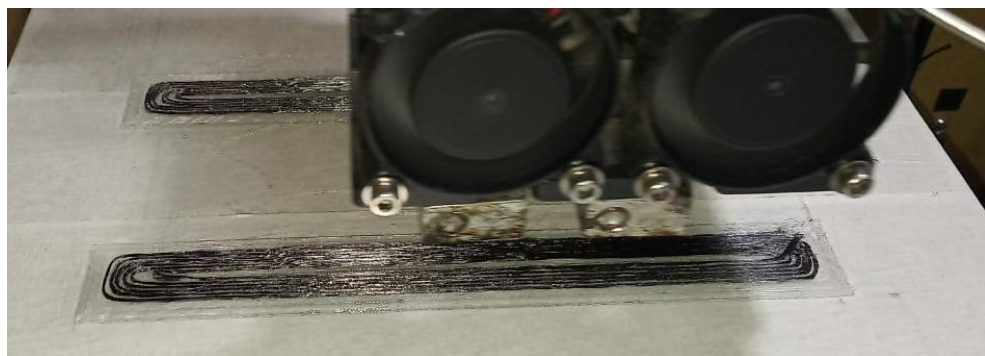


Figure 32 Schematic of in tandem printing of tensile samples

Tensile Properties for the L₁₆ OA

11. Table 18 provides the summary of the results while figure 33-36 shows the combined graphical representation of results at each setting for Tensile Testing. Graphically, results have

been segregated based upon the materials. The trend here shows that the effect of inducing a gap between the thread layer is very less, if any, compared to the effect of number of thread layers.

12. Here error bars have also been displayed to show the difference of strengths obtained from different samples. Larger error bars prompted fabrication of more samples and hence, for larger error more than 02 samples have been tested to achieve a good data convergence.

Table 18 Summary of results for Tensile Testing of Composites

S No	Material	Count	Gap	Tensile Strength				
				T1	T2	T3	T4	Avg
1	PLA	12	0	63.746	59.93	70.93	69.34	65.99
2	PLA	24	1	85.853	79.31			82.58
3	PLA	36	2	87.952	93.19			90.57
4	PLA	48	3	109.51	95.01	116	99.4	104.97
5	ABS	12	1	41.857	42.44			42.15
6	ABS	24	0	57.805	60.98			59.39
7	ABS	36	3	67.676	72.08			69.88
8	ABS	48	2	88.639	84.02			86.33
9	PLA-C	12	2	61.256	59.37			60.31
10	PLA-C	24	3	71.492	73.99			72.74
11	PLA-C	36	0	82.894	84.3			83.60
12	PLA-C	48	1	92.998	95.93			94.46
13	PLA-Cu	12	3	52.458	52.13			52.30
14	PLA-Cu	24	2	55.396	58.31			56.85
15	PLA-Cu	36	1	72.287	68.13			70.21
16	PLA-Cu	48	0	101.42	96.64	77.04	86.33	90.36

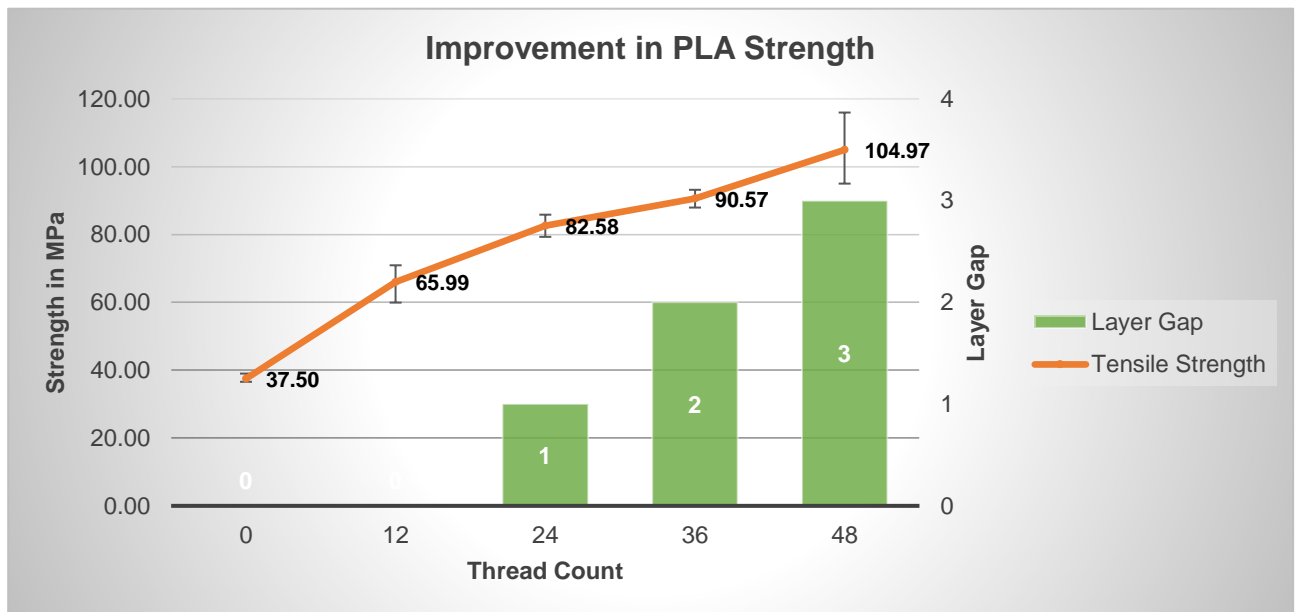


Figure 33 Combined Results for Tensile Testing of PLA Composite

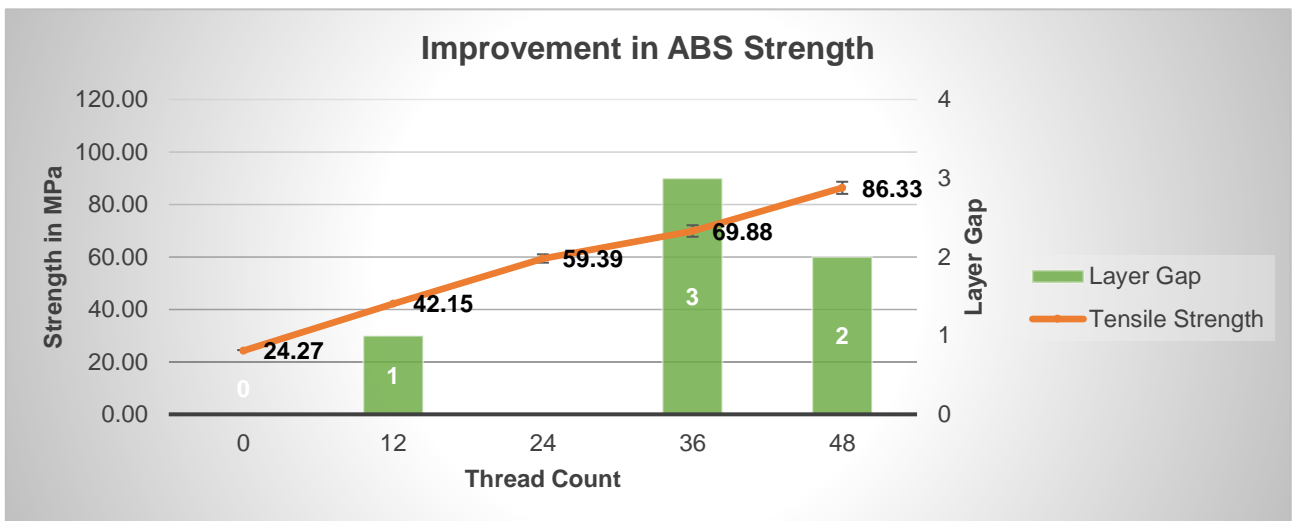


Figure 34 Combined Results for Tensile Strength of ABS Composites

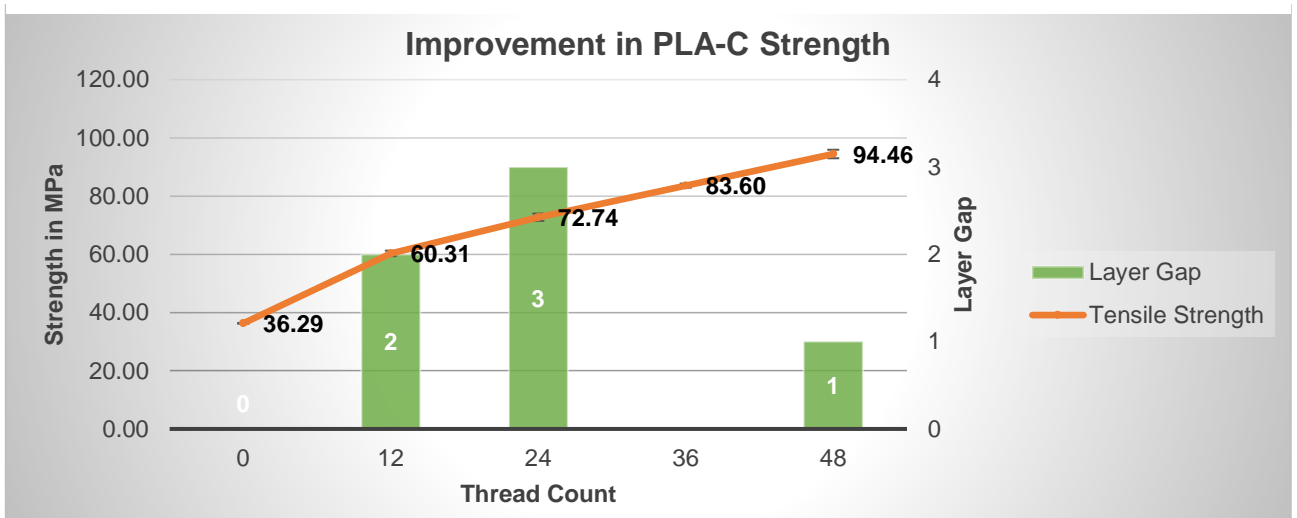


Figure 35 Combined Results for Tensile Testing of PLA-C Composite

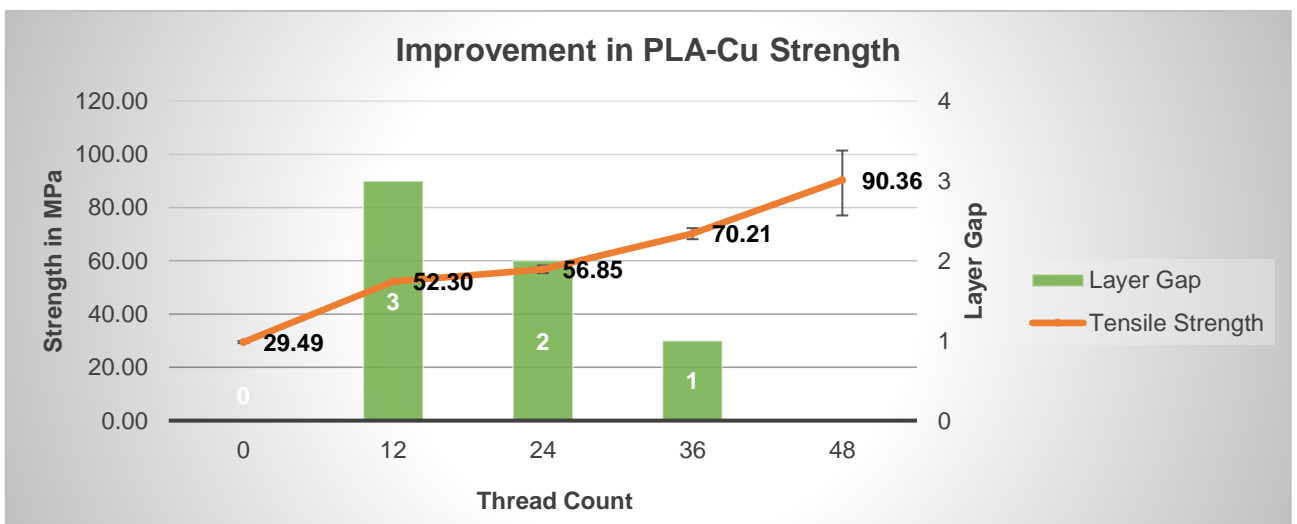


Figure 36 Combined Results for Tensile Testing of PLA-Cu Composites

13. Samples having a difference in the outcome over 10% have been repeated to achieve a better data rationality. While as the strength has improved drastically from the baseline values, it also corroborates the hypothesis that the Volume fraction of fiber, V_f , is above the minimum value, V_{min} . Similar to the above comparison, Stress Strain Curves for individual materials at each trial run have also been made and available in attached excel workbooks. From those curves, young's modulus have been calculated presented in Table 19 for each sample.

Table 19 Tensile Modulus for Complete OA

S No	Material	Count	Gap	Tensile Modulus Calculation				
				Y1	Y2	Y3	Y4	Avg
1	PLA	12	0	591.253	504.672	677.49	647.169	605.15
2	PLA	24	1	645.38	699.536			672.46
3	PLA	36	2	673.656	732.306			702.98
4	PLA	48	3	720.657	620.803	788.636	756.438	721.63
5	ABS	12	1	388.98	350.423			369.70
6	ABS	24	0	464.598	436.529			450.56
7	ABS	36	3	551.487	557.481			554.48
8	ABS	48	2	613.587	555.984			584.79
9	PLA-C	12	2	734.778	690.119			712.45
10	PLA-C	24	3	815.682	794.98			805.33
11	PLA-C	36	0	804.343	846.627			825.48
12	PLA-C	48	1	977.943	857.696			917.82
13	PLA-Cu	12	3	678.522	653.427			665.97
14	PLA-Cu	24	2	620.412	919.231			769.82
15	PLA-Cu	36	1	740.948	668.049			704.50
16	PLA-Cu	48	0	906.726	715.509	556.442	610.785	697.37

Signal-to-Noise Ratio Using Minitab

14. Data presented in Table 18 was input into Minitab software, to calculate S/N ratio with the type being larger the better. Minitab can only take equal number of replicates for all trials to estimate SN ratio, therefore, trial runs with more than 02 replicates were reduced to 02 by taking average and input into the software. The results obtained are presented in Table 20 while the main effects plot is presented in figure 37.

15. Here the columns labeled 'UTS-1' & 'UTS-2' are the experimentally measured values of tensile strength. 'SNRA1' is the standard notation used by Minitab to denote Signal to Noise ratio, 'STDE1' represents standard deviation of the replicates and 'MEAN1' is the mean value of the replicates of a trial run. As the aim was to maximize tensile strength, largest Signal to Noise ratio is the desired outcome. For the OA used, S No 4 of the table represents the highest achieved S/N ratio.

Table 20 Calculated SN Ratio for Tensile Strength using Minitab

S No	Material	Thread Count	Layer Gap	UTS-1	UTS-2	SNRA1	STDE1	MEAN1
1	PLA	12	0	66.544	65.429	36.3882	0.78888	65.987
2	PLA	24	1	85.853	79.314	38.3174	4.62393	82.583
3	PLA	36	2	87.952	93.188	39.1288	3.70225	90.570
4	PLA	48	3	104.456	105.487	40.4211	0.72952	104.972
5	ABS	12	1	41.857	42.441	32.4951	0.41279	42.149
6	ABS	24	0	57.805	60.982	35.4654	2.24632	59.393
7	ABS	36	3	67.676	72.076	36.8736	3.11107	69.876
8	ABS	48	2	88.639	84.016	38.7136	3.26891	86.327
9	PLA-C	12	2	61.256	59.371	35.6052	1.33275	60.314
10	PLA-C	24	3	71.492	73.993	37.2319	1.76838	72.742
11	PLA-C	36	0	82.894	84.305	38.4431	0.99751	83.599
12	PLA-C	48	1	92.998	95.929	39.5022	2.07267	94.464
13	PLA-Cu	12	3	52.458	52.133	34.3692	0.22939	52.296
14	PLA-Cu	24	2	55.396	58.306	35.0862	2.05779	56.851
15	PLA-Cu	36	1	72.287	68.134	36.9166	2.93647	70.210
16	PLA-Cu	48	0	89.230	91.484	39.1172	1.59378	90.357

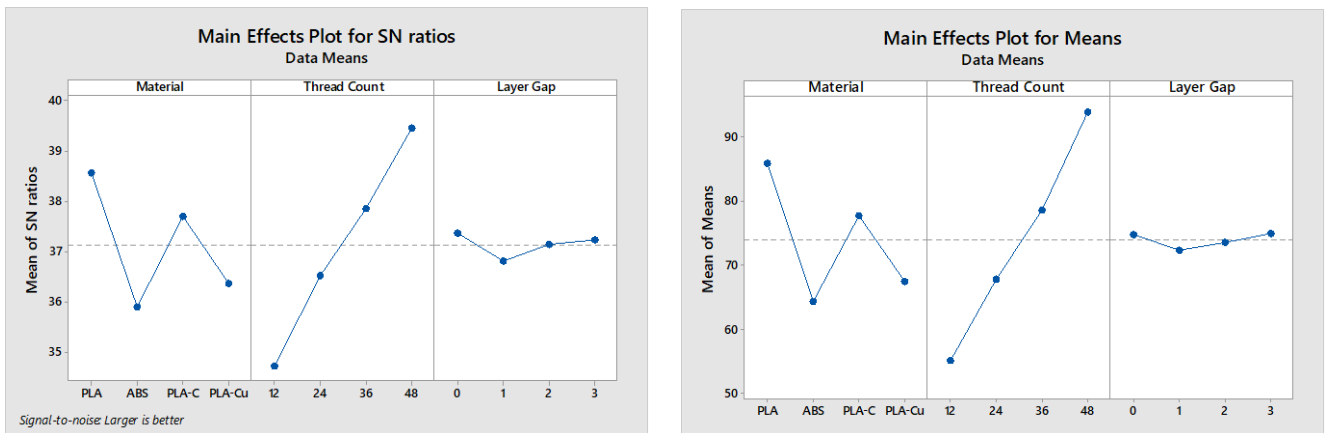


Figure 37 Main Effect plot for Tensile Strength using Minitab

16. Main effect plots shown in figure 37 are only for Tensile strength of complete OA. It is clear from these plots that layer gap, induced to improve bonding between fiber and matrix, has little to no effect on the strength of the part while thread count has a directly proportional effect on maximizing strength. Response table summary presented in table 21 also shows that out of the variables considered for this study, layer gap has the least effect. Here it must also be noted that these tables show factor levels in coded units and the ranking of the factors is interpreted as the effect of each factor on the desired outcome. This ranking is based on the difference generated in SN ratio / mean for each level of a factor. Thus, factor with largest Delta has the highest impact on the outcome and it is Ranked first.

17. For each response that is generated using Minitab, a regression coefficient table is also generated. As already described in the previous chapter, Minitab calculates these coefficients for factor levels one less than the total factor levels. Table 22 provides the summary of this estimated regression model. Here last column represents the significance levels of each factor. The p-value also corroborates that layer gap plays an insignificant role in improving tensile strength of parts. This test is necessary to reduce the experimentation and modeling to only significant parameters. Here the parameters in the last row indicate the fitness of the model as a whole, that how much data can be predicted accurately using this model.

Table 21 Response Tables for Tensile Strength using Minitab

Level	Response Table for Means			Response Table for Signal to Noise Ratios Larger is better		
	Material	Thread Count	Layer Gap	Material	Thread Count	Layer Gap
1	86.03	55.19	74.83	38.56	34.71	37.35
2	64.44	67.89	72.35	35.89	36.53	36.81
3	77.78	78.56	73.52	37.70	37.84	37.13
4	67.43	94.03	74.97	36.37	39.44	37.22
Delta	21.59	38.84	2.62	2.68	4.72	0.55
Rank	2	1	3	2	1	3

Table 22 Estimated Regression model co-efficient for SN ratio of Tensile Strength

Term	Co-eff	SE Co-eff	T	p
Constant	37.1297	0.1556	238.678	0.000
Material PLA	1.4342	0.2694	5.323	0.002
Material ABS	-1.2427	0.2694	-4.612	0.004
Material PLA-C	0.5659	0.2694	2.100	0.080
Thread C 12	-2.4153	0.2694	-8.964	0.000
Thread C 24	-0.6045	0.2694	-2.243	0.066
Thread C 36	0.7109	0.2694	2.638	0.039
Layer Ga 0	0.2238	0.2694	0.831	0.438
Layer Ga 1	-0.3218	0.2694	-1.194	0.277
Layer Ga 2	0.0038	0.2694	0.014	0.989
S = 0.6223 R-Sq = 96.6% R-Sq(adj) = 91.6%				

18. Subsequently, ANOVA on these SN ratios has also been carried out and the results are summarized in Table 23. This tables also validates the finding that the layer gap in case of tensile strength is statistically insignificant.

Table 23 ANOVA for SN ratios of Tensile Strength

Source	DF	Seq SS	Adj SS	Adj MS	F	p
Material	3	17.9807	17.9807	5.9936	15.48	0.003
Thread Count	3	48.1401	48.1401	16.0467	41.44	0.000
Layer Gap	3	0.6503	0.6503	0.2168	0.56	0.661
Residual Error	6	2.3232	2.3232	0.3872		
Total	15	69.0943				

Predicted SN Ratios for Full Factorial Design

19. In table 20, SN ratios have been calculated for the OA. Using equations delineated in chapter 2, SN ratios for the optimum level can also be calculated by using the main effects plot as reference for determining the optimum factor levels. It must be noted that this is an estimate for the system performance at optimum. Minitab has further extended this by making it possible to predict the most probable SN ratio at all the possible factor combination according to Full Factorial design. Table 24 shows the remaining factorial design runs, that were not tested in Taguchi DOE, and calculations made using Minitab software for SN ratio, expected mean and standard Deviation calculations.

20. Here 'PSNRA' represents the predicted SN ratio, 'PMEAN' represents the expected mean value of tensile strength and 'PSTDE' represents the range over which it varies. As the

aim of this study was to maximize Tensile Strength, therefore, S No 3 of the table below is the target factor levels. This result is also validated from the main effects plot from figure 37.

Table 24 Predicted SN ratio for full factorial design of Tensile Strength using Minitab

S No	Material	Thread Count	Layer Gap	PSNRA	PMEAN	PSTDE
1	PLA	24	0	38.18323	80.91802	2.55782
2	PLA	36	0	39.49855	91.58951	2.570543
3	PLA	48	0	41.09654	107.0556	1.799939
4	PLA	12	1	35.82676	65.72949	1.679514
5	PLA	36	1	38.9529	89.10709	3.675385
6	PLA	48	1	40.55088	104.5731	2.904781
7	PLA	12	2	36.15236	66.8932	1.758473
8	PLA	24	2	37.96317	79.59932	3.741621
9	PLA	48	2	40.87648	105.7369	2.98374
10	PLA	12	3	36.24288	68.34914	0.627636
11	PLA	24	3	38.05369	81.05525	2.610784
12	PLA	36	3	39.36901	91.72674	2.623507
13	ABS	12	0	33.69549	46.62044	0.373302
14	ABS	36	0	36.82162	69.99804	2.369173
15	ABS	48	0	38.41961	85.4641	1.59857
16	ABS	24	1	34.96065	56.84413	3.461292
17	ABS	36	1	36.27597	67.51562	3.474015
18	ABS	48	1	37.87396	82.98168	2.703412
19	ABS	12	2	33.47543	45.30173	1.557103
20	ABS	24	2	35.28625	58.00785	3.540251
21	ABS	36	2	36.60156	68.67933	3.552974
22	ABS	12	3	33.56595	46.75767	0.426266
23	ABS	24	3	35.37676	59.46378	2.409414
24	ABS	48	3	38.29007	85.60133	1.651534
25	PLA-C	12	0	35.50413	59.96394	-0.34365
26	PLA-C	24	0	37.31495	72.67005	1.639502
27	PLA-C	48	0	40.22825	98.8076	0.881622
28	PLA-C	12	1	34.95848	57.48152	0.761196
29	PLA-C	24	1	36.76929	70.18763	2.744344
30	PLA-C	36	1	38.08461	80.85912	2.757067
31	PLA-C	24	2	37.09489	71.35135	2.823303
32	PLA-C	36	2	38.41021	82.02283	2.836026
33	PLA-C	48	2	40.00819	97.4889	2.065423
34	PLA-C	12	3	35.37459	60.10117	-0.29068
35	PLA-C	36	3	38.50073	83.47877	1.705189
36	PLA-C	48	3	40.09871	98.94483	0.934586
37	PLA-Cu	12	0	34.18085	49.61258	-0.18212
38	PLA-Cu	24	0	35.99166	62.31869	1.801032

S No	Material	Thread Count	Layer Gap	PSNRA	PMEAN	PSTDE
39	PLA-Cu	36	0	37.30698	72.99017	1.813755
40	PLA-Cu	12	1	33.63519	47.13015	0.922726
41	PLA-Cu	24	1	35.44601	59.83627	2.905874
42	PLA-Cu	48	1	38.35932	85.97382	2.147993
43	PLA-Cu	12	2	33.96079	48.29387	1.001685
44	PLA-Cu	36	2	37.08692	71.67147	2.997556
45	PLA-Cu	48	2	38.68491	87.13753	2.226952
46	PLA-Cu	24	3	35.86212	62.45592	1.853996
47	PLA-Cu	36	3	37.17744	73.1274	1.866719
48	PLA-Cu	48	3	38.77543	88.59347	1.096115

Flexural Properties for the L₁₆ OA

21. On similar grounds, calculations for flexural testing were made. Table 25 represents the data of flexural strengths achieved for the complete OA using 3 point bending test. Similarly, Figure 38-41 graphically compares the baseline strength to progressive improvement in strength with Layer Gap and amount of thread. Graphs have been segregated on the basis of materials. Error bars have also been shown, while it may be noted here that in all the cases that the error exceeds 10%, more than 02 samples are fabricated and tested.

22. In comparison to the trend for Tensile testing, flexural strength did not follow the same trend of improvement with higher number of threads. In this case however, Layer gap induced more effect than Tensile specimen. Here it must also be noted that each flexural specimen testing took over 20 mins due to lower displacement rate. However, the rate was not changed to keep the data consistent.

Table 25 Results for Flexural Testing of complete OA

S No	Material	Count	Gap	Flexural Strength				
				B1	B2	B3	B4	Avg
1	PLA	12	0	87.761	87.9			87.83
2	PLA	24	1	97.246	97.95			97.60
3	PLA	36	2	109.37	99.81			104.59
4	PLA	48	3	131.9	123.8			127.85
5	ABS	12	1	66.002	62.82			64.41
6	ABS	24	0	75.348	72.57			73.96
7	ABS	36	3	118.9	115.6	75.41	83.08	98.26
8	ABS	48	2	88.114	111.3	76.21	80.84	89.13
9	PLA-C	12	2	70.315	70.88			70.60
10	PLA-C	24	3	79.313	80.39			79.85
11	PLA-C	36	0	101.34	98.47			99.91
12	PLA-C	48	1	107.73	108.3			107.99
13	PLA-Cu	12	3	89.812	84.68			87.25
14	PLA-Cu	24	2	95.253	92.95			94.10
15	PLA-Cu	36	1	88.132	86.59			87.36
16	PLA-Cu	48	0	94.128	88.44			91.28

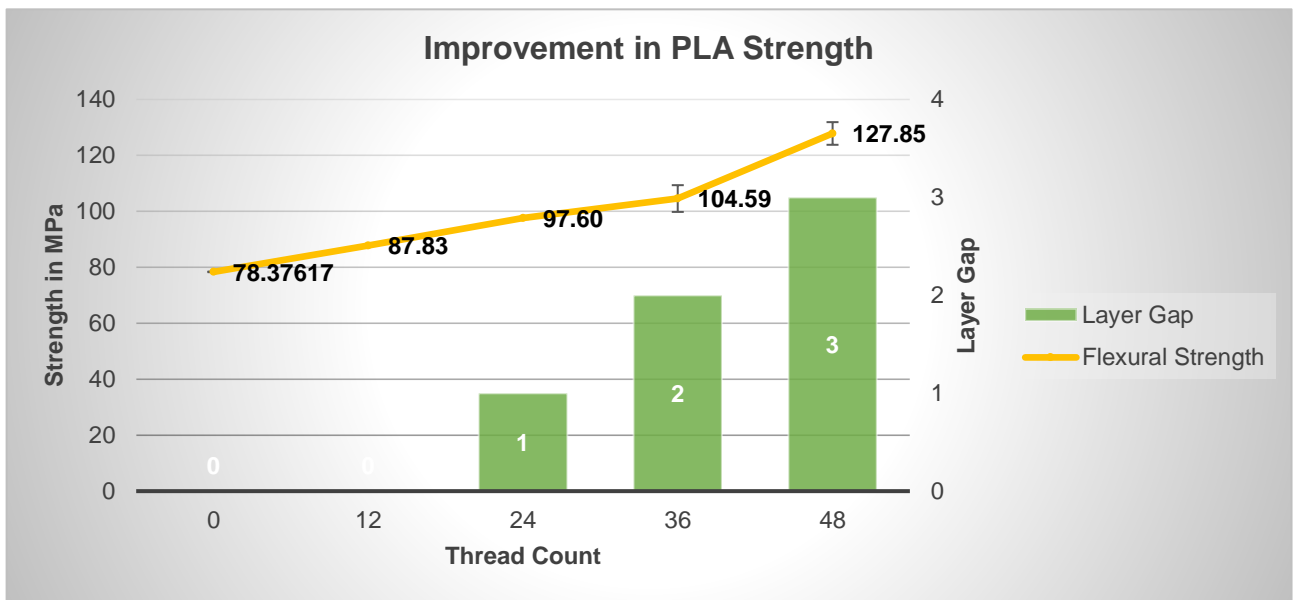


Figure 40 Combined Results for Flexural Strength of PLA Composites

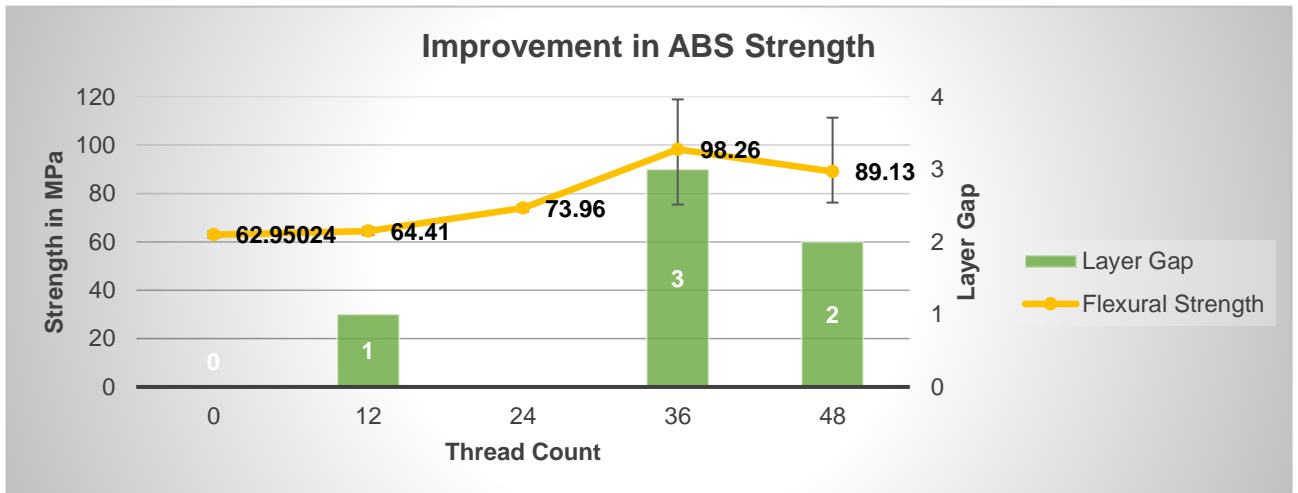


Figure 38 Combined Results for Flexural Strength of ABS Composites

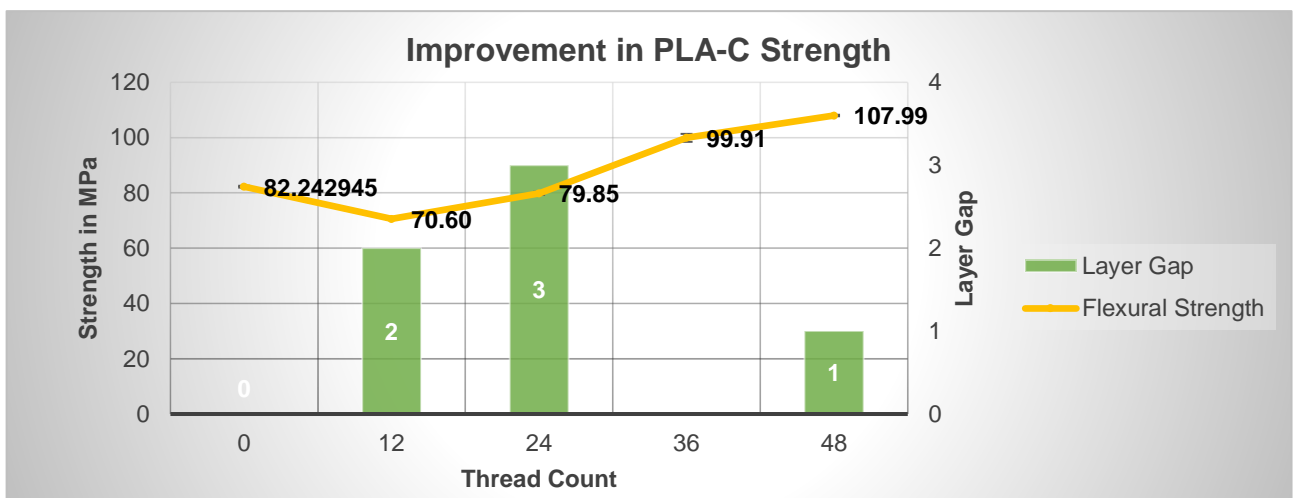


Figure 39 Combined Results for Flexural Strength of PLA-C Composites

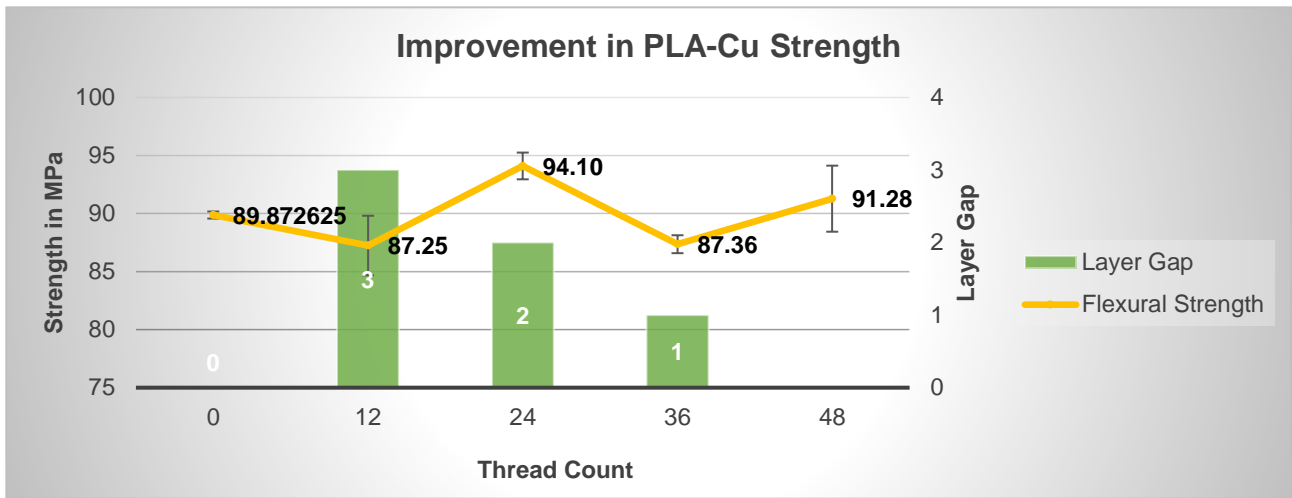


Figure 41 Combined Results for Flexural Strength of PLA-Cu Composites

23. Stress-strain curves for the complete OA were also constructed using data acquired from the UTM. These curves have been used to calculate the modulus at each trial run of OA. Significant improvement was observed in load bearing capacity of the samples. Table 26 shows the details of the Modulus estimated using the stress strain curves for flexural testing. Even though improvement in the flexural strength was less, the improvement in flexural modulus was significant.

Table 26 Flexural Modulus for Complete Array

S No	Material	Count	Gap	Flexural Modulus Calculation				
				E1	E2	E3	E4	Avg
1	PLA	12	0	4009.59	3779.96			3894.77
2	PLA	24	1	4607.41	4403.41			4505.41
3	PLA	36	2	4848.7	4541.15			4694.93
4	PLA	48	3	4870.8	4726.03			4798.41
5	ABS	12	1	3568.6	3276.88			3422.74
6	ABS	24	0	3894.26	3748.43			3821.34
7	ABS	36	3	5417.96	5184.81	3052.6	2900.89	4139.07
8	ABS	48	2	4059.13	4785.73	3503.83	3701.71	4012.60
9	PLA-C	12	2	3829.16	3839.37			3834.26
10	PLA-C	24	3	4354.75	4452.7			4403.73
11	PLA-C	36	0	5464.57	5402.28			5433.42
12	PLA-C	48	1	5630.56	5559.04			5594.80
13	PLA-Cu	12	3	4694.01	4475.08			4584.54
14	PLA-Cu	24	2	4891.11	5029.75			4960.43
15	PLA-Cu	36	1	4958.62	4834.49			4896.56
16	PLA-Cu	48	0	5303.62	4834.87			5069.24

Signal to Noise Ratio Using Minitab

24. Experimentally collected data shown in Table 25 was input into Minitab for determination of S/N ratio in a similar manner to the method adopted for Tensile strength. Trial runs having more than 02 replicates were reduced to 02 replicates by taking averages, similar to the case of Tensile Strength. Columns marked 'FS-1' & 'FS-2' represent the experimental results for flexural strength.

25. Results obtained for SN ratio show that in this case, addition of layer gap has an impact on maximizing the flexural strength. This is evident from the main effect graphs shown in Figure 42. This may be because the most common defect causing loss of flexural strength is formation of voids. Introduction of thermoplastic layers between layers of fiber inhibits the formation of these discontinuities. Hence, layer gap may have a stronger effect on flexural strength than on tensile strength. For the OA used, S No 4 in the table below shows highest S/N ratio.

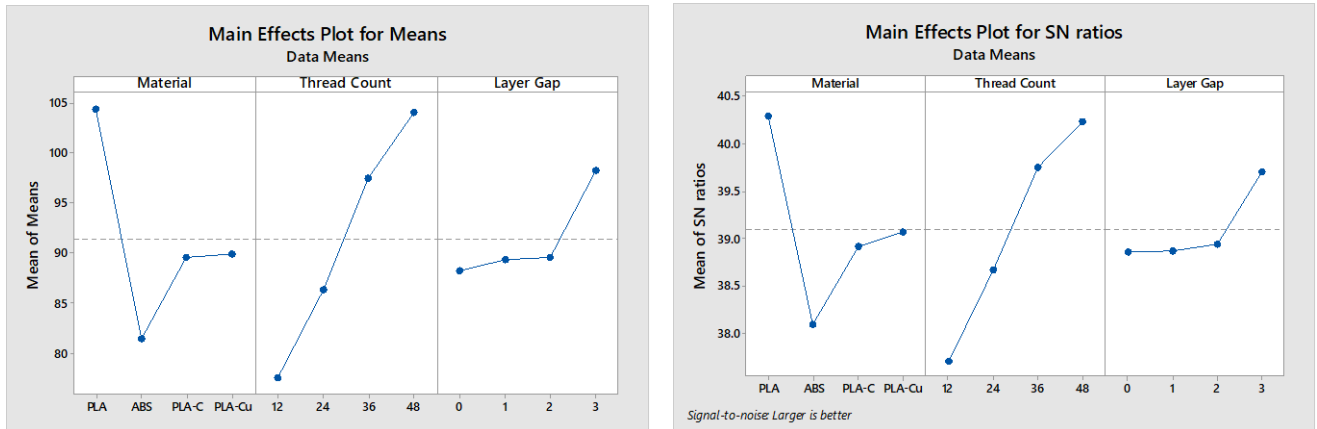


Figure 42 Main Effects plot for Flexural Strength using Minitab

Table 27 Summary of SN ratio results for Flexural Strength using Minitab

S No	Material	Thread Count	Layer Gap	FS-1	FS-2	SNRA1	STDE1	MEAN1
1	PLA	12	0	87.761	87.897	38.8728	0.09624	87.829
2	PLA	24	1	97.246	97.948	39.7886	0.49643	97.597
3	PLA	36	2	109.373	99.813	40.3628	6.76022	104.593
4	PLA	48	3	131.900	123.798	42.1209	5.72933	127.849
5	ABS	12	1	66.002	62.818	36.1711	2.25171	64.410
6	ABS	24	0	75.348	72.568	37.3751	1.96550	73.958
7	ABS	36	3	97.155	99.340	39.8448	1.54503	98.248
8	ABS	48	2	84.477	93.755	38.9638	6.56054	89.116
9	PLA-C	12	2	70.315	70.881	36.9756	0.40019	70.598
10	PLA-C	24	3	79.313	80.387	38.0449	0.75986	79.850
11	PLA-C	36	0	101.342	98.473	39.9893	2.02881	99.908
12	PLA-C	48	1	107.725	108.259	40.6678	0.37738	107.992
13	PLA-Cu	12	3	89.812	84.679	38.8036	3.62959	87.245
14	PLA-Cu	24	2	95.253	92.950	39.4700	1.62864	94.101
15	PLA-Cu	36	1	88.132	86.588	38.8252	1.09167	87.360
16	PLA-Cu	48	0	94.128	88.436	39.1951	4.02472	91.282

26. Response tables for SN ratio and means have been summarized in Table 28. Analysis shows that factor of layer gap induces the least of impact on maximizing the outcome variable. However, in case of flexural specimen the impact of layer gap is more significant than in case of tensile specimen. As layer gap causes the smallest change in the value of mean / SN ratio with change in its levels, it is ranked the last. In resemblance to response table for Tensile strength, amount of thread has the highest impact on SN ratio.

Table 28 Response Tables for Flexural Strength Using Minitab

Level	Response Table for Means			Response Table for Signal to Noise Ratios Larger is better		
	Material	Thread Count	Layer Gap	Material	Thread Count	Layer Gap
1	104.47	77.52	88.24	40.29	37.71	38.86
2	81.43	86.38	89.34	38.09	38.67	38.86
3	89.59	97.53	89.60	38.92	39.76	38.94
4	90.00	104.06	98.30	39.07	40.24	39.70
Delta	23.03	26.54	10.05	2.20	2.53	0.85
Rank	2	1	3	2	1	3

27. Similarly, an approximate regression model for flexural case was also constructed and analyzed, summary is presented in Table 29. Here, it must be noted that although the p-value for layer gap is quite large (in-significant), however, it is lesser than the value calculated in case of Tensile specimen. Moreover, it must also be noted that in this case the R-squared value is lower thus the model build does not comprehensively encompass the complete data. The p-values have also not been estimated for the highest level for thread count and layer gap which are predicted as the most suitable as per the main effects plot presented in figure 42.

Table 29 Estimated Regression Model Coefficients for SN ratio of Flexural Strength

Term	Co-eff	SE Co-eff	T	p
Constant	39.0919	0.2347	166.577	0.000
Material PLA	1.1943	0.4065	2.938	0.026
Material ABS	-1.0033	0.4065	-2.468	0.049
Material PLA-C	-0.1725	0.4065	-0.425	0.686
Thread C 12	-1.3862	0.4065	-3.410	0.014
Thread C 24	-0.4223	0.4065	-1.039	0.339
Thread C 36	0.6636	0.4065	1.633	0.154
Layer Ga 0	-0.2339	0.4065	-0.575	0.586
Layer Ga 1	-0.2288	0.4065	-0.563	0.594
Layer Ga 2	-0.1489	0.4065	-0.366	0.727

S = 0.9387 R-Sq = 83.8% R-Sq(adj) = 59.4%

28. ANOVA for the SN ratios for Flexural Strengths was also performed and it is summarized in table 30. Here material is significant on a scale of $\alpha=0.1$ while the layer gap is statistically insignificant according to ANOVA of SN ratio, further analysis of it will be covered in the next chapter.

Table 30 ANOVA for SN ratio of Flexural Strength

Source	DF	Seq SS	Adj SS	Adj MS	F	p
Material	3	9.852	9.852	3.2840	3.73	0.080
Thread Count	3	15.404	15.404	5.1348	5.83	0.033
Layer Gap	3	2.013	2.013	0.6710	0.76	0.555
Residual Error	6	5.287	5.287	0.8812		
Total	15	32.557				

Predicted SN ratio for Full Factorial Design

29. SN ratios for the full factorial design were also predicted using Minitab, summary of this calculation is presented in Table 31. Detailed analysis of the data presented below shows that

the highest SN ratio is for the factor level design S No 4 of Taguchi OA. This is also confirmed by the main effects plot that show that flexural strength maximizes for PLA 48 thread with 3 layer gap. Table 23 & 30 both clearly show that higher SN ratios are achieved at higher thread count while layer gap has little effect on the mechanical properties.

Table 31 Predicted SN ratio for full factorial design of Flexural Strength using Minitab

S No	Material	Thread Count	Layer Gap	PSNRA	PMEAN	PSTDE
1	PLA	24	0	39.63004	96.34586	1.593745
2	PLA	36	0	40.71594	107.4962	3.237569
3	PLA	48	0	41.19727	114.0292	4.554133
4	PLA	12	1	38.67128	88.58545	1.001052
5	PLA	36	1	40.72106	108.5919	2.26305
6	PLA	48	1	41.2024	115.1248	3.579614
7	PLA	12	2	38.75116	88.84762	3.78415
8	PLA	24	2	39.71504	97.70369	3.402324
9	PLA	48	2	41.28228	115.387	6.362713
10	PLA	12	3	39.51166	97.54365	2.862707
11	PLA	24	3	40.47554	106.3997	2.480881
12	PLA	36	3	41.56144	117.5501	4.124705
13	ABS	12	0	36.46859	64.45549	1.78571
14	ABS	36	0	38.51837	84.46193	3.047708
15	ABS	48	0	38.99971	90.99486	4.364272
16	ABS	24	1	37.43759	74.40721	0.429365
17	ABS	36	1	38.5235	85.55759	2.073189
18	ABS	48	1	39.00483	92.09051	3.389753
19	ABS	12	2	36.5536	65.81331	3.59429
20	ABS	24	2	37.51747	74.66938	3.212463
21	ABS	36	2	38.60338	85.81976	4.856288
22	ABS	12	3	37.3141	74.50934	2.672846
23	ABS	24	3	38.27797	83.36541	2.29102
24	ABS	48	3	39.84521	101.0487	5.251409
25	PLA-C	12	0	37.2993	72.60966	-0.40342
26	PLA-C	24	0	38.26318	81.46573	-0.78525
27	PLA-C	48	0	39.83042	99.14903	2.175142
28	PLA-C	12	1	37.30442	73.70531	-1.37794
29	PLA-C	24	1	38.2683	82.56138	-1.75977
30	PLA-C	36	1	39.3542	93.71176	-0.11594
31	PLA-C	24	2	38.34818	82.82355	1.023333
32	PLA-C	36	2	39.43408	93.97393	2.667158
33	PLA-C	48	2	39.91542	100.5069	3.983722
34	PLA-C	12	3	38.1448	82.66351	0.483716
35	PLA-C	36	3	40.19458	102.67	1.745715
36	PLA-C	48	3	40.67592	109.2029	3.062278

S No	Material	Thread Count	Layer Gap	PSNRA	PMEAN	PSTDE
37	PLA-Cu	12	0	37.45335	73.0198	1.298671
38	PLA-Cu	24	0	38.41722	81.87587	0.916845
39	PLA-Cu	36	0	39.50312	93.02625	2.560669
40	PLA-Cu	12	1	37.45847	74.11545	0.324151
41	PLA-Cu	24	1	38.42235	82.97152	-0.05767
42	PLA-Cu	48	1	39.98958	100.6548	2.902714
43	PLA-Cu	12	2	37.53835	74.37762	3.10725
44	PLA-Cu	36	2	39.58813	94.38407	4.369249
45	PLA-Cu	48	2	40.06946	100.917	5.685812
46	PLA-Cu	24	3	39.26272	91.92972	1.803981
47	PLA-Cu	36	3	40.34863	103.0801	3.447805
48	PLA-Cu	48	3	40.82996	109.613	4.764369

Fracture Surface Analysis

30. Fracture surface of the specimen subjected to tensile testing was analyzed visually. The surface showed evidence of brittle failure which was also supported by the stress-strain curves obtained for each specimen. It was found that fiber pull out occurred in all the fractures with thermoplastic failure occurring prior to the failure of threads. Also, there was evidence found for lack of a strong bond between fibers and thermoplastic in all the cases. This failure pattern was common for all tensile and flexural samples.

31. Figure 43 contains cross sectional views of broken flexural samples, showing fiber pull out and weak interface between plastic and fiber. This is a common failure type in composites that exhibit weak interface between fiber and matrix. In this failure mode the fibers elongate to support matrix until failure. In case of high strength fibers, it is common that they continue to bear the applied load subsequent to matrix failure. It may also be noted, as highlighted in figure 44, that there are void formation in places of fiber which is another indicator of weak fiber to thermoplastic interface. Any void/ discontinuity is a precursor for failure in an object under load.

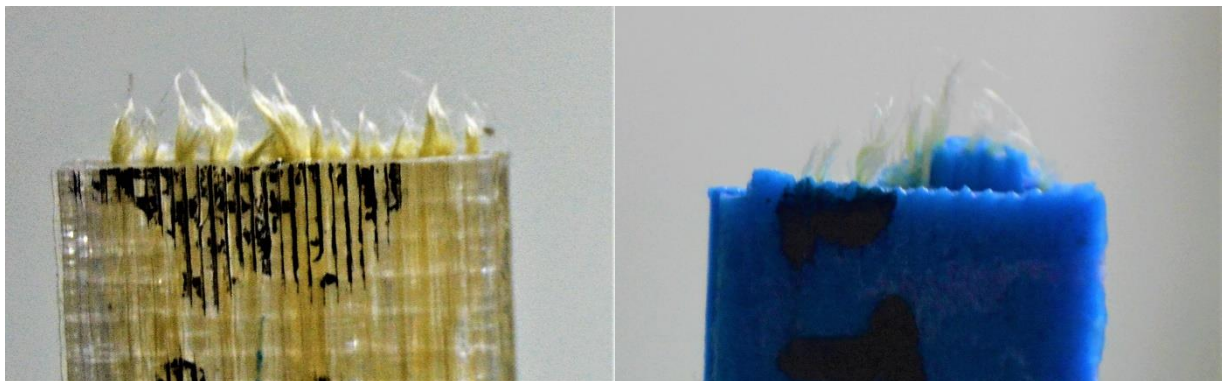


Figure 43 Broken Flexural Sample sideview



Figure 44 Cross-sectional view of Flexural sample

32. Similarly, tensile testing of samples also yielded similar results of fiber pull out and void formation. Figure 45 shows the fiber pull out phenomena for tensile sample, here also matrix failure occurred first. However, thread was not strong enough to elongate subsequent to failure of matrix and broke immediately after the failure of matrix which is evident from stress-strain curves for tensile samples. This was true for all the types of thermoplastics used in this research work. Figure 46 shows the cross-sectional view of tensile sample showing void formations similar in nature to flexural samples. These voids are smaller than the voids formed in case of flexural samples due to the type of load applied.

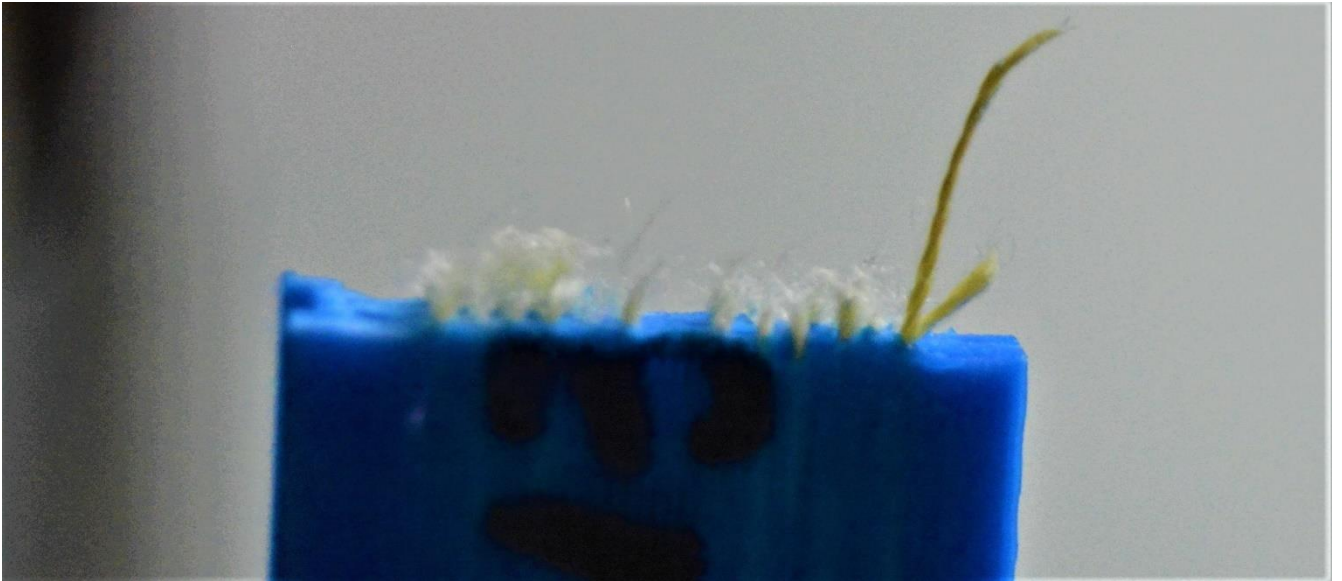


Figure 45 Fiber Pull-out phenomena in Tensile Sample



Figure 46 Cross-sectional view of Tensile sample and void formation

Theoretical Estimation of Tensile Strength

33. Rule of Mixtures (ROM) is a very useful theoretical way of estimating tensile strength for a unidirectional composite. As discussed in Chapter 2, experimental data is the most reliable source for mechanical properties of composites. However, ROM estimates can be a good starting point for establishing a direction.

34. ROM theory suggests that the tensile strength of fibers claimed by the OEM is always higher than the value achieved experimentally. Therefore, a more practical approach is to perform testing of samples at one level of volume fraction and back calculate the apparent tensile strength of fibers. Then use this apparent tensile strength, F_{ft} , to estimate the tensile strength of composite at rest of the levels of volume fraction that are to be investigated. F_{ft} can be estimated using the ROM equation discussed in Chapter 2.

35. It must be kept in mind that the theoretical equations assume a perfect bond between fiber and matrix, which is not the case in most composite layup methods. In this technique as no binder is used, fused thermoplastic and the fiber remain immiscible for most part. Literature review already revealed that most of the defects, such as voids, occur at the interface between fiber and matrix. Having said that, it is also pertinent to mention here that these imperfections may not play a vital role depending upon the application in which the part is used. Also, few researchers have already proposed ways and means to improve permeability between fiber and matrix. This experimental study does not cover that technique, however, it has the capability to adopt that advancement along with the added benefits of having a thermoplastic shell suggested here.

36. Aforementioned approach was used to estimate tensile strength of the complete OA. Table 11 shows the F_{ft} estimated from experimental data for lowest volume fraction for each material, using these values Tensile Strength of the composite have been estimated. These estimated values of Tensile Strength were then compared with the average of experimentally achieved Tensile Strength for each trial run, Table 32 provides a summary of these calculation. It must also be kept in mind that ROM is only applicable to Tensile mode of failure, flexural properties cannot be estimated using these mathematical relations.

37. At baseline values for all the materials, predicted and achieved strength has zero difference because F_{ft} has been estimated using the experimental values at these values. Moreover, with increase in amount of fiber there is a significant difference in the values achieved and predicted which will be analyzed in detail in the forthcoming chapter.

38. According to the literature review, no analytical relationships were available to predict the flexural properties of unidirectional composites. Therefore, no comparison data could be generated.

Table 32 Tensile Strength Estimation using ROM

S No	Material	Count	Gap	Experimental Strength	% V_f	F_{ft}	Predicted Strength	Difference
1	PLA	12	0	65.99	1.30	3344.16	65.986465	0.00
2	PLA	24	1	82.58	2.60		109.1604365	26.58
3	PLA	36	2	90.57	3.90		152.3344079	61.76
4	PLA	48	3	104.97	5.20		195.5083794	90.54
5	ABS	12	1	42.15	1.30	2380.47	42.14895	0.00
6	ABS	24	0	59.39	2.60		72.94495889	13.55
7	ABS	36	3	69.88	3.90		103.7409678	33.87
8	ABS	48	2	86.33	5.20		134.5369767	48.21
9	PLA-C	12	2	60.31	1.30	3009.00	60.31384	0.00
10	PLA-C	24	3	72.74	2.60		99.14848316	26.41
11	PLA-C	36	0	83.60	3.90		137.9831263	54.38
12	PLA-C	48	1	94.46	5.20		176.8177695	82.35
13	PLA-Cu	12	3	52.30	1.30	2495.55	52.29565	0.00
14	PLA-Cu	24	2	56.85	2.60		84.47363237	27.62
15	PLA-Cu	36	1	70.21	3.90		116.6516147	46.44
16	PLA-Cu	48	0	90.36	5.20		148.8295971	58.47

CHAPTER 5

DISCUSSION & ANALYSIS

Research Gap & Process Development

1. Aim of this research was to try and eliminate the limitations that were found in the procedures developed to fabricate CFRTPCs during the course of literature review. Following is the summary of these limitations:

(a) **Environmental Effect on the fiber.** Barbero (2017) states that usual practice while fabricating PMCs is to cover up the fiber with matrix to ensure safeguard of fiber from environment. While the current procedures available for fabricating CFRTPCs had no method of ensuring this automatically.

(b) **Surface Finish.** Parts that are fabricated for installation in large mechanisms have close tolerances and fine surface finish. Formation of voids due to immiscibility of fiber with matrix impedes the surface quality and increases surface roughness. Also, the use of large diameter nozzles to accommodate fiber extrusion with the thermoplastic hinders surface finish.

(c) **Volume Fraction.** Fabricating CFRTPCs using a single extruder system has an inherent limitation that as long as the part is being print, fiber is continuously extruded in each layer. There may be methods to indirectly control the volume fraction by either increasing flow rate of thermoplastic or cutting the fiber. However, both these techniques limit the fiber layup that can be achieved.

2. Aforementioned limitations of fabricating CFRTPCs using FDM were kept in mind while designing this experimental study. A single point solution for all these limitations was the use of a dual nozzle FDM system instead of a single nozzle system that has been used in all the previous study. Dickson et al. (2017) have attempted a similar feat using Carbon/ Nylon/ Kevlar reinforced Nylon composites printed with a dual extruder printing setup. However, as already described, this procedure does not offer the flexibility to just use any fiber.

3. Therefore, a new procedure was developed using commercially available dual nozzle FDM setup. This procedure addresses the above stated issues amicably while providing the flexibility to use any fiber type that can bear the nozzle temperature.

DOE & Results

4. Developing the procedure required in depth knowledge of the FDM setup capability and limitations. Over 100 trial runs were carried out to develop understanding of operation with single nozzle. Subsequently, another 100 trial runs were carried out to comprehensively understand dual nozzle operations. These trial runs also included the operation of the setup with the Kevlar fiber.

5. Subsequently, procedure was finalized and its parameters settled to ensure process repeatability. This was followed by identification of variables to be considered for study,

summary has been presented in Table 10. Taguchi DOE was selected to reduce the experimental load, based upon the availability of resources and raw materials. This decision led to the reduction of trial runs from a large total of 272 to 80 runs including all the replicates and samples for baseline materials. This figure increased to 100, due to variability in a few results and sample damage during fabrication. Even with this reduction to 1/3rd, the time required for testing and fabrication was nearly two months.

6. Results so obtained have already been covered in depth in the previous chapter. Following are the conclusion drawn from results obtained:

(a) **Volume Fraction Analysis.** Analysis was performed on the minimum volume fraction and volume fraction achieved using analytical relationships available in literature. Table 12 shows the minimum volume fraction and apparent fiber strength calculated for all four categories of material. Subsequently, Table 15 presents volume fraction for flexural and tensile samples at each setting of complete OA. Tensile specimen were larger in size as compared to flexural specimen, therefore, fiber volume fraction achieved for tensile specimen is slightly less than flexural specimen at corresponding factor levels. This difference was negligibly small, therefore, no changes in sample design were made.

(b) **Effect of Different materials.** Results show that out of the four materials used, PLA yields the highest tensile strength without addition of fiber. Flexural strength for PLA-C is superior than rest of the materials. This also corroborates the claims that addition of short carbon fiber to thermoplastics improves material stiffness.

(c) **Impact of adding Kevlar Fiber on Mechanical Properties.** It is evident from results for all the materials that tensile strength and fiber quantity has a direct relationship. Strength enhances significantly at high quantity of fibers. Tensile strength has increased up to 3 times from the base value while flexural strength has enhanced by almost twice the baseline value. In case of flexural strength, improvement also show effects of layer gap which will be discussed in forthcoming paragraphs.

(d) **Effect of inducing Layer Gap.** Software used in this study had no direct provision of adding fiber and thermoplastic alternatively with the outer shell being fabricated only from thermoplastic. G-code was studied in depth to achieve this feat. Each code was generated using Cura and edited to meet the requirements of each trial by using Repetier-Host. Therefore, formation of a separate G-code file for each setting of the selected OA was necessary. A single layer gap here meant a 0.2 mm layer of thermoplastic. Results show that addition of layer gap has no significant effect on tensile strength as shown in main effect graphs presented in figure 34. However, for the case of flexural strength, main effect graphs presented in figure 39 show that inducing a layer gap of 3 layer has a positive impact. 03 layer gap corresponds to 0.6 mm of thermoplastic in between 02 layers of fiber.

(e) **Apparent Fiber Strength.** Barbero (2017) states that the OEM provided fiber strength is often too large to achieve. Therefore, a more practical approach adopted is to calculate tensile strength experimentally at one volume fraction and then use it to back calculate apparent fiber strength, F_{ft} , using ROM equation. Table 12 has presented a

summary of these calculations. It is noteworthy that the fiber exhibits different strength for different material, following are the probable causes:

- i. Fiber strength experimentally calculated is strongly dependent on interaction of matrix and fiber to hold the part under loading. Therefore, as this interaction varies from one material to another, the fiber strength also varies.
- ii. Additives in thermoplastic filament increases voids in the parts fabricated (Ning et al., 2017a, Ning et al., 2017b). These voids may have been further enhanced due to immiscible behavior of Kevlar fiber with the thermoplastics. Hence, due to lesser interaction between matrix and fiber, the apparent strength of fiber reduced.

(f) **Optimized Settings & Confirmatory Experiments.** Aim of this study was to maximize both tensile and flexural strength in the bracket under analysis. 'Larger the better' SN ratio was utilized for this purpose as replicates for each factor level design were available. Following optimized factor levels were determined by superimposing calculations made:

- i. For tensile strength, PLA with 48 threads and 0 layer gap was the optimized setting. It was found that layer gap addition had no apparent benefit for tensile strength of a part.
- ii. For flexural strength, PLA with 48 threads and 3 layer gap was the optimized setting. Layer gap at its highest level had a positive impact on the flexural strength of the fabricated specimen.

Inducing layer gap had a positive impact on the flexural strength of the part while no impact was observed on tensile strength. It is also clear from the results for tensile strength listed in Table 18 & 22 that SN ratio only drops slightly for adding layer gap. Also, for flexural strength results listed in Table 25 & 29 reducing layer gap has a significant impact on the mean flexural strength and SN ratios. Therefore, keeping these factors in view, optimized setting that will maximize tensile as well flexural strength is using PLA as material with 48 threads (04 layers of threads) and inducing 03 layer gap between successive thread layers.

There was no need to perform confirmatory experiments as the optimized factor setting has already been tested. Tensile strength has been enhanced 2.8 times the base value while the flexural strength has enhanced 1.6 times the base value.

(g) **ANOVA.** SN ratio were subjected to ANOVA using Minitab software. This analysis revealed that material and thread were statistically significant while layer gap was not. However, in case of flexural strength, the p-value for layer gap was much lower than that for tensile strength. This means that the impact induced by Layer gap is much smaller than the rest of the parameters considered. Therefore, if required, layer gap can be omitted from mathematical relation for the system under investigation. It must be noted that even with small impact that layer gap has, the increase in flexural strength is significant while the effort involved is minimal. Hence, based upon the requirement of the system under consideration, layer gap may still be utilized.

(h) **ROM & Tensile Strength.** Rule of mixtures is a simple mathematical technique used to ascertain tensile properties of composites reinforced with unidirectional continuous fibers. This rule is only applicable to tensile properties parallel and perpendicular to the fiber direction. ROM is not applicable to flexural strength estimation and no such analytical relationship exists. Calculation for tensile strength parallel to fiber direction have only been made as only this was considered in this study. Summary of the tensile strength calculated using ROM and comparison with experimental results has been presented in Table 28. It is evident that predicted strengths are significantly larger than the experimentally determined strength. This may be because of the underlying assumption made for determining ROM mathematical relation. ROM assumes a perfect bond between fiber and the matrix which is not true in real circumstances. For this reason, Barbero (2017) suggests the use of ROM only to predict the stiffness of parts and use experimental data for the remaining mathematical properties. Even with this severe limitation, ROM can serve as the baseline to determine expected effects of a volume fraction on the tensile properties of a composite. It must also be kept in mind that no such mathematical predictor exists for the flexural properties.

Minitab Results

7. Minitab is a powerful software primarily designed for statistical analysis of data. This software was used for DOE and subsequent analysis of the data collected through experimentation. Calculation of SN ratio, ANOVA and main effects plots were generated using this software. Conclusions drawn from this data has been covered in previous paragraphs.

8. Regression analysis was performed for the data collected to identify a single equation for tensile as well as flexural strength of the system under consideration. These equations made the finding discussed above even more clear that Material and Thread count has a primary impact on the strength of a part. Layer gap had a negligibly small, albeit positive impact on tensile strength. While, significantly large impact was observed on flexural strength at highest gap selected for this study.

$$\begin{aligned}
 UTS = & 73.918 + 12.11 \textit{Material_PLA} - 9.48 \textit{Material_ABS} + 3.86 \textit{Material_PLA} - C - 6.49 \textit{Material_PLA} - Cu \\
 & - 18.73 \textit{Thread_Count_12} - 6.03 \textit{Thread_Count_24} + 4.65 \textit{Thread_Count_36} \\
 & + 20.11 \textit{Thread_Count_48} + 0.92 \textit{Layer_Gap_0} - 1.57 \textit{Layer_Gap_1} - 0.40 \textit{Layer_Gap_2} \\
 & + 1.05 \textit{Layer_Gap_3}
 \end{aligned}$$

$$\begin{aligned}
 FS = & 91.37 + 13.10 \textit{Material_PLA} - 9.94 \textit{Material_ABS} - 1.78 \textit{Material_PLA} - C - 1.37 \textit{Material_PLA} \\
 & - Cu - 13.85 \textit{Thread_Count_12} - 4.99 \textit{Thread_Count_24} + 6.16 \textit{Thread_Count_36} \\
 & + 12.69 \textit{Thread_Count_48} - 3.13 \textit{Layer_Gap_0} - 2.03 \textit{Layer_Gap_1} - 1.77 \textit{Layer_Gap_2} \\
 & + 6.93 \textit{Layer_Gap_3}
 \end{aligned}$$

9. Co-efficient of each variable signify the relative impact on the outcome variable, Flexural strength and Tensile strength in this case. It is evident from analyzing these equations that layer gap has a relatively large impact on the flexural strength when layer gap is 03 while very small although positive impact on tensile strength. Keeping all these factors in view, it is reiterated that the optimum factor level settings are as follows:

MATERIAL : PLA THREAD COUNT : 48 LAYER GAP : 03

Fracture Surface Analysis

10. Thermoplastic exhibited brittle failure as evident from the stress-strain curves for each along with visual inspection of the fractured specimen. This is in line with the literature review carried out prior to research work as all of the previous research work have identified brittle behavior of thermoplastics. Nature of the composites fabricated was also brittle as the matrix was brittle. Fracture in thermoplastic and composite samples was instantaneous on a macroscale with no neck formation.

11. Cross sectional surface of thermoplastic shows that the bonding between the layers is slightly lower in strength, evident from the fact that individual layers can be identified. Moreover, the samples also show signs of crack propagation at microscale followed by instantaneous failure which is also consistent with brittle fracture theory. Figure 25 provides the necessary evidence for this interpretation.

12. Fiber pull out phenomena occurs in composite failure when the bond formation between the fiber and matrix is weak. In this failure category, the matrix of composite fails first which may or may not be followed by the failure of fiber. In case of this research work, matrix failure was immediately followed by the failure of fiber. This is also an indication of the fact that aramid fiber, though have very high strength, do not exhibit the high tensile strength claimed by the OEM. This is also in line with the established fact that OEM provided data cannot be relied upon while designing composites and it is better to test mechanical properties of any designed composite experimentally (Barbero, 2017).

13. Moreover, visual analysis of the fracture surface provides evidence that void formation was initiated at the interface of fiber and thermoplastic which directly contributed to failure. Figure 43-46 provide the evidence of this interpretation. In reality, perfect bond formation cannot be achieved between fiber and thermoplastic, however, quality of bond formed using conventional techniques is superior than that achieved using FDM. Strength was over-estimated using ROM because of the assumption that a perfect bond is formed between fiber and thermoplastic which is not the case. Hence, albeit the superior improvement in tensile strength, it was very inferior to the estimated values using ROM.

CHAPTER 6

CONCLUSION & RECOMMENDATIONS

Conclusion

1. A new procedure was developed to address the limitations of CFRTPCs fabrication process using FDM. Variable selection was done based upon the resources available, setup limitations and the previous research work available. Taguchi DOE was successfully implemented to reduce the amount of data generated followed by tensile and flexural testing using UTM for the L₁₆ OA.
2. Based on the data generated optimum factor levels were selected to maximize tensile and flexural strength. The process shows promising results with tensile strength improvement of up to 3 times that of the thermoplastic and flexural strength improvement of up to almost 2 times at a very low volume fraction.
3. Mechanical characteristics of any part are directly dependent upon the strength of bond between its constituents. Composites are not different here, the mechanical properties are primarily dependent upon the strength of interface between fiber and matrix. Conventional techniques use pressure and temperature along with catalysts to improve miscibility that in turn yield favorable mechanical characteristics. Use of FDM process for fabricating unidirectional composites yields weaker interface between fiber and matrix in the absence of any the above mentioned agents. Therefore, it is strongly suggested that the parts produced using this technique be termed as 'HYBRIDS' instead of 'Composites'.

Recommendations

4. Analysis on the capability of the process has been assessed by carrying out flexural and tensile testing. Behavior under impact load, creep behavior and fatigue testing may also be carried out to ascertain the practicality of this process. Testing may also be carried out under various environmental conditions.
5. In this research work, unidirectional CFRTPCS have been investigated while the process is capable of producing multidirectional CFRTPCs which would further enhance mechanical properties. This may also be further investigated.
6. Theoretically, the process is appropriate for all fibers as long as they can bear the temperature at the nozzle assembly. However, testing may be carried out with other fiber categories (natural, synthetic and metal) to determine special requirements, if any, for adoption of this procedure.
7. Tested samples show that there is a weak interface between plastic and fiber that has contributed to failure. The mechanical strength of the samples can further be improved by treating fiber or thermoplastic with chemicals that improve miscibility of thermoplastic with fiber. Similarly, gluing agents such as epoxy can also be added to fiber layers in the samples during the process which may also enhance mechanical properties.

REFERENCES

- AFROSE, M. F., MASOOD, S., IOVENITTI, P., NIKZAD, M. & SBARSKI, I. 2016. Effects of part build orientations on fatigue behaviour of FDM-processed PLA material. *Progress in Additive Manufacturing*, 1, 21-28.
- ASTM, I. 2007. Standard test methods for flexural properties of unreinforced and reinforced plastics and electrical insulating materials. *ASTM D790-07*.
- BARBERO, E. J. 2017. *Introduction to Composite Materials Design, Third Edition*, CRC Press.
- BELLEHUMEUR, C., LI, L., SUN, Q. & GU, P. 2004. Modeling of bond formation between polymer filaments in the fused deposition modeling process. *Journal of Manufacturing Processes*, 6, 170-178.
- BENIAK, J., KRIŽAN, P. & MATUŠ, M. 2015. A comparison of the tensile strength of plastic parts produced by a fused deposition modeling device.
- BROOKS, H. & MOLONY, S. 2016. Design and evaluation of additively manufactured parts with three dimensional continuous fibre reinforcement. *Materials & Design*, 90, 276-283.
- CHACÓN, J., CAMINERO, M., GARCÍA-PLAZA, E. & NÚÑEZ, P. 2017. Additive manufacturing of PLA structures using fused deposition modelling: Effect of process parameters on mechanical properties and their optimal selection. *Materials & Design*, 124, 143-157.
- DICKSON, A. N., BARRY, J. N., MCDONNELL, K. A. & DOWLING, D. P. 2017. Fabrication of continuous carbon, glass and Kevlar fibre reinforced polymer composites using additive manufacturing. *Additive Manufacturing*, 16, 146-152.
- GOH, G., DIKSHIT, V., NAGALINGAM, A., GOH, G., AGARWALA, S., SING, S., WEI, J. & YEONG, W. 2018. Characterization of mechanical properties and fracture mode of additively manufactured carbon fiber and glass fiber reinforced thermoplastics. *Materials & Design*, 137, 79-89.
- HAFSA, M., IBRAHIM, M., WAHAB, M. & ZAHID, M. Evaluation of FDM pattern with ABS and PLA material. *Applied Mechanics and Materials*, 2014. Trans Tech Publ, 55-59.
- INTERNATIONAL, A. 2015. *Standard test method for flexural properties of polymer matrix composite materials*, ASTM International.
- KIM, H., PARK, E., KIM, S., PARK, B., KIM, N. & LEE, S. 2017. Experimental study on mechanical properties of single-and dual-material 3D printed products. *Procedia Manufacturing*, 10, 887-897.
- KRUTH, J.-P. 1991. Material increment manufacturing by rapid prototyping techniques. *CIRP Annals-Manufacturing Technology*, 40, 603-614.
- LEE, C., CHUA, C., CHEAH, C., TAN, L. & FENG, C. 2004. Rapid investment casting: direct and indirect approaches via fused deposition modelling. *The International Journal of Advanced Manufacturing Technology*, 23, 93-101.
- LI, N., LI, Y. & LIU, S. 2016. Rapid prototyping of continuous carbon fiber reinforced polylactic acid composites by 3D printing. *Journal of Materials Processing Technology*, 238, 218-225.
- LIU, F. W. 2007. *Rapid prototyping and engineering applications: a toolbox for prototype development*, Crc Press.
- LIU, S., LI, Y. & LI, N. 2018. A novel free-hanging 3D printing method for continuous carbon fiber reinforced thermoplastic lattice truss core structures. *Materials & Design*, 137, 235-244.

- MAGALHÃES, L., VOLPATO, N. & LUERSEN, M. 2014. Evaluation of stiffness and strength in fused deposition sandwich specimens. *Journal of the Brazilian Society of Mechanical Sciences and Engineering*, 36, 449-459.
- MATSUZAKI, R., UEDA, M., NAMIKI, M., JEONG, T.-K., ASAHARA, H., HORIGUCHI, K., NAKAMURA, T., TODOROKI, A. & HIRANO, Y. 2016. Three-dimensional printing of continuous-fiber composites by in-nozzle impregnation. *Scientific reports*, 6, 23058.
- NING, F., CONG, W., HU, Y. & WANG, H. 2017a. Additive manufacturing of carbon fiber-reinforced plastic composites using fused deposition modeling: Effects of process parameters on tensile properties. *Journal of Composite Materials*, 51, 451-462.
- NING, F., CONG, W., HU, Z. & HUANG, K. 2017b. Additive manufacturing of thermoplastic matrix composites using fused deposition modeling: A comparison of two reinforcements. *Journal of Composite Materials*, 51, 3733-3742.
- NOORANI, R. 2006. Rapid prototyping: principles and applications.
- ONUH, S. O. & YUSUF, Y. Y. 1999. Rapid prototyping technology: applications and benefits for rapid product development. *Journal of intelligent manufacturing*, 10, 301-311.
- ONWUBOLU, G. C. & RAYEGANI, F. 2014. Characterization and optimization of mechanical properties of ABS parts manufactured by the fused deposition modelling process. *International Journal of Manufacturing Engineering*, 2014.
- PEREZ, A. R. T., ROBERSON, D. A. & WICKER, R. B. 2014. Fracture surface analysis of 3D-printed tensile specimens of novel ABS-based materials. *Journal of Failure Analysis and Prevention*, 14, 343-353.
- ROSS, P. J. 1996. *Taguchi techniques for quality engineering : loss function, orthogonal experiments, parameter and tolerance design*, Second edition. New York : McGraw-Hill, [1996] ©1996.
- ROY, R. K. 1990. *A primer on the Taguchi method*, New York (N.Y.) : Van Nostrand Reinhold.
- SOOD, A. K., OHDAR, R. K. & MAHAPATRA, S. S. 2010. Parametric appraisal of mechanical property of fused deposition modelling processed parts. *Materials & Design*, 31, 287-295.
- STANDARD, A. D3039. Standard test method for tensile properties of polymer matrix composite materials. American Society for Testing Materials, 2003.
- STANDARD, A. 2009. Standard test method for tensile properties of plastics, D 638–08. *Annual book of ASTM standards*, 8.
- TANOTO, Y. Y. & ANGGONO, J. 2017. *PROCESSING AND MATERIALS EFFICIENCY IN FUSED DEPOSITION MODELING: A COMPARATIVE STUDY ON PARTS MAKING USING ABS AND PLA POLYMERS*. Petra Christian University.
- TIAN, X., LIU, T., YANG, C., WANG, Q. & LI, D. 2016. Interface and performance of 3D printed continuous carbon fiber reinforced PLA composites. *Composites Part A: Applied Science and Manufacturing*, 88, 198-205.
- WU, W., GENG, P., LI, G., ZHAO, D., ZHANG, H. & ZHAO, J. 2015. Influence of layer thickness and raster angle on the mechanical properties of 3D-printed PEEK and a comparative mechanical study between PEEK and ABS. *Materials*, 8, 5834-5846.
- YANG, C., TIAN, X., LIU, T., CAO, Y. & LI, D. 2017. 3D printing for continuous fiber reinforced thermoplastic composites: mechanism and performance. *Rapid Prototyping Journal*, 23, 209-215.
- ZHONG, W., LI, F., ZHANG, Z., SONG, L. & LI, Z. 2001. Short fiber reinforced composites for fused deposition modeling. *Materials Science and Engineering: A*, 301, 125-130.
- ZIEMIAN, C., SHARMA, M. & ZIEMIAN, S. 2012. Anisotropic mechanical properties of ABS parts fabricated by fused deposition modelling. *Mechanical engineering*. InTech.

G-Code Sheet

Comm	Parameters	Description	Example
G0	Axis [X/Y/Z] Position	Rapid Movement	G0 X50
G1	Axis [X/Y/Z/E] Position Feed [F]	Controlled Movement	G1 F150 X10
G20	none	Set units to inch	G20
G21	none	Set units to mm	G21
G28	<Axis [X/Y/Z]>	Home	G28 X Y
G90	none	Absolute Positioning	G90
G91	none	Relative Positioning	G91
G92	Axis [X/Y/Z/E] Value	Set Position to value	G92 X5 Y10
M17	none	Enable all stepper motors	M17
M18	none	Disable all stepper motors (move freely)	M18
M20	none	List files at the root folder of the SD Card	M20
M24	none	Start / Resume SD Card Print (see M23)	M24
M25	none	Pause SD Card Print (see M24)	M25
M27	none	Report SD Print status	M27
M42	none	Stop if out of material (if supported)	M42
M43	none	Like M42 but leave heated bed on (if supported)	M43
M92	Steps per unit[X]	Program set S steps per unit (resets)	M92 X123
M104	Temperature[S]	Set extruder temperature (not waiting)	M104 S100
M105	none	Get extruder Temperature	M105
M106	Fan Speed	Set Fan Speed to S and start	M106 S123
M107	none	Turn Fan off	M107
M109	Temperature[S]	Set extruder Temperature (waits till reached)	M109 S123
M112	none	Emergency Stop (Stop immediately)	M112
M114	none	Get Current Position	M114
M115	none	Get Firmware Version and Capabilities	M115
M116	none	Wait for ALL temperatures	M116
M117	none	Get Zero Position in steps	M117
M119	none	Get End-stop Status	M119
M140	Degrees[S]	Set heated bed temperature to S (not waiting)	M140 S55
M141	Degrees[S]	Set chamber temperature to S (not waiting)	M141 S30
M143	Degrees[S]	Set maximum hot-end temperature	M143 S275
M203	Offset[Z]	Set Z offset (stays active even after power off)	M203 Z-0.1
M226	none	Pauses printing (like pause button)	M226
M227	Steps[P/S]	Enables Automatic Reverse and Prime	M227 P1500 S1500
M228	none	Disables Automatic Reverse and Prime	M228
M229	Rotations[P/S]	Enables Automatic Reverse and Prime	M229 P1.0 S1.0
M230	[S]	Enable / Disable wait for temp.	M230 S1
M245	none	Start cooler fan	M245
M246	none	Stop cooler fan	M246
T	No.	Select extruder no. (starts with 0)	T1